Study of New Mid-Pole Bonding Mitigation System to Wooden Pole Ladder Network Model to address Pole-Top Fire Issue

A thesis submitted in fulfillment of the requirements for the degree of
Doctor of Philosophy

Mohd Fadli Rahmat

B.Eng. (Electrical Engineering), University Technology of Malaysia, Malaysia

M.Eng. (Electrical Power), University Technology of Malaysia, Malaysia

School of Electrical and Computer Engineering
College of Science, Engineering and Health
RMIT University

October 2010

Declaration

I certify that except where due acknowledgement has been made, the work is that of the author alone; the work has not been submitted previously, in whole or in part, to qualify for any other academic award; the content of the thesis is the result of work which has been carried out since the official commencement date of the approved research program; any editorial work, paid or unpaid, carried out by a third party is acknowledged; and, ethics procedures and guidelines have been followed.

Mohd Fadli Rahmat

October 2010

Acknowledgment

First of all, I would like to express my heartfelt gratitude and appreciation to my supervisor, Dr. Alan Wong, for his brilliant advice, encouragement and excellent support during my Phd study in RMIT University. His patience and invaluable assistance has made me a better person and it will always inspire me in the future. I would also like to extend my thanks to my co-supervisor, Prof. Luiping Wang for her advice and help.

Special thanks to my employer, Universiti Teknologi Malaysia, for giving me an opportunity to further my research study in Australia. My deepest gratitude to the staff of the Ministry of Higher Education, Malaysia for their assistance, cooperation, understanding and generosity. The financial support given by this department made this research work possible.

My appreciation to all administrative and academic staff at in the School of Electrical and Computer Engineering, RMIT University, Melbourne, Australia. Their support was invaluable. I would like to acknowledge the assistance of the technical staff, Ivan Kiss and Sinisa Gavrilovic, for setting up the wooden poles and cross-arms in the RMIT University High Voltage laboratory. Thanks also to Dr. Kamram Ghorbani for his kindness in allowing me to use the thermographic camera for my laboratory testing.

Further thanks to all my research colleagues, Azizi, Wai Siang, Jonathan, Tanwir, Rick, Hanif, Nasrul, Zamharir and others. I was very grateful for their company and help during my candidature. Thanks, also to my editor Ruth Fluhr, for her close scrutiny of my writing.

To my lovely wife, Norhaida Talib, thank you very much for your companionship, patience, understanding and support throughout our stay in Melbourne. To my son, Nazmi and my daughter, Nabila, you have been my inspiration. To my parents, thanks for your prayers and for everything. I love you all.

Finally, my gratitude and thankfulness to God for giving me good health, ideas and wisdom during my PhD study. Hopefully my work will benefit humankind and the further pursuit of knowledge. Amen.

Contents

Declaration ii

Acknowledgment iii

List of Figures viii

List of Tables xi

List of Symbols xii

Abstract 1

1 Introduction 2

1.1 Background and Introduction . . . 2
1.2 Objectives of the Thesis . . . 9
1.3 Thesis Organization . . . 11
1.4 Outcomes of the Thesis . . . 13

2 Literature Review 15

2.1 Introduction . . . 15
2.2 Wooden Pole Deterioration . . . 17
2.3 Wooden Pole Treatment and Preservation . . . 19
2.4 Failure of Wooden Poles . . . 21
2.5 Pole-Top Fire . . . 24
2.5.1 Effect of Leakage Current . . . 28
2.5.2 Current Pole-Top Fire Mitigation Techniques . . . 29
2.6 Wooden Pole Models . . . 34

3 Study of Leakage Current Effect using Ladder Network Model 39
3.1 Introduction 39
3.2 Wooden Pole Modeling based on Ladder Network 40
3.3 Leakage Current Effect using Ladder Network Model 44
3.3.1 Pole Resistance 46
3.3.2 Current Distribution of Dry and Wet Wooden Pole 49
3.3.3 Radial Current Distribution of Wooden Pole 51
3.4 Summary 53

4 Proposed Pole-Top Fire Mitigation Technique: Mid-pole Bonding System 54
4.1 Introduction 54
4.2 Proposed Mid-Pole Bonding System 56
4.2.1 System Description 56
4.3 Enhanced Ladder Network Model for Simulating Mid-Pole Bonding System 63
4.4 Performance Study of Mid-Pole Bonding System and Simulation Comparison 68
4.4.1 Simulation Results 73
4.5 Simulation of Three-Phase Leakage Current 78
4.6 Summary 82

5 Experimental Study on Novel Mid-Pole Bonding System 85
5.1 Introduction 85
5.2 Experimental Setup 86
5.3 Mid-Pole Bonding System Study on Wooden Pole 91
5.4 Thermographic Study of Cross-Arm 95
5.4.1 Thermographic Study of Wooden Cross-Arm with Leakage Current of 5 mA and 14 mA 96
5.4.2 Thermographic Study of Steel Cross-Arm with Leakage Current of 5 mA and 14 mA 99
5.4.3 Thermographic Study of Mid-Pole Bonding System 103
5.5 Summary 105

6 Conclusions and Future Works 106
6.1 Conclusions 107
6.2 Recommendation for Future Work 111

Appendix A Wooden Pole 113

Bibliography 115

List of Figures

1.1 Typical transmission and distribution line structures in electrical power network [1] . . . 4
1.2 Stobie pole in South Australian electrical distribution network [2] . . . 5
1.3 Recorded pole-top fire events over South-West Interconnected System (SWIS) in Western Australia from 1993 to 2004 [3] . . . 8
1.4 Pole-top fire in Dunsborough electrical distribution network [4] . . . 9

2.1 Wood deterioration as a result of termite attack [5] . . . 18
2.2 Pole destruction by lightning strike [6] . . . 23
2.3 Typical H-frame wooden pole structure in transmission lines [7] . . . 25
2.4 Pole-top fire event in Southmoor distribution line [8] . . . 27
2.5 Operator spraying silicone compound on pole-top insulators [9] . . . 30
2.6 Pole bonding configuration [10] . . . 33
2.7 Application of pole bonding to the cross-arm [11] . . . 33

3.1 A complete leakage current model . . . 41
3.2 Resistance of wooden pole with king bolt insertion . . . 42
3.3 Wooden pole ladder network model . . . 45
3.4 Resistance of dry wooden pole . . . 48
3.5 Resistance of wet wooden pole . . . 48
3.6 Current distribution for sapwood resistance . . . 50
3.7 Current distribution for radial resistance . . . 50
3.8 Current distribution for heartwood resistance . . . 51
3.9 Current distribution of wet radial resistance with different locations of king bolt . . . 52

4.1 Mid-pole bonding system . . . 57

4.2 New mid-pole bonding arrangement 58
4.3 Metallic band 59
4.4 Cable terminations for mid-pole bonding system 61
4.5 Wooden pole with cross-arm and supporting steel bars 64
4.6 Electrical model for mid-pole bonding system (including steel bar and king bolt) 65
4.7 Comparison of radial current distribution in mid-pole bonding system and normal system 66
4.8 Radial current distribution of mid-pole bonding system 68
4.9 Shunting arrangement 1 for cross-arm by Ross [12] 69
4.10 Shunting arrangement 2 for cross-arm by Ross [12] 70
4.11 Electrical model for Ross shunting arrangement 1 70
4.12 Electrical model for Ross shunting arrangement 2 71
4.13 Wooden pole with cross-arm and supporting steel bars 72
4.14 Electrical model for wooden pole and steel cross-arm(including steel bar and king bolt) 72
4.15 Comparison of radial current distribution between wooden and steel cross-arm under wet conditions 74
4.16 Radial current distribution of Ross's shunting arrangement 1 74
4.17 Radial current distribution of Ross's shunting arrangement 2 75
4.18 Radial current distribution of mid-pole bonding system with bypass at section 10 75
4.19 Radial current distribution of mid-pole bonding system with bypass at section 7 77
4.20 Radial current distribution of mid-pole bonding system with bypass at section 4 77
4.21 Comparison of radial current distribution for phase-to-phase leakage current with wooden cross-arm with grounding 79
4.22 Comparison of radial current distribution for phase-to-phase leakage current with wooden cross-arm without grounding 81
4.23 Pole-top fire at steel bar holder bolt due to leakage current phenomena 83

5.1 An experimental setup for mid-pole bonding system study 87
5.2 High voltage transformer 88
5.3 Voltage divider for high voltage measurement 88

5.4 1 MΩ high voltage resistor 89
5.5 Wooden cross-arm 90
5.6 Steel cross-arm 90
5.7 Thermovision A320 thermal camera 91
5.8 Mid-pole bonding system on wooden pole for leakage current from top section of wooden pole to ground 93
5.9 Mid-pole bonding system on wooden pole for leakage current from cross-arm to ground 94
5.10 Thermographic images for wooden cross-arm at 5 mA 97
5.11 Thermographic images for wooden cross-arm at 14 mA 98
5.12 Thermographic images for steel cross-arm at 5 mA 100
5.13 Thermographic images for steel cross-arm at 14 mA 101
5.14 King bolt temperature for steel and wooden cross-arm 102
5.15 Comparison of king bolt temperature with steel cross-arm 103
5.16 Linear regression of king bolt temperature with mid-pole bonding system for steel cross-arm 104

List of Tables

1.1 Electricity related ignitions in Victorian bushfires, 7 February 2009 [13] . . . 7

2.1 Australian timber pole species [14, 15] . . . 16
2.2 Specification for preservative treatment of timber [16] . . . 20
2.3 Current methods to reduce pole-top fire risk . . . 31

3.1 Pole model moisture gradient relative to sapwood and heartwood along wooden pole [17] . . . 43
3.2 Resistances of dry pole . . . 46
3.3 Resistances of wet pole . . . 47

4.1 Metallic band dimensions and parameters . . . 60
4.2 Heat dissipation of designed heat sink . . . 60
4.3 Developed mitigation system . . . 69
4.4 Comparison of simulation results for ladder network model . . . 84

5.1 Average I_{Ratio} for both experimental setups at each bypass termination 95
5.2 Average I_{Ratio} for both simulation setups at each bypass termination 95

A.1 Physical dimensions of pole . . . 113
A.2 Resistances of dry pole . . . 114
A.3 Resistances of wet pole . . . 114

List of Symbols

kV	kilovolt
V	voltage
C	celsius
cm	centimeter
%	percentage
ft	foot
i	current
R	resistance
mA	miliampere
$\mathbf{R}_s$	sapwood resistance
$\mathbf{R}_h$	heartwood resistance
$\mathbf{R}_s$	radial resistance
$\mathbf{R}_w$	rain resistance
MC	moisture content
ρ	resistivity
ℓ	length
A	cross-sectional area
R	pole radius
P	heartwood depth
$\mathbf{R}_c$	conductor resistance
$\mu\Omega$	miliohm
$\mathbf{M}\Omega$	megaohm
m	meter
$\mathbf{k}\Omega$	kiloohm
$\mathbf{R}_{kb}$	king bolt resistance

$\mathbf{R}_{st}$	steel resistance
$\mathbf{R}_{b}$	bolt resistance
$\mathbf{R}_{shCA}$	cross-arm shunting resistance
$\mathbf{R}_{shP}$	pole shunting resistance
$\mathbf{R}_{AIR}$	air resistance
$\mathbf{R}_{steelCA}$	steel cross-arm resistance
$\mathbf{R}_{steelend}$	steel end cross resistance
mm	milimeter
$\mathbf{R}_{rCA}$	cross-arm radial resistance
$\mathbf{R}_{sCA}$	cross-arm sapwood resistance
$\mathbf{R}_{HS}$	heat sink thermal resistance
$\mathbf{A}_{base}$	based Cross-sectional area
$\mathbf{A}_{fin}$	fin Cross-sectional area
$\boldsymbol{h}$	convective heat transfer coefficient
$\boldsymbol{n}$	fin efficiency
m	fin parameter
H	metallic band height
W	metallic band width
t	metallic band thickness
$\mathbf{H}_{fin}$	fin height
$\mathbf{W}_{fin}$	fin width
$\mathbf{t}_{fin}$	fin thickness
$\mathbf{k}_{fin}$	fin thermal conductivity
$\mathbf{V}_{Leakage}$	leakage voltage
$\mathbf{V}_{Shunt}$	shunting voltage
$\mathbf{V}_{Ground}$	ground voltage
$\mathbf{I}_{Leakage}$	leakage current
$\mathbf{I}_{Shunt}$	shunting current
ACA	Ammonia Copper Arsenate
PCP	Pentachloropenol
ACZA	Ammonia Copper Zinc Arsenate
CCA	Chromated Copper Arsenate

BIL	Basic Impulse Level
AUD	Australian Dollar
CAIDI	Customer Average Interruption Duration Index
SAIDI	System Average Interruption Duration Index
ESTA	Electricity Trust of South Australia Utilities
MATLAB	MATrix LABoratory software
RMIT	Royal Melbourne Institute Technology
IEEE	Institute of Electrical and Electronics Engineers
AUPEC	Australasian Universities Power Engineering Conference
ISH	International Symposium on High Voltage Engineering
SWIS	South-West Interconnected System

Abstract

This thesis presents an original study of pole-top fire in electrical distribution networks by using the ladder network model. A new mid-pole bonding mitigation method has been proposed and developed in this research to overcome the pole-top fire issue. A complete wooden pole model with cross-arm has been developed for further investigation of pole-top fire. Leakage current concentration at the wood-bolt insertion is demonstrated by significant information about radial current distribution along wooden pole structures. Replacing wood with steel cross-arm was unsuccessful in decreasing the fire-prone risk. On the other hand, Ross shunting methods depict a similar result and caused higher current concentration on the king bolt insertion compared to wood and steel cross-arm. A time-lapsed thermographic study on wood and steel cross-arms with poles have shown that the temperatures that developed on the king bolts were almost similar for both materials. The application of a mid-pole bonding system on a wooden pole structure proved successful in reducing the pole-top fire risk by at least 50%. The mid-pole bonding system offers better performance compared to the current method. This new system will provide a better solution for the pole-top fire problem.

Chapter 1

Introduction

1.1 Background and Introduction

Electrical distribution networks in Australia and around the world face great challenges in maintaining the reliability and efficiency of power systems. There is tremendous pressure for power utility companies to meet the high demand from consumers with economic and capacity constraints [18, 19]. One of the challenges is to upgrade aging facilities and equipment to enhance the overall system reliability. Continuous system upgrades will improve the power system performance and reliability of indices such as the System Average Interruption Duration Index (SAIDI) and the Customer Average Interruption Duration Index (CAIDI). Lack of resources to improve the present distribution network may compromise safety levels and also lead to power disruptions such as blackout or brownout [14]. Hence, appropriate maintenance strategies such as regular line inspection and monitoring of the condition of power equipment are important in maintaining the system reliability and therefore preventing unexpected power disturbances.

Since the early' 50s, wooden pole structural systems have been adopted by power utility companies in Australia and around the world as an economical and frugal method for supporting overhead power distribution lines. Technically, wooden pole is a selected forest product, usually hardwood timber which possesses the required mechanical properties and high durability to support overhead conductors. The Australia standard, AS 2209, sets out requirements for timber poles intended primarily for use in overhead lines for electrical distribution networks. The standard classifies timbers into groups of durability class 1, 2, 3 and 4 [15]. Most of the in-service wooden poles in Australia are harvested from native or local grown forest and the majority of the timbers are from the durability class 1 and 2 species. These groups of timbers do not require full-length preservative treatment due to their high pole strength compared to timbers in durability class 3 and 4. In Australia, blackbutt, spottted gum (durability class 2) and messmate, mountain ash and alpine ash (durability class 3 and 4) are the most common timber species currently used [14]. Typically, these types of timbers are expected to have a service lifespan of between 30 and 50 years.

Technically, wooden poles are used either in the transmission and distribution of electrical power networks as depicted in Figure 1.1. Depending on the placement of wooden poles in the electrical power network, certain overhead lines are used to provide the minimum technical requirement for each design. These include the mechanical design of poles, cross-arms and foundations with weather loads, conductor sags and tension effects, as well as the conductor characteristics and selection according to standard practices [15, 20, 21]. For example, 38-feet (12 meters) wooden poles are used for 12 kV to 34.5 kV distribution overhead lines and up to 85 feet (26 meters) wooden poles are used for 138 kV H frame or single circuit in sub-transmission lines. On top of that, these in-service poles still require protection systems, regular line inspection and maintenance to reduce

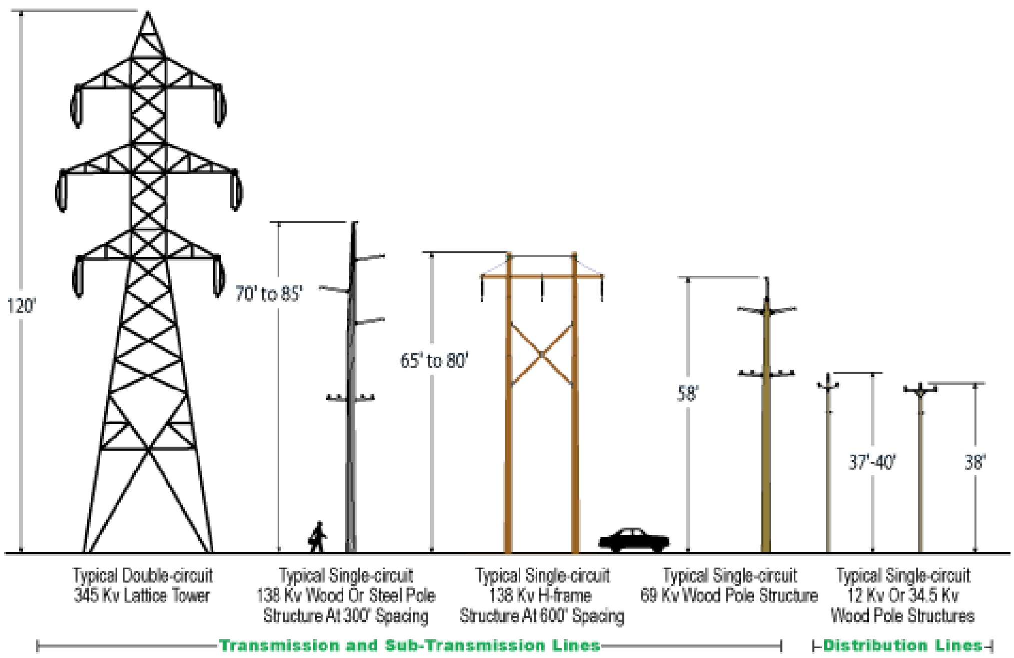

Figure 1.1: Typical transmission and distribution line structures in electrical power network [1]

power disturbances and improve the safety and security level of the system. Finally, a systematic remedial and refurbishment strategy is needed to provide good repair and extend the lifespan of wooden pole systems.

Over the last few decades, other types of utility poles have been introduced as an alternative to wood. These poles consist of concrete, tubular steel, fibre glass, fibre-reinforced polymer or aluminium. For example, "Stobie Pole", which is made up of a metal-concrete composite was developed by the Electricity Trust of South Australia Utilities (ETSA), as shown in Figure 1.2. It was introduced into South Australian distribution networks to overcome the limited availability of wood supply [2]. According to [14], almost 100% of in service poles in the Northern Territory distribution networks are made of steel. This is due to the severe local climate, which has the most destructive hazard level, making wooden poles very

Figure 1.2: Stobie pole in South Australian electrical distribution network [2]

unsuitable for this region. Nevertheless, wooden pole is still a favourable choice for most power utility companies around the world because of the reasonable cost, natural durability and excellent insulating characteristic of timber.

Currently, there have been great concerns over the build-up of greenhouse gases in the atmosphere, particularly over deforestation to accommodate the needs of power utilities for their electrical networks. If over 20,000 new poles are required each year for replacement in existing lines in Australia, more forest must be cleared for these purposes [14]. However, with efficient forest management practices, re-forestation and rehabilitation are successfully increasing the area of forested land. Wood still holds a big volume of carbon in its cells after it has been harvested. On the other hand, a very small amount of energy is used during timber production compared to alternative poles. For example, an alternative pole such as tubular steel consumes four times more energy in production than concrete and wooden poles [22]. According to this report [22], the global warming potential of a regular wooden pole is about one fifth of a concrete pole and about one thirtieth of that of tubular steel. Therefore, it is clear that wooden pole is substantially more environmentally benign compared to alternative poles. Regarding pole utilization of energy and potential, alternative poles contribute more carbon dioxide to the atmosphere, which promotes global warming.

Most wooden poles in service are still exposed to risks even though comprehensive inspections, maintenance and rehabilitation have been made regularly. The ignition of bushfires could be attributed to pole-top fires and defective fittings on wooden pole structures. Polluted insulators allow leakage current to flow from power lines, which will ignite fire, especially at the metal wood insertions such as king bolts and pin insulators. Improper and inefficient inspection to detect faulty fittings during regular pole maintenance could also cause a risk of mechanical failure. Both events can cause power lines to fall and trigger a spark amongst dry vegetation on the ground. In summer, the possibility of bushfires occurring is high, especially during dry hot conditions. According to [23], more than 30 major bushfires have been recorded in Victoria since 1851, burning millions of hectares of land, destroying thousands of buildings, killing millions of livestock and hundreds of people. As reported in [24–26], 119 people in Kilmore were killed during the Victorian Black Saturday fires in 2009. Some speculations were made in these reports that the failure of power line assets was responsible for the bushfire tragedy. The final report of the results of the investigation by the 2009 Victorian Bushfires Royal Commission [13] stated that electricity asset failure caused 5 of the 11 major fires on 7 February 2009 as summarized in Table 1.1.

Location	Causes	Descriptions
Kilmore East	-due to conductor failure as a result of fatigue of conductor strands, partly caused by helical termination being incorrectly seated in thimble. -the failed conductor had contact with a cable stay supporting pole and caused arcing that ignited vegetation near the base of pole.	One hundred and nineteen fatalities, two hundred and thirty-two casualties, 1,242 houses destroyed and 125,383 hectares burnt.
Horsham	-due to failure of pole cap to secure conductor on pole. -as a result the conductor hit the ground and caused fire to start.	No fatalities, no casualties, thirteen houses destroyed and 2,346 hectares burnt.
Coleraine	-tie wire that held conductor in place on top of pole broke, causing conductor to swing in wind. -contact between conductor and tree, causing arcing that ignited foliage near top of tree which subsequently fell to the ground.	No fatalities, one casualties, one house destroyed and 713 hectares burnt.
Pomberneit	-electrical fault occurred as result of clashing of 66 kV and 22 kV conductors or the 22 kV and 22 kV conductors, or both. -clashing caused emission of molten particles, which ignited vegetation by side of Princes Highway.	No fatalities, no casualties, no house destroyed and 1,008 hectares burnt.
Beechworth-Mudgegonga	-tree had fallen on power line, pulling conductor furthest from road off supporting insulators at poles. -arcing between energized conductor and pole was the probable cause of fire, which started in vegetation at base of pole.	Two fatalities, twelve casualties, thirty-eight house destroyed and 33,577 hectares burnt.

Table 1.1: Electricity related ignitions in Victorian bushfires, 7 February 2009 [13]

In addition, hundreds of pole-top fire cases were recorded in the electrical network of SWIS after a change in pole-top fire mitigation techniques during the period 1993 to June 2004, as shown in Figure 1.3. There is still a big number of pole-top fire cases recorded, even though line washing, pole bonding and silicone

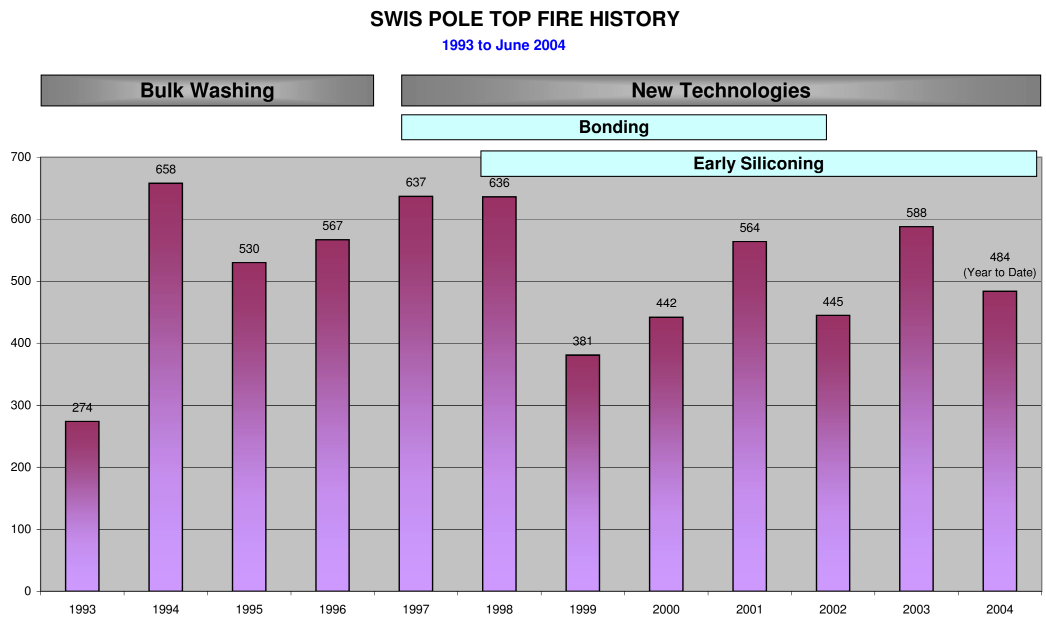

Figure 1.3: Recorded pole-top fire events over South-West Interconnected System (SWIS) in Western Australia from 1993 to 2004 [3]

coating have been applied in the Western Australian south-west electrical network. According to an electrical incident report by EnergySafety Western Australia in [4], a bushfire which occured near Cape Natural Lighthouse, Dunsborough on 7 February 2009 was caused by pole-top fire. As a result of pole burning at the attached insulator, the falling hot ember ignited vegetation under the power line and triggered a bushfire, as shown in Figure 1.4. A similar report was released by EnergySafety Western Australia that investigated the possible causes of fire ignition from high voltage power lines in the Toodyay bushfires [27]. The arcing between conductors in the span between poles T303-12 and T303-43 could have ignited the fire. Other sources of the fire ignition, such as lightning, vandalism, vehicle movement and pole-top fire were considered and eliminated. Therefore, wooden pole safety is aimed at preventing wildfire ignition and protecting the sur-

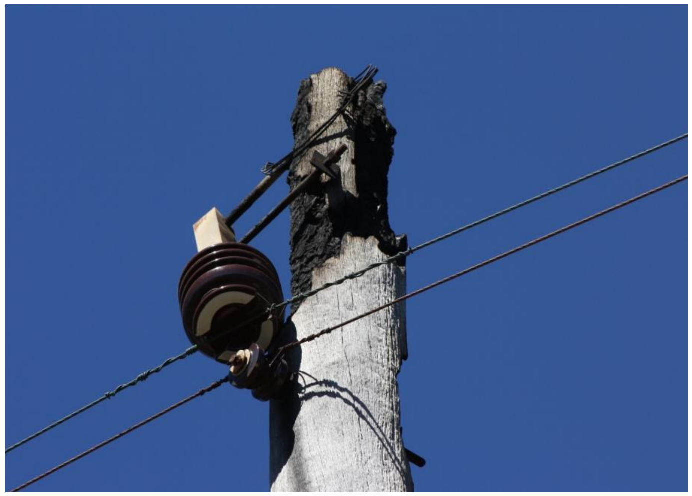

Figure 1.4: Pole-top fire in Dunsborough electrical distribution network [4]

rounding public from injury and electrocution. Further study and continuation of any research that is linked to bushfire issues and power networks is imperative. The research outcomes could supply the solution to overcoming fire prone events in the electrical distribution networks and eliminate any fire risks.

1.2 Objectives of the Thesis

This research is focused on the investigation of leakage current flow using wooden pole computer simulations and an experimental approach. A new effective pole-top fire mitigation technique that allows leakage current to flow to the ground is designed and tested. To investigate the feasibility of the pole-top fire problem, a ladder network model introduced by R. Filter in [17] has been manipulated to achieve our main research objective. The primary objectives of this research are:

- To develop a wooden pole electrical model that is based on the ladder network model, then, investigate and determine significant result from simulation works that can be used to explain leakage current effects on the king bolt insertion point along the wooden pole structure. In detail, the work is carried out in a MATLAB software environment, which represents the real wooden pole in service. The effects of moisture content, type of chemical treatments, physical dimension, step size, pollution levels on insulators and also weather conditions, such as dry and wet, are included in this study.

- To modify and manipulate the existing ladder network model purposely to include and introduce a novel electrical wooden cross-arm model for a complete case study. The developed cross-arm model is based on the ladder network model in which radial and king bolt resistances are used as a reference point.

- To introduce an electrical model of the P.M Ross mitigation technique, steel cross-arm and novel mid-pole bonding system to the enhanced model. The performance of the new mid-pole bonding system is investigated and compared with the Ross shunting method and steel cross-arm method; the performance is based on the leakage current concentration at the metal insertion.

- To verify the performance of a mid-pole bonding system simulation study with an experimental work. A metallic bonding for mitigation purposes is designed and the performance of a bypass technique is investigated as a function of the bypass current ratio. This will be compared with the ladder network computer model.

- An investigation of the leakage current effect is conducted to find out the developed temperature on the king bolt with steel and wooden cross-arm. The performance of the mid-pole bonding system in terms of king bolt temperature development is also investigated.

In this research, a 12-meter wooden pole with treated Chromated Copper Arsenate (CCA) was chosen to develop the ladder network model using MATLAB software. In addition, a 2-meter standard length of wooden and steel cross-arm was also used as part of the enhanced wooden pole model. The sapwood, heartwood and current radial distributions along wooden pole sections were determined after a comprehensive simulation study. The simulations were performed under an 11 kV system and the leakage current was assumed to flow in either a single phase or phase-to-phase form, depending on case studies. The comparative performance measures of the Ross shunting technique, the steel cross-arm and mid-pole bonding systems were made under wet conditions.

For the laboratory work, a 6.5-meter wooden pole with treated CCA was used for the experimental study. This was due to the limitation of laboratory working space and wooden pole delivery transportation. Another computer model was developed to correspond to the tested wooden pole. The testing was run with only a single phase of 11kV power supply and a series of high voltage resistances were used to simulate the pollution levels. A thermographic camera was also used to capture the temperature on the pole cross-arm junction, especially at the king bolt during the leakage current testing. An aluminium sheet was used to fabricate a metallic band for the mid-pole bonding purposes. Finally all the experimental studies were done in the RMIT University High Voltage laboratory.

1.3 Thesis Organization

The background and introduction of the thesis are clearly presented in Chapter 1. Brief descriptions of the remaining chapters are as follows:

- Chapter 2 discusses an overview of wooden pole technical literatures in the electrical network services. A concise explanation of wooden pole deterioration, treatment and preservation is presented in Chapter 2. A discussion of the failure of wooden poles in terms of mechanical and electrical aspects is also included in this chapter. A detailed study, particularly on the attributing factors that relate to pole-top fire issues is also addressed. Finally the evolution of a wooden pole model and the current solutions for pole-top fire issues are discussed in the last two sections of Chapter 2.

- Chapter 3 presents the development of a wooden pole ladder network model that is associated with pole dimensions, type of treatment, moisture content in the wood and the effect of weather. In general, the moisture level of the wood is the major factor that influences the magnitude of the wooden pole at each section compared to the type of treatment as depicted in Chapter 3. Current distribution of each resistance of each section of wooden pole is examined and analyzed from simulation works in the last section of Chapter 3. As a result, the radial current distribution shows a significant result in terms of explaining the effect of leakage current on the bolt insertion.

- Chapter 4 describes the enhancement and modification of the ladder network model, particularly the introduction of the cross-arm element into the original model. Electrical configuration of the Ross shunting technique is developed on the enhanced ladder network model to determine the performance of this mitigation method. The steel cross-arm model is also included in Chapter 4 as part of the research study. A new mid-pole bonding system is proposed in this simulation study to overcome the disadvantages of the steel cross-arm and the Ross shunting technique. The comparative work is done with radial current distribution evaluation. Lastly, the simulation study works are made under circumstances of single phase and phase-to-phase leakage current phenomena.

- Chapter 5 presents the laboratory experiment to verify the performance of the mid-pole bonding system compared with the simulation works. An observation of the temperature development on the king bolt for both wooden and steel cross-arm is made. The experimental setup is also explained in Chapter 5, particularly as to how the specific current is measured with a floating oscilloscope; the use of a thermographic camera to record the developed temperature at the pole cross-arm junction is also discussed. Finally, the performance of the mid-pole bonding system based on temperature growth at the king bolt is also included in Chapter 5.

- Chapter 6 is a conclusion and summary of the research findings, with recommendations for possible future works.

1.4 Outcomes of the Thesis

A few papers have been published in refereed journals and local conference notes by the author as outcomes of his PhD study. Most of the information delivered in these papers is included in this thesis.

- K.L. Wong and **M.F. Rahmat**,"Study of leakage current distribution in wooden pole using ladder network model", *IEEE Transaction on Power Delivery*, vol. 25(2), pp. 995-1000, April 2010.

- K.L. Wong and **M.F. Rahmat**,"Feasibility study of leakage current shunting method based on ladder network model", *IEEE Transaction on Power Delivery*, vol. 25(2), pp. 1133-1137, April 2010.

- R.H. Lunuwilage and **M.F. Rahmat** and K.L. Wong, "Study of Leakage Current Distribution in a Wooden Pole using a Three Dimensional Resistance Model",*In AUPEC '10 Australasian Power Engineering Conference*, 2010, pp. 1-5, Dec. 2010.

- **M.F. Rahmat** and K.L. Wong,"Thermographic study of stainless steel cross-arm on overhead distribution system", *In AUPEC '09 Australasian Power Engineering Conference*, 2009, pp. 1-6, Sept. 2009

- K.L. Wong and **M.F. Rahmat**,"Investigation of leakage current in wooden pole using ladder network model", *In AUPEC '08 Australasian Power Engineering Conference*, 2008, pp. 1-5, Dec. 2008.

- K.L. Wong and **M.F. Rahmat**,"Feasibility study of pole shunting method based on ladder network model", *Poster presentation in ISH '09 International Symposium on High Voltage Engineering*, 2009, Aug. 2009.

- **M.F. Rahmat** and K.L. Wong,"Thermographic Study of Stainless Steel Cross-arm on Overhead Distribution System", *IEEE Transaction on Power Delivery*,(Submitted for review on 14 Oct. 2009).

Chapter 2

Literature Review

2.1 Introduction

Electricity supply is distributed by an electrical distribution network either through overhead lines or underground cables. Overhead lines become the most cost-effective and convenient method to distribute electric power in both suburban and rural areas. This system offers a simple voltage operation, accessibility for repair and extension with low-cost lines construction. Most of the distribution overhead lines are operated with a voltage of 33/11 kV or 240/415 V. On the other hand, underground cables are more suitable for highly populated urban areas, rivers or other obstacle-prone areas. Underground cables experience less faults per km than overhead lines, but any faulty aspects are difficult to locate and more costly to repair [28]. In Australia more than 80% overhead lines are supported by wooden poles compared to alternative poles such as those made of concrete, metal and fibreglass-reinforced plastic composite materials [14].

Wooden poles have been used as part of the energy utility structure since the first electrical distribution network was constructed in the late 1880s [29]. Wooden poles are popular among power utility industries due to their natural insulation properties, high mechanical strength, long lifecycle, availability, low initial cost, simple foundation preparation and ease of maintenance for overhead line structures [30]. Therefore, a lot of countries around the world, such as the United States [31], the United Kingdom [28], Scandinavian countries [32] and Brazil [33] are still using wooden poles to transfer electricity to their consumers. For example, the United States has about 110 million poles in service and Brazil utilizes over 2 million wooden poles to support distribution and transmission lines.

Table 2.1 summarizes the major timber pole species that have been used in the Australian energy network. There is no significant number of timber poles used in Northern Territory and South Australia, due to very high termite hazard, cyclone weather and meagre timber resources. Most of the timbers are classified into durability classes which depend on the inherent resistance of a pole species

	Durability Class	**Species**
New South Wales	1 and 2	Eucalyptus pulilaris (blackbutt) Corymbia (spotted gum)
Queensland	1 and 2	Corymbia (spotted gum) Pinus elliottii (slash pine)
Victoria	1,2 and 3	Eucalyptus pulilaris (blackbutt) Corymbia (spotted gum) Pinus radiata (radiata pine)
Western Australia	1 and 2	Eucalyptus marginata (jarrah) Eucalyptus diversicolor (karri) Corymbia calophylla (marri)
Tasmania	3 and 4	Eucalyptus regnans (mountain ash) E. delegatensis (alpine ash) E. obliqua (messmate)
Australia Capital Territory	1 and 2	Eucalyptus pulilaris (blackbutt) Corymbia (spotted gum)
South Australia and Northern Territory	nil	nil

Table 2.1: Australian timber pole species [14, 15]

to decay, or to insect or marine borer attack [34]. According to [34], the probable above-ground life expectancy for durability class 1 timber is more than 40 years and the probable marine-borer-resistance life expectancy is more than 60 years. In contrast, timber pole from durability class 4 can only last about 5 to 7 years for both conditions. However, with full-length preservative treatment that depends on biological hazard conditions, these durability class 4 timbers will have a life expectancy greater than 20 years [14]. A detailed list and general requirements of timbers for overhead lines can be referred to in the AS2209 standard [15].

In the next section, a brief discussion about wooden pole deterioration, pole treatments and preservations, pole inspections, maintenance programs, pole structural reliability, as well as pole management is presented. Then, a detailed discussion relating to the electrical performance of wooden poles, especially on the issue of wooden pole-top fires is included. On top of that, previous and current practices for pole-top fire mitigation methods is also discussed in this chapter. Finally, models of wooden pole are presented in the last section of this chapter.

2.2 Wooden Pole Deterioration

All erected wooden poles in transmission and distribution lines are exposed to extreme weather conditions, biological attacks and fire [35]. The effect of knots and cracks on wooden pole body structures can be easily detected, especially in seasonal countries. This occurs during sudden transitions from hot to cold weather for long periods of time. Fungi and termite attack might also occur on the sapwood section of the wooden pole that has contact with the ground. Fungal rot eats the wood cell slowly, leading to softening and decay. In addition, termite colonies nest underground in old tree stumps or root systems, attacking and feeding on

Figure 2.1: Wood deterioration as a result of termite attack [5]

the wooden pole through their built tunnel system. Last but not least, borers live in wooden pole cracks laying eggs before burrowing out of the wood at the adult stage and flying off to breed. For example, beetles, pinhole and marine borers digging flight holes from inside may weaken the pole considerably. As a result, the pole will attract woodpeckers to peck the wood for feeding, especially during warmer months [36]. Finally, most fire events are related to insulator failure which undermines the mechanical strength of wooden poles and leads to structural failure.

Most of the deterioration agents are linked to the role of moisture content and moisture distribution along the wooden pole structure. Based on Wallis, fungal decay only occurs when the moisture level of the wood is above 20 percent [37]. Therefore, before the wooden poles are installed for service, they need to go through a preparation and pre-treatment process to reduce the exposure to fungi and termites. These preparation procedures include a process of peeling, drying and conditioning [38]. The bark and inner cambium layer of the poles are stripped out during the peeling process. Once the peeling process is completed, the poles are dried to remove water until an equilibrium moisture content level is reached. This is purposely done to reduce the shrinkage and crack effects. The poles are dried either: by a heat-steam conditioning method in a pressurized cylinder; through a long seasoning air-dry process; or by an accelerated kiln-drying controlled method. Then the preservation treatment process is ready for the prepared poles.

2.3 Wooden Pole Treatment and Preservation

Pre-treating and preserving wooden poles is important in increasing the service life of poles. Highly toxic chemicals have been used to preserve wooden poles from the effects of moisture, fungi and wood-destroying insects, besides creating weather protection. Oil-based/borne and water-based chemicals are the two common preservative types in commercial use for wooden pole preservation treatment [29, 39–42]. Oil-based preservative is a product of distilled bitumen coal such as coal-tar creosote, beechwood creosote and creosote bush resin. On the other hand, oil-borne preservative is a blend of petroleum co-solvent with carrier oils. For example, pentachlorophenol (penta or PCP) with 5% to 9% mixture has been used in the treating of wooden poles until now, especially in the United States. However, water-based preservative is based on chemical salts dissolved in water at various concentrations of 2% to 5%. A water mixture of chromated copper arsenate (CCA), and ammoniacal copper zinc arsenate (ACZA) are the most popular water-based preservatives. A very high-pressure cylinder or vacuum pressure plant is used for most oil preservative and waterborne treatment for better penetration and impregnation of wooden poles. The hot and cold bath method is the most effective alternative for non-pressurized treatment. It depends on atmospheric pressure utilized by first heating the medium and then cooling it in preservative [43].

Apparently, the relative toxicity of preservatives is successful in making wooden poles inedible. Good preservative penetration is also crucial to meet most requirements of standardized treatments to ensure effective resistance to decay, insect and borer attack [40]. On the other hand, these treatment processes do not reduce the high natural insulation features after treatment. According to [44], water-borne preservative-treated wood exhibits better immunity to fires than oil preservative-treated wood. It is also reported that the CCA-treated pole has a less hazardous body-current level resulting from human contact with poles, compared to PCP preservative treatment. The durability of CCA-treated poles displays no significant differences to that of untreated poles after a standard strain mechanical test, for either ground-line strength of stiffness as reported in [45]. Unavoidable soil and water contamination surrounding pole butt due to the presence of toxic chlorinated compounds in the preservative mixtures may become a risk to the environment as well as to those who work close to wooden poles, especially linesman [29]. Therefore, a careful procedure should be taken when dealing with any treated wooden poles. Finally, Table 2.2 shows the current approved treatment practice for hazard class 5 service conditions in Australia where timber is in contact with the ground or fresh water [16].

Treatment	**Species**	**Preservative level**
CCA **(% copper + % chromium + % arsenic)**	Softwood Hardwood	1.00 % 1.20 %
Creosote (% creosote)	Softwood Hardwood	24.50 % 13.00 %

Table 2.2: Specification for preservative treatment of timber [16]

Thermal treatment of wooden pole without the addition of any toxic chemicals is reported in [46]. This environmentally-friendly method improves the resistance to wood decay, increases the dimensional stability and darkens the colour of wood. However, a slight decrease in the flexibility of the wooden pole with increasing temperatures has been observed when it is used in contact with the ground. The study showed that large cracks were observed on existing cracks which were created during the 180-215^{o}C drying periods. Preliminary results demonstrated that the poles could be used only by bucket truck linesmen and were not suitable for climbing purposes. A standard international practice for preservation of wooden poles in distribution and transmission lines has been published and it provides a basic guideline for all engineers as to what is necessary for specific needs [47].

2.4 Failure of Wooden Poles

The proper management of wooden pole structures in distribution and transmission lines could minimize any mechanical and electrical failures [48–53]. Wooden pole management, including combinations of conventional and advance inspections, pole reliability assessments from structural analysis, and action incorporating replacements, rehabilitations or maintenances has significant economic considerations. Instances of wooden pole external decay, such as cracks, holes or corrosions are assessed by regular visual inspection and internal rot is usually detected through hammer tests, drilling or with non-destructive testing methods (sonic vibration, ultrasonic sound, infrared camera) [54–68]. With extreme weather conditions, such as ice loading, wind gust and hot spells, an efficient structural assessment study plays an important role in improving the reliability of distribution and transmission lines. Then cable clashing due to support failure and icing problems, and pole foundation failure caused by strong winds or even unexpected bushfires during hot conditions could be avoided. Therefore, well organized maintenance and rehabilitation programs will improve the pole aging in service and effective replacement plans could save millions of dollars per year based on efficient management decisions [69–78].

On the other hand, the insulation strength of wooden poles becomes a major concern in transmission and distribution lines. As reported in [41], a typical dry wooden pole has 10^{17}-10^{18} ohm-cm resistivity which represents great insulator properties. However the resistivity of wooden poles drops dramatically to 10^{8}-10^{9} ohm-cm and 10^{5}-10^{6} ohm-cm as moisture content increases to 12% at the fiber saturation point. On top of that, the resistivity changes of water-based and oil-based/borne treated wooden poles have much less effect compared to the changes caused by moisture content [17, 44]. For example, untreated, PCP-treated and CCA-treated poles have almost similar resistivity magnitude at 14% of moisture content, but it changes dramatically as moisture level increases. Thus, these become a great challenge when dealing with high voltage phenomena such as switching impulse, lightning impulse and leakage current effects.

Lightning strikes often occur during thunderstorms, a rare problem for wooden poles. However, a direct and indirect strike of lightning can cause major mechanical damage such as pole splitting, conductor damage, flashovers between line phases and pole-mounted equipment (at the insulators and transformers) and, even worse, can cause injury or loss of human life [28, 41, 79]. Therefore, for this uncontrollable phenomenon, action has been taken to overcome the faulty conditions within the budgetary limit of available techniques. For example, arc gaps, surge arresters and overhead earthwires have been installed on wooden pole structures along with earthing rod to protect overhead lines, transmission lines

Figure 2.2: Pole destruction by lightning strike [6]

and substations that are based on protection strategies [80–84]. At the end, the proposed schemes should minimize the risk of lightning strike to public safety, electricity supply interruption and also to the loss of economic value. Similar to lightning strike protection, an identical strategy is used to overcome the switching impulse issue with the same implementation but different specifications [85, 86].

The natural shrinkage and cracking of the wood due to natural aging of wooden pole may cause loosening of metal to wood connection that will allow a spark discharge inside the bolt hole [41, 87]. With sufficient leakage current magnitude and extra air supply provided by wind, the hole becomes more readily ignitable than sound wood. The leakage current is thought to be finally concentrated in a small zone in the volume of wood under the bolt washer. It is believed the heat generated (i^2R) together with an incident spark discharge is sufficient to ignite the wood. Finally, the pole-top fire issue will be discussed in detail in the next section. This includes causes of pole-top fire, types of damage, the possible trigger of leakage current, current mitigation techniques and also the wooden pole modeling .

2.5 Pole-Top Fire

Unexpected and unplanned power outages can happen at any time in the short or long term and are able to affect tens of thousands of electricity customers. One reason for power disturbances caused by the damaging of wooden pole structures in the transmission and distribution system is pole-top fire. Wooden pole structure failure could lead to phase-to-phase or phase-to-ground faults. In the worst case, this scenario tends to initiate bushfire by the triggered electrical spark between fallen live wires and dry vegetation such as leaves, grasses or bushes.

The causes of pole-top fire have been attributed to several factors. Pole-top fire may be caused by the effect of capacitive coupling or high electric field intensities between pole and phase wires or in the high voltage transmission system. On the other hand, flows of leakage current over the failed insulators from phase wires to the wooden pole structure can become another cause of pole-top burning especially at the metal insertion sections such as king bolt, bolt and insulator pins. Therefore a lot of essential work has been reported in the last few decades that relates to pole-top fire investigations [12, 41, 44, 80, 87–99].

Johnson and Walraven investigated the unexplained fire phenomenon that occurred across 160 miles of 345 kV H frame transmission wooden poles [88]. During a climbing inspection, they found 60 burn areas in sizes from 1 inch diameter and 1 inch deep to 6 ft long, 6 inch wide, and 2 inches deep along ground wires in

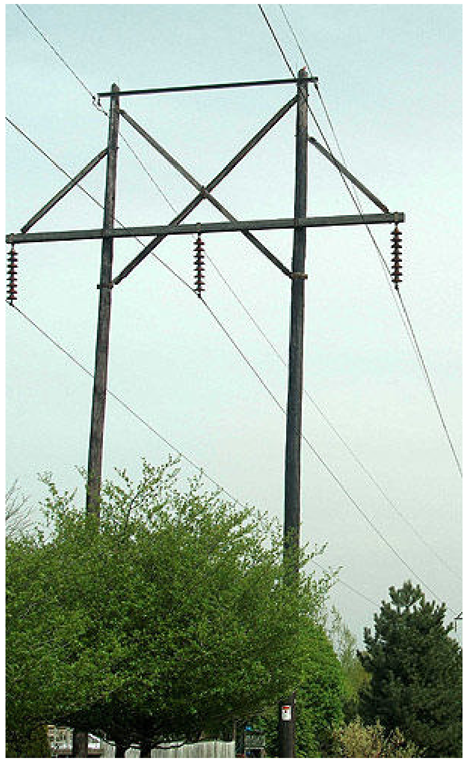

Figure 2.3: Typical H-frame wooden pole structure in transmission lines [7]

an area 10 ft above to 10 ft below levels of the bundles of phase wire. The five possible mechanisms, such as heating due to dielectric losses, inductive ferromagnetic heating, heating by leakage current, electromechanical heating and heating by discharge current were investigated. The results of this intensive study states that the high intensity of electric fields between earthing wire fasteners/clips and high-voltage phase wire caused dielectric losses inside the wooden pole and slowly triggered a fire. As a result, a small modification was made on the 345kV H frame, especially at the earthing wire fasteners by re-clipping it with a stainless steel type, increasing the distance between fasteners and also bonding the pole-top brace hardware with earthing wire. The success of this protective adaptation will only be proven after a few years in service with regular climbing inspections by experienced operators. However, there is no subsequent report based on their work.

Lusk and Mak found that fires in the H frame of wooden high voltage transmission line towers were attributable to surface leakage current or lightning strike [89]. The excessive internal Joule (i^2R) losses in wooden poles at the metal insertion point were identified as a main cause associated with the existence of capacitive coupling and high electric field intensities between pole and phase wires. The Joule loss depends on the electrical conductivity of wooden pole that relies on the current moisture content and magnitude of the charging current due to capacitive and electric field effects. In the above study, the metal fasteners that were nailed into the wood and held the pole earthing wire on the pole surface became current collecting points or current burden drainage points, especially during wet conditions. Two laboratory tests were run to validate the hypothesis of current discharge and the constricted drain of the induced charge. As a result, they proposed adding more metal fasteners on a single earthing wire to reduce the per fastener current drainage burden. Thus, they hope to provide an extra effect of the Faraday shield that tend to reduce the total capacitive coupling and high electric field passing through the wood.

Leakage current flow over the surface of contaminated insulators may cause the wood to burn, especially at the medium voltage line in the overhead distribution system. Ross found that during prolonged dry periods, contamination accumulates on the insulator surfaces and, if followed by fog, rain mist or snow, reduces the surface resistance and allows leakage current flow [12, 90]. Two types of burn damage, tree burning and pocket burning, often occur on wooden pole structures. Both types of burning depends on leakage current magnitudes and voltage dropped across the uneven wet wooden surfaces. The tree burning type, which is more common than pocket burning, has a tree-like burn pattern on the pole surface and usually the replacement of wooden pole structure member is unnecessary. However, the pocket burning always extends into the wooden pole body and occurs only if a small portion of the pole is dry. Light winds create a dampening condition on the pole and insulator surfaces and produce a"shadow" area. The high resistance of the shadow area in series with low leakage current resistance causes a concentration of voltage across the dry area. A fire will be triggered if the voltage drop is sufficient and causes a short electrical breakdown across the dry zone. The replacement of the wooden pole structure member is needed in this instance. Figure 2.4 shows the failure of the wooden cross-arm due to pole-top fire.

Figure 2.4: Pole-top fire event in Southmoor distribution line [8]

Under controlled conditions in the laboratory, a study of the various factors contributing to pole burning was made to evaluate the importance of the different variables and to develop means of prevention [91]. The tests were set up with several insulators and pin types by using methods of artificial contamination and fogging. Pole fire was produced under dirty and foggy conditions, resulting in burning similar to that which has been observed in the field during laboratory testing. It was concluded that pole fires cannot be attributed to any single factor, but are the result of a combination of several factors to be fulfilled simultaneously such as leakage current, overall surface resistances, light wind and moisture. For instance, localized Ohmic heating (I^2R) on the wooden pole dry-band surfaces will accelerate the fire initiation and then can cause wood burning. According to this study, pole fires are most likely to occur at the joint between the pole and cross-arm junction. Based on the results of a potential distribution graph, nearly 50% of the voltage gain occurred in this small section compared to the whole test circuit. The wood in the region understudy was relatively dry so the prime requisites for arc and fuel were present. Finally, pocket burning or"pocket fire" occurred where there was smouldering without an open flame as a result of a deep "pocket" burned inside the wood.

2.5.1 Effect of Leakage Current

A few studies were carried out by [44, 93–95, 98] about leakage current magnitude related to pole-top fire. Based on a laboratory study, Chen and Chang reported that the overall leakage current was below 1 mA under severe artificial pollution of the insulator surfaces [94]. However, a leakage current measuring more than 4.4 mA on testing equipment was recorded during wet conditions. Similar to [93], it was found that a current of 5 mA is sufficient to ignite wood and 1 mA to sustain the ignition. Loxton et al. in [98] also supported these findings by concluding from their laboratory work that miliamperes of current magnitudes are needed to cause the ignition of wood. In [44], Filter referred to this current as the fire inception current. Depending on the age profile of the woods and insulator contamination levels, the current could vary between microamperes to miliamperes [95]. Based on their observations, in some instances, wood smouldering was noticed at the heated king bolt that was connected into the wooden pole and cross-arm during the test. Finally, the type of preservative treatments may have affected the overall leakage current magnitude from the top to the bottom of the wooden pole as reported in [44]. Laboratory tests indicated that for poles treated with water-borne preservative, such as Ammonia Copper Arsenate (ACA) and CCA, fire inception currents are two to three times greater than pentachlorophenol-treated poles. During foul weather conditions and as the result of polluted insulators, 4 mA to 6 mA leakage currents were deemed possible for poles treated with water-borne preservative.

2.5.2 Current Pole-Top Fire Mitigation Techniques

In the past, several pole fire mitigation techniques were proposed for the electrical distribution network. Table 2.3 summarizes the practice that has been employed over the last few decades in order to eliminate pole-top fire risk. Line insulator washing has been part of a live-line maintenance operation especially for those areas where pollution was very high, such as coastal areas, desert regions and others [100]. A helicopter fitted with a water tank and spraying nozzle has been used for those difficult access areas to clean and tidy up polluted insulator surfaces with high-pressure water under a strict practices code [101]. On the other hand, a crane operated by several washer crews has been used for easily accessible areas. Usually, silicone coating was applied onto insulator surfaces after the washing process had finished. This method managed to break up water film and encapsulate particles so that they worked effectively and did not cause flashovers and leakage current flow when wet [102]. The main drawback has been that this silicone compound needs to be removed and cleaned up from the insulator surfaces after a few years in service. Besides that, insulator washing has not been very useful in environments exposed to polluting conductive mist conditions, such as marine salt fogs. Figure 2.5 depicts the application of silicone coatings on pole-top insulators by line operators.

Replacing or upgrading insulators and cross-arms has become a common option for the electricity distribution company to improve their operation reliability. For example, adding a creepages extender is able to upgrade the electrical strength of insulators and reduce the leakage current and electrical stress, even without coating [108]. Replacing insulators and cross-arms with better material and design can improve the mechanical strength and pollution classification from a light to a heavy

Figure 2.5: Operator spraying silicone compound on pole-top insulators [9]

Existing Technology	Features	Drawbacks
Regular/periodic insulator washing [100–103]	-uses high water pressure to clean up surface of insulator.	-sometimes does not cover every surface of insulator. -needs regular washing. -costly.
Silicone Coating [102, 104–107]	-sprays a silicone coating onto insulators surface after line wash process. - silicone coating acts like gel absorbing dust, moisture and pollution.	-after lines are washed, silicone coating is sprayed onto insulators using gun attached to compressor pump. -silicone then acts like gel absorbing moisture, dust and pollution. -need to clean up insulator after several years in service. -costly.
Replacing or Upgrading insulator [94, 108, 109]	-adds plastic hood or protective creep-age on top of insulator. -uses better insulator to reduce risk of leakage current such as hybrid insulator.	-costly. -require line to be de-energized during replacement.
Steel/Fibre Cross-Arm [9, 110]	-changes/replaces wooden cross-arm to steel or fibre glass type.	-line de-energized during cross-arm replacement. -over years, surface of fibre glass/steel becomes contaminated with dust. -costly.
Leakage Current Monitoring [111–114]	-online monitoring of leakage current.	-very costly as many monitoring units are required to be installed along the power lines.
Pole Bonding [10–12, 80, 87, 90, 98, 99]	-attaches conductive material plates that have integral punched out teeth that acts as current collector and shunts leakage current at wooden pole and cross-arm junction.	-nailed/punched effect onto wooden pole allows another leakage current concentration point.
Line Pole Grounding [93, 115–118]	-shunts leakage current to ground.	-reduce basic impulse level of the wooden pole. -earthing rod needed for this configuration and it's very costly.

Table 2.3: Current methods to reduce pole-top fire risk

pollution category [9, 109, 110]. The disadvantage has been that the line needs to be de-energised during the replacement operation and this procedure is very costly. It has been reported in [119], that a budget of about AUD 10-15 million was estimated for the replacement process cost of the thousands of wooden cross-arms on rural Victorian power poles. Replacement of all cross-arms with steel or fibre glass may reduce the pole-fire risk, but cannot prevent insulator failure.

An online monitoring system which detects leakage current and partial discharge activities on an insulator surface has been discussed in [111–114]. This system comprises of: a sensor unit attached at the last shed of the insulator or at the insulator pin; signal conditioning and data acquisition for detecting, processing and transmitting monitored leakage current; and finally a protection system installed to avoid the risk of any voltage spikes to the electronic systems. According to Metwally et al. in [113], pole fire normally occurs at the weakest point along an axial point length, where there are one or more deep cracks and current entry and exit points on the pole. The leakage current monitoring system or Pollution Monitoring System can be used as a good warning in order to predict a pole-fire event. Therefore, an optimal precaution action can be taken, such as live-line washing or replacement of defective insulators at the appropriate time. However, due to the total cost and complexity of this system, it presents a great challenge for distribution and transmission companies to invest in this technology.

The main purpose of the pole bonding is to eliminate the voltage stress between uneven wet surfaces across wooden pole structures, especially at the king bolt sections. Therefore a conductive copper plate has been used and stapled across the cross-arm surfaces and connected to the king bolts in many configurations to overcome the pole fire problem [12, 87, 90]. In another configuration, a copper plate with integral punch-out teeth was bonded to the cross-arm or wooden pole

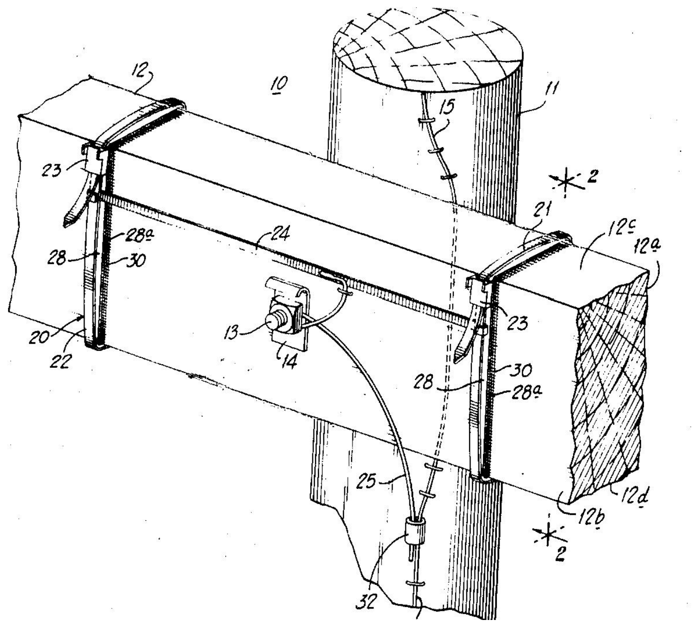

Figure 2.6: Pole bonding configuration [10]

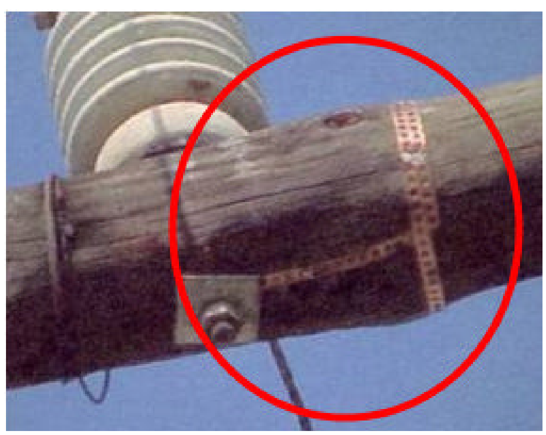

Figure 2.7: Application of pole bonding to the cross-arm [11]

surface in order to decrease current concentration at the king bolt section [10, 11, 80, 98, 99]. However, with time, the wires, plates or other bonding elements tended to become loose due to shrinkage of the wood as it was exposed to the elements over a number of years. It was found that this loosening of the staples or teethed copper plates in conjunction with wood shrinkage substantially worsened the already poor electrical contact between the conductive bonding elements and the wood surfaces it was desired to protect. It has also been proven in [120] that the pole-bonding method caused leakage current concentration at the king bolt junction due to the bonding arrangement.

Finally, line pole grounding has become a current popular method to overcome the pole-top fire problem [93, 115–118]. Based on this technique, all the secured metals such as the king bolts, insulator pins and bolts that hold the steel holders were shunted through grounding cables to the earthing rod. Thus, any leakage current flow phenomena that was caused by failed insulators was diverted to the ground. However, it involved a lot of investment, especially for the earthing rod expenses and installation costs. It also reduced the overall basic impulse level of the wooden pole structure in which the grounding wire arrangement eliminated the natural insulation that was provided by the wooden pole. Even with line pole grounding installed and in service, a pole-top fire was reported in the Northern Beaches area in Sydney [121].

2.6 Wooden Pole Models

Technically, the wooden pole can be represented as an electrical resistances model [41, 122–125], a thermal model [66, 67, 126] and a finite element model [127–131]. Depending on the purpose of the research, the model of the wooden pole is based either on whole pole measurements, laboratory studies such as wood stakes or computer simulation works, especially in the thermal and finite element models. Whole pole evaluations techniques are based on on-site, full-length resistance measurements of the wooden pole structure by inserting electrode rods at the top and bottom sections [122–124]. This on-site assessment provides practical electrical test data of the in-service wooden poles. However, to generalize wooden pole electrical resistance is difficult due to the contact resistance, moisture content, treatment gradient and pole dimension factors. Therefore, intensive examinations of each type of treatment and pole species are needed for many other in-service wooden poles.

Conversely, wood stake studies were established by examining, under controlled laboratory conditions, the resistivity of a uniform wood stake undergoing various wood moisture levels, type of treatments and species effects [41, 125]. However, such studies ignored real service conditions such as weather factors, that can affect the wood properties. Therefore, an ideal wood electric property was presented but did not describe a precise full-length wooden pole characteristic due to the internal complexities of a wooden pole.

The thermal model of a wooden pole involves solving the equation formulated by Fourier with a partial differential solver and a finite element method [66, 67]. In this study, internal through hole, external and microwave heating types were investigated with MATLAB simulations for wooden pole inspection purposes. Due to the large defect depths, low wood thermal diffusivity, and the wood dependencies upon temperature, moisture, species and fiber orientation, an infrared camera was used to detect defect types that were close to the wood surface. Meanwhile, Younsi et al. used a diffusion equation with variables diffusion coefficients, and the incompressible Reynolds averaged Navier-Stokes equation for cases of high thermal treatment of wooden poles with a three-dimensional numerical simulation [126]. Based on the above study, the proposed numerical algorithms were useful for designing high-temperature wood treatment processes. The effects of initial moisture content, wood aspect ratio and final gas temperature on temperature and moisture content distribution were determined and included in this study.

In [127–129], a three-dimensional finite element of the wooden pole model was developed for stress distribution prediction purposes. The developed model was used to measure and predict the mechanical strength and failure location in full-size wooden poles. This research dealt with the enhancement of the laminar fluid flow program to quantify the effect of knots and their associated cross grains on the stress distribution of wooden poles. The study results demonstrated good similarity between theoretical and numerically predicted pole stresses. Therefore, this technique could be used as a part of non-destructive testing for improving visual grading methods for wooden poles.

In summary, the thermal and finite element models offer many advantages in terms of wooden pole inspections and assessments. However, whole pole evaluation and the wood stakes method will provide better platforms for electrical study, especially for basic insulation level and leakage current studies on the wooden pole structure. For example, an impedance model was proposed by Rathsman et al. for a wood-insulator combination subjected to a lightning impulse [132]. On the other hand, Filter and Mintz combined whole pole evaluation and wood stake approaches to determine an accurate wooden pole model for leakage current effect on the human body [17]. The integrated knowledge of these two methods allowed them to overcome all the limitations, such as variety of pole species, wood treatment and weather conditions and to develop a computer-based electrical equivalent circuit of a wooden pole. This improved model was termed the ‘ladder network model’. This ladder network model offers great simplicity and with a small modification, it is suitable for explaining pole-top fire events [120, 133].

All the above studies were based on experimental laboratory work and computer simulation studies. In particular, the leakage current became main mechanism causing the pocket-burning or tree-burning events on the wooden pole structure, especially for medium-voltage power lines. In addition, the capacitive coupling effect was able to be used to explain the pole-top fire events along high voltage transmission systems. However, none of those previous studies were established on the ladder network model of the wooden pole developed by Filter in [17]. Therefore, this study provides the starting point and offers an opportunity to begin investigation founded on a computer model for further understanding of the wooden pole-top fire. The computer simulation of a wooden pole model could provide another angle for an explanation of pole-top fire. The great advantage is that the ladder network model of the wooden pole can be manipulated for other purposes, especially for pole-top fire mitigation studies. In particular, this is the first pole-top fire study which based on wooden pole ladder network model.

In conclusion, power utility companies already spend a lot of money executing these mitigation techniques specifically to overcome the pole-top fire issue. On top of that, the outcomes are not convincing and pole-top fires are still occurring and reported. Weather factors such as humidity, rain, dust and wind play an important role in the surface contamination of insulators; this is understandable and beyond our control. However, if the flow of leakage current along the pole structure can be diverted properly away from the current concentration spots, such as king bolt and pin insulator sections, then the risk of wood fire igniting can be reduced significantly. It will be seen that the contribution of the wooden pole ladder network model study is able to easily solve this difficult challenge. As a result, all the disadvantages of current practices can be overcome with the so-called mid-pole bonding system. Theoretically, this new mitigation method can be retrofitted to any pole structure configuration and will be relatively cheap. A further description, the method of implementation and the successfulness of this method are presented in Chapters 3, 4 and 5 in detail.

Chapter 3

Study of Leakage Current Effect using Ladder Network Model

3.1 Introduction

Wooden poles are commonly used to support overhead power lines in electricity distribution networks. Wooden poles have become a highly popular support structure around the world in the last few decades due to the ease of supply and cost-effectiveness. There are more than 5 million wooden poles currently in service all around Australia's distribution network and up to 70% were installed more than 20 years ago. Based on economic figures, millions of dollars of capital expenditure is needed for pole replacement over the next decade [14]. Typically, the life expectancy of a wooden pole is within the range of 30 to 40 years. It's reported that the annual wooden pole failures in the Western Australian network are between 1.88 and 4.34 pole failures per year per 10 000, in comparison with the industry target of 1 pole failure per year per 10 000 poles [134]. Therefore, it is really important to maintain continuous research into wooden pole performance to improve their reliability in service.

Pole-top fire is a wood-structure burning phenomenon and usually it happens at the mounted cross-arm region, especially at the metal insertion sections. Commonly pole-top fires are related to insulator failure that allows an excessive amount of current flow from the live conductors. Under severe conditions, it causes power lines to collapse, power breakdowns and the conductor to hang down. As a result, this falling conductor could trigger a spark when it touches dry vegetation and start a flame leading to unwanted bushfire.

In a previous chapter, a detailed study relating to pole-top fire has been discussed. A new insight into the leakage current distribution along wooden pole structures using the ladder network model is presented in the next section. This model takes into consideration species effect and treatment variation, pole dimension, moisture gradient, and weather effects such as rain. It also describes the ladder network modelling, including environmental simulation and other assumptions. The results in this chapter will help us to find a new solution in eliminating the occurrence of pole fire. This work will highlight the important fact that a complete wooden pole should be adopted in leakage current studies since the leakage current is a function of line voltage and the total resistance consists of insulator resistance and wood resistance, as depicted in Figure 3.1. Finally, a new finding based on an intensive simulation study is presented in the last section of this chapter.

3.2 Wooden Pole Modeling based on Ladder Network

The principal objective of the ladder network model development was to determine the hazard of leakage current on humans under a variety of operations and fault

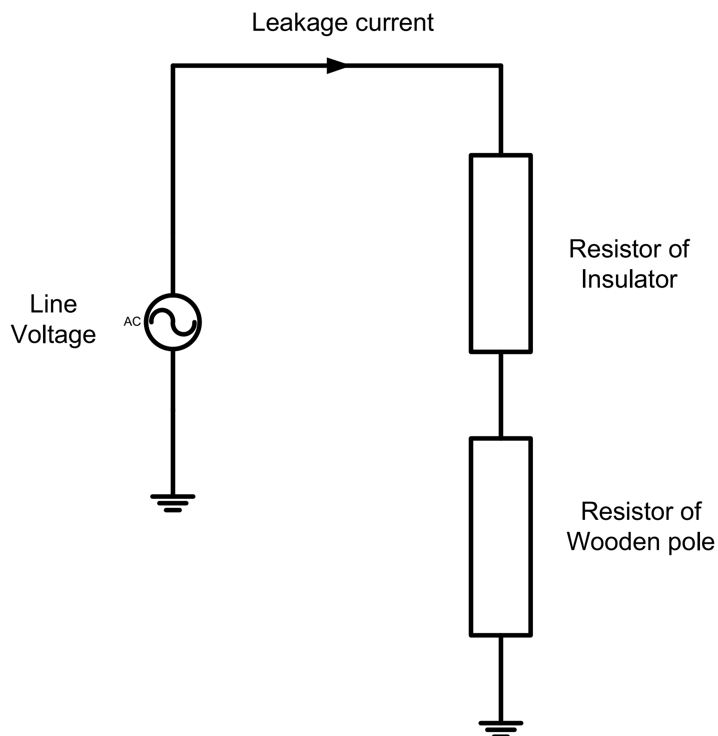

Figure 3.1: A complete leakage current model

conditions resulting from contact at the wooden pole structure. It also focussed on the feasibility of using the electrical properties of wooden poles as diagnostic aids to allow simple and reliable assessment of internal rot. Based on laboratory and field measurements, a wood pole equivalent circuit was developed accounting for wood species, treatment types and weather conditions [135].

The ladder network model consists of three wood resistances i.e. sapwood resistance $\mathbf{R}_s$, heartwood resistance $\mathbf{R}_h$ and radial resistance $\mathbf{R}_r$ as shown in Figure 3.2. The model provides possible connection points for other resistances representing pole hardware, cross arm or metal insertions. Rain resistance can be added to the model using suitable external bridging resistors, $\mathbf{R}_w$ connected between the nodes along the pole length.. The resistances in this model are determined by pole

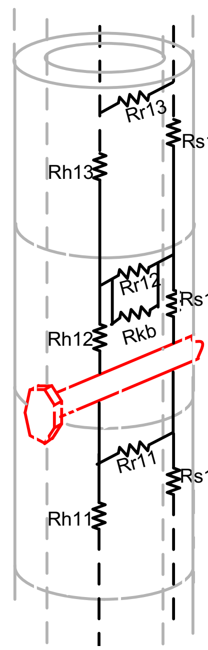

Figure 3.2: Resistance of wooden pole with king bolt insertion

species, type of preservative treatment and moisture content percentage **(MC)%** of the pole. The relationships between wood resistivity ρ, moisture content and type of treatment can be expressed in the form of equations (3.1).

$$\text{Untreated wood} \qquad \rho = 10^{(-0.137(MC\%)+7.27)}\Omega - m \tag{3.1a}$$

$$\text{Penta treated wood} \qquad \rho = 10^{(-0.135(MC\%)+7.36)}\Omega - m \tag{3.1b}$$

$$\text{CCA treated wood} \qquad \rho = 10^{(-0.250(MC\%)+9.12)}\Omega - m \tag{3.1c}$$

$$\text{ACA treated wood} \qquad \rho = 10^{(-0.303(MC\%)+9.51)}\Omega - m \tag{3.1d}$$

In general, these three resistance components are interconnected in the ladder network which can be determined from the equation (3.2) based on wood resistivity ρ, pole length ℓ and cross-sectional area of wood modeled $\mathbf{A}$. The resistances for

$\mathbf{R}_s$ and $\mathbf{R}_h$ are dependent on the wooden pole radius, $\mathbf{R}$ and the heartwood depth $\mathbf{P}$, as shown in (3.3) and (3.4). The scaling factor 1.83 is applied for the $\mathbf{R}_r$ reflected to the $\mathbf{R}_s$ according to Darveniza in [135] and moisture content is limited to no more than 30% for $\mathbf{R}_s$ as shown in Table 3.1. As a result of ground moisture wicking into the pole, first meter of the pole above the ground line has high moisture content. Therefore, bottom section of wooden pole (up to 1.5 meter) contain greater amount of water. However, the top pole is exposed more too drying influence of the air and sun light, the moisture content in the top meter of the pole substantially reduced form value measured near the middle height [17].

$$R = \frac{\rho \ell}{A} \tag{3.2}$$

$$R_h = \frac{\rho \ell}{\pi (R - P)^2} \tag{3.3}$$

$$R_s = \frac{\rho \ell}{2\pi P (R - P)} \tag{3.4}$$

$$R_r = 1.83 R_s \tag{3.5}$$

For the ladder network model, we selected 0.75 meter steps will provide details leakage current distribution along wooden pole structure and suitable section

	Moisture Content in	
Location on Pole	Sapwood	Heartwood
Top 1.5 meter	(MC)%	(MC + 5)%
Central Portions	(MC)%	(MC + 9)%
Bottom (0.75 - 1.5)meter	(MC + 5)%	((MC/2 + 19.5)%
Bottom (0.00 - 0.75)meter	(MC + 5)%	30%

Table 3.1: Pole model moisture gradient relative to sapwood and heartwood along wooden pole [17]

length especially for the extended ladder network model (with cross-arm). Thus, a 12-meter pole is represented by a 16-step model. This step size is sufficient to describe the behaviour at the bottom, middle and top sections of the pole during the simulation study. Section 1 represents the section closest to ground and section 16 is the highest section above ground, as shown in Figure 3.3. In our simulations, we selected a typical 12-meter red-pine pole height without cross-arm configuration. The top and bottom radius is 11 cm and 18 cm respectively and the top and bottom heartwood radius is 8.15 cm and 14.2 cm with 0.75 meter steps; the pole was assumed to be treated with CCA. As depicted in Figure 3.3, a king bolt of 2 $\mu\Omega$ resistance was installed at section 12. The magnitude of leakage current depended on the degree of insulator contamination and the overall pole resistance. Conductor resistance $\mathbf{R}_c$ and rain resistance $\mathbf{R}_w$ effect were not included in this study.

3.3 Leakage Current Effect using Ladder Network Model

In this section, the discussion is focussed on how to draw out all the important and significant information from the electrical ladder network model. The computer simulations for the leakage current study are based on MATLAB software environment for this research. The whole 16 wooden pole sections have been established by using the SimPowerSystem toolbox to build the electrical ladder network model. Section 1 represents the closest section to the ground and section 16 is the highest section above the ground, as shown in Figure 3.3. The 1 MΩ insulator resistor has been used to create the leakage current flow at a certain level from the 11 kV line voltage source with the overall resistances of the ladder network. Based on the simulation study, the resistances and leakage current information

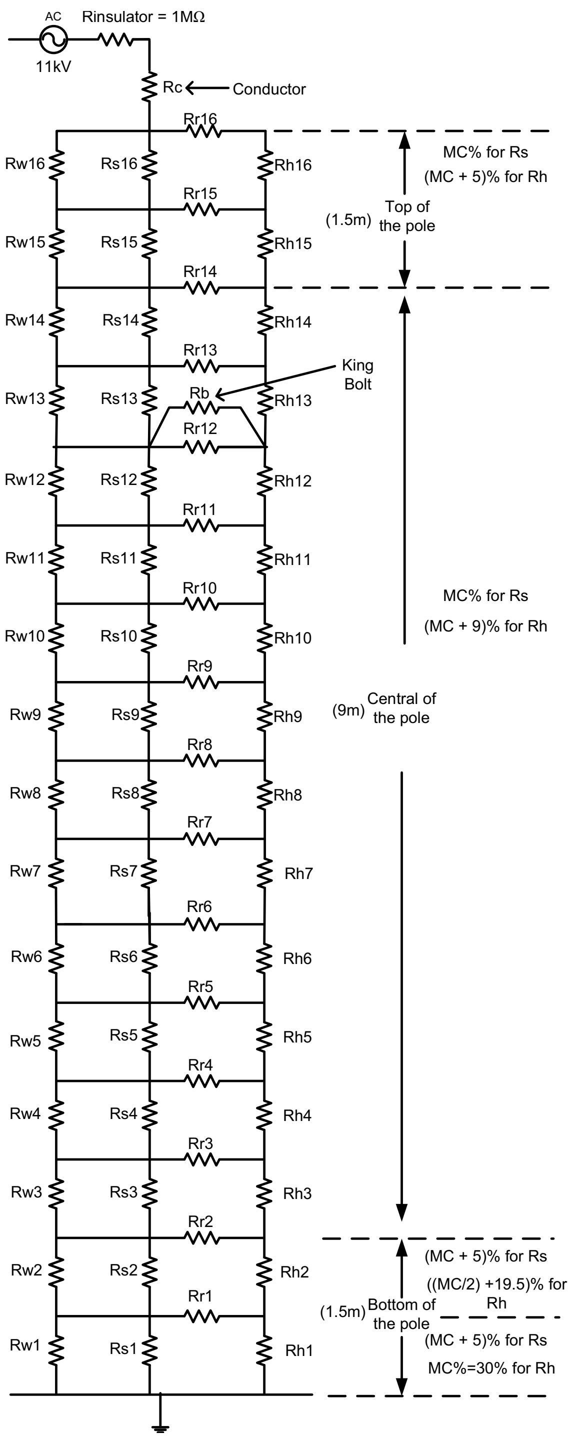

Figure 3.3: Wooden pole ladder network model

from the radial, heartwood and sapwood are presented and discussed. The effect of metal insertion in the wooden pole structure is included in this study, located at section 12. Finally, the modelled simulations have been run under dry (11.7% MC) and wet (22.7% MC) conditions to demonstrate the different weather effects which appropriate for the Australian weather condition [136–138]. Table 3.2 and 3.3 summarizes the resistances magnitude for both dry and wet poles. Detailed information can be referred to in Appendix A.

3.3.1 Pole Resistance

The pole resistances at each section of the ladder network model have been studied. Each pole section consists of sapwood, heartwood and radial resistances. Based on the proposed ladder network model, Figure 3.4 and Figure 3.5 depicts the value of the three resistances in dry and wet conditions (11.7% and 22.7% of moisture content). For the dry pole study, the heartwood, sapwood and radial resistances, located at section 16 (the highest section above ground) were 2.89 MΩ, 74.91 MΩ

Section	**Height (m)**	$\mathbf{R}_s$ (Ω)	$\mathbf{R}_h$ (Ω)	$\mathbf{R}_r$ (Ω)
1	0.00 to 0.75	1.87 MΩ	493.55 Ω	3.43 MΩ
2	0.75 to 1.50	1.96 MΩ	7.57 kΩ	3.58 MΩ
3	1.50 to 2.25	36.42 MΩ	116.44 kΩ	66.66 MΩ
4	2.25 to 3.00	38.18 MΩ	123.31 kΩ	69.88MΩ
5	3.00 to 3.75	40.15 MΩ	130.61 kΩ	73.48 MΩ
6	3.75 to 4.50	42.20 MΩ	138.80 kΩ	77.22 MΩ
7	4.50 to 5.25	44.40 MΩ	147.78 kΩ	81.26 MΩ
8	5.25 to 6.00	46.66 MΩ	157.66 kΩ	85.39 MΩ
9	6.00 to 6.75	49.24 MΩ	168.57 kΩ	90.11 MΩ
10	6.75 to 7.50	51.89 MΩ	180.66 kΩ	94.96 MΩ
11	7.50 to 8.25	55.05 MΩ	193.72 kΩ	100.75 MΩ
12	8.25 to 9.00	58.39 MΩ	208.66 kΩ	106.85 MΩ
13	9.00 to 9.75	62.05 MΩ	225.40 kΩ	113.55 MΩ
14	9.75 to 10.50	65.85 MΩ	244.23 kΩ	120.52 MΩ
15	10.50 to 11.25	70.43 MΩ	2.64 MΩ	128.89 MΩ
16	11.25 to 12.00	74.91 MΩ	2.89 MΩ	137.09 MΩ

Table 3.2: Resistances of dry pole

Section	Height (m)	$\mathbf{R}_s$ (Ω)	$\mathbf{R}_h$ (Ω)	$\mathbf{R}_r$ (Ω)
1	0.00 to 0.75	3.33 kΩ	493.55 Ω	6.10 kΩ
2	0.75 to 1.50	3.48 kΩ	521.06 Ω	6.38 kΩ
3	1.50 to 2.25	64.77 kΩ	550.95 Ω	118.54 kΩ
4	2.25 to 3.00	67.90 kΩ	583.47 Ω	124.26 kΩ
5	3.00 to 3.75	71.40 kΩ	617.99 Ω	130.67 kΩ
6	3.75 to 4.50	75.04 kΩ	656.74 Ω	137.33 kΩ
7	4.50 to 5.25	78.97 kΩ	699.24 Ω	144.51 kΩ
8	5.25 to 6.00	82.97 kΩ	746.01 Ω	151.85 kΩ
9	6.00 to 6.75	87.56 kΩ	797.63 Ω	160.25 kΩ
10	6.75 to 7.50	92.28 kΩ	854.80 Ω	168.87 kΩ
11	7.50 to 8.25	97.90 kΩ	916.59 Ω	179.16kΩ
12	8.25 to 9.00	103.83 kΩ	987.28 Ω	190.02 kΩ
13	9.00 to 9.75	110.34 kΩ	1.06 kΩ	201.92 kΩ
14	9.75 to 10.50	117.11 kΩ	1.15 kΩ	214.32 kΩ
15	10.50 to 11.25	125.25 kΩ	4.71 kΩ	229.21 kΩ
16	11.25 to 12.00	133.22 kΩ	5.15 kΩ	243.79 kΩ

Table 3.3: Resistances of wet pole

and 137.09 MΩ respectively. The value of the resistance varied as the diameter of the pole increased from the bottom to the top. The linearity between the pole resistance and pole diameter could be clearly seen, particularly from pole section 3 to section 14, where the moisture content remained constant. The effect of the king bolt insertion at section 12 was visible in both Figure 3.4 and Figure 3.5, especially when the wooden pole was subjected to moisture.

The moisture content has a significant role in wooden pole modelling. In accordance with the original model developed by Filter and Mintz [17], the moisture content increases from 9% at the central position to 19.5% at 0.75 m to 1.5 m from the ground and eventually 30% at the section just above the ground. The effect of moisture content can be clearly seen in Figure 3.4. The heartwood section of a wooden pole has the lowest resistance level and this is a result of the higher percentage of moisture content level residing in the heartwood section [135].

When the wooden pole is exposed to rain, the rain effect increases the overall moisture content. In this simulation study, we selected a moisture level of

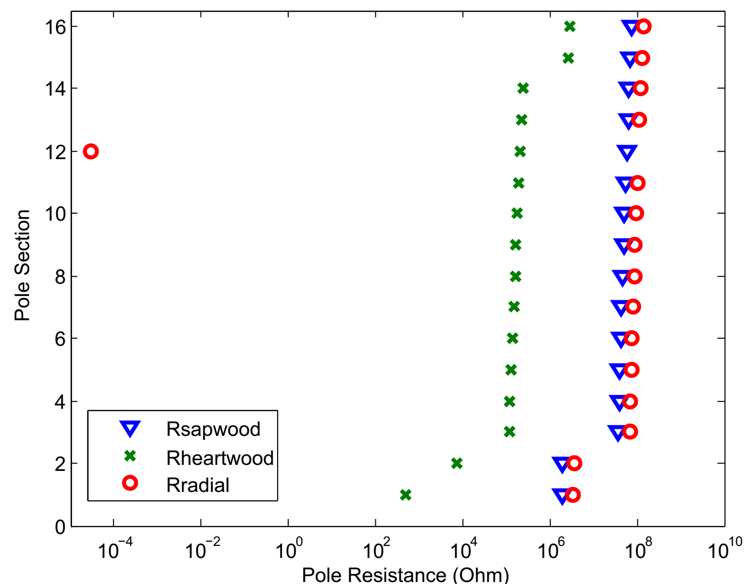

Figure 3.4: Resistance of dry wooden pole

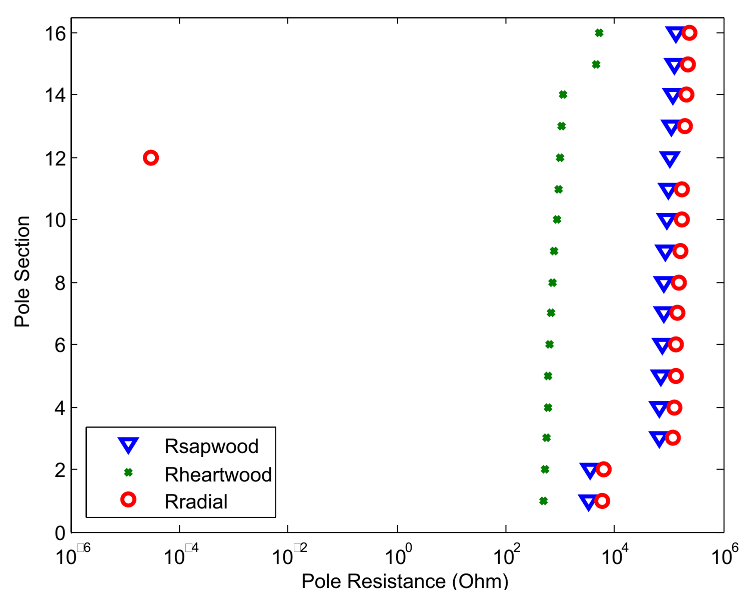

Figure 3.5: Resistance of wet wooden pole

22.7% to represent the wet condition of the pole and the results can be found in Figure 3.5. The moisture content significantly reduces the value of the three resistive components of the wood. In comparison to the values under dry conditions, the heartwood, sapwood and radial resistances at the pole section 16 under wet conditions were now 5.15 kΩ, 133.22 kΩ and 243.79 kΩ respectively.

3.3.2 Current Distribution of Dry and Wet Wooden Pole

In pole fire study, the insight into leakage current distribution across various pole sections is critical. Figure 3.6, Figure 3.7 and Figure 3.8 depict the current distribution for pole sections 1 to 16 under both dry and wet conditions. In dry conditions, the sum of the current across the three resistances was almost zero or negligible. The simulated results show that was the case when the insulation level of the high voltage insulator was reduced significantly due to surface pollution; the high value of the wood's resistance limited the total current flow and the effect of the king bolt insertion at section 12 had minimum effect on the current distribution.

As the moisture level was set to 22.7%, which represented a typical damp condition occurring after rain, the overall leakage current increased to mA range. In the case of sapwood and heartwood resistance, the highest current of 4.9 mA appeared across pole section 16, which is the pole top. Under wet conditions, the effect of the king bolt insertion could be clearly observed. From Figure 3.7, we could see a current “spike” at pole section 12 where the king bolt was located. Other observations included the proportion of current flowing through the heartwood section. These sections carry most of the current through the heartwood section down to the ground. Also, the change in current distribution at the bottom pole section (0 to 1.5 m from the ground) was contributed to by the higher moisture level.

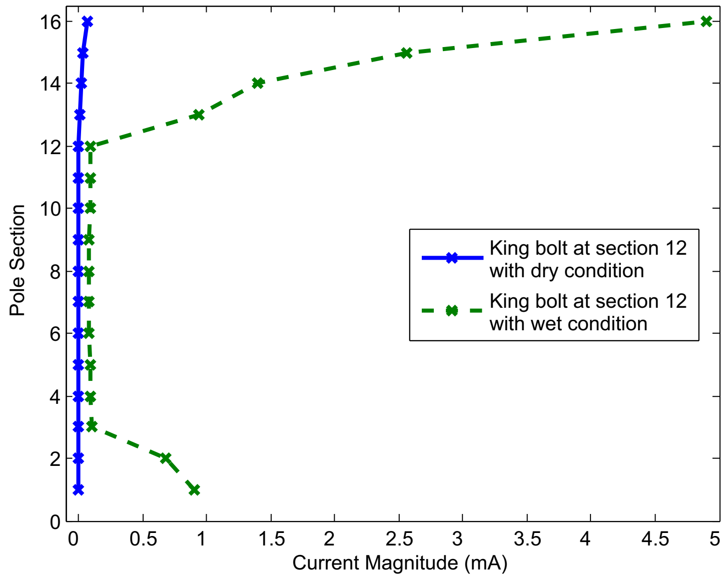

Figure 3.6: Current distribution for sapwood resistance

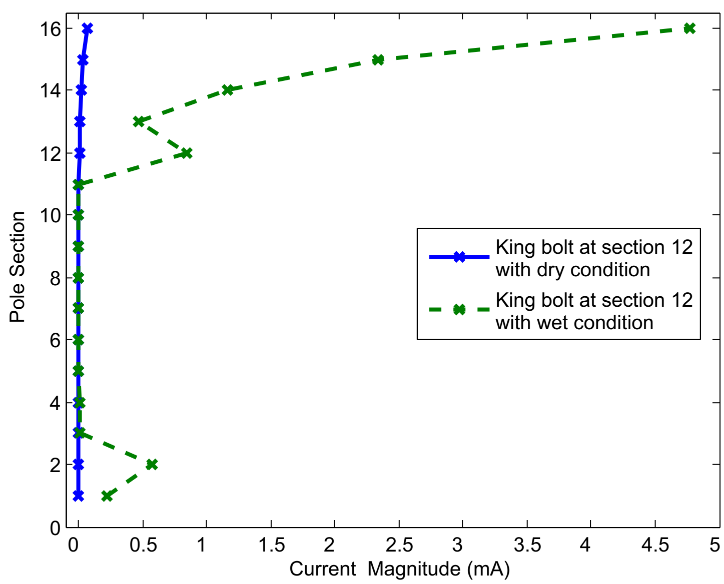

Figure 3.7: Current distribution for radial resistance

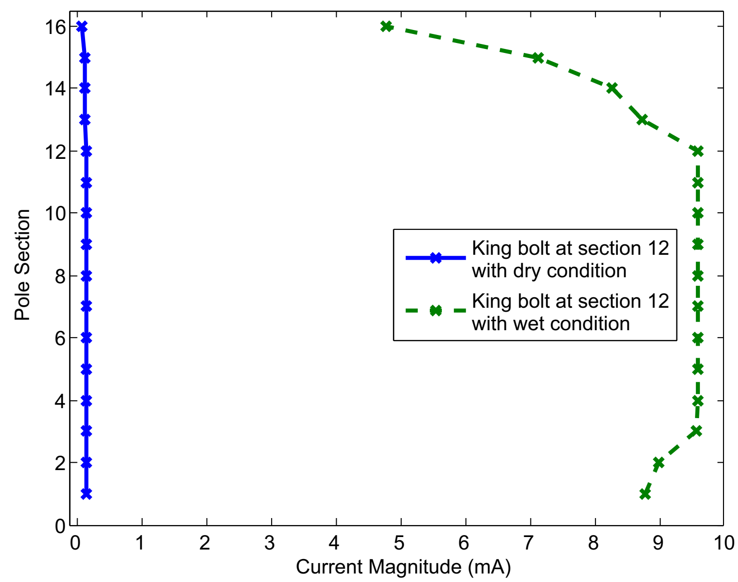

Figure 3.8: Current distribution for heartwood resistance

Leakage current with a value of 9.5 mA was recorded in the center section of the pole.

3.3.3 Radial Current Distribution of Wooden Pole

The damage to wooden poles due to pole fires frequently takes place at the cross-arm junction where the attachment of the king bolt or the insulator's metal support is located. Figure 3.9 depicts a graph of how the metal insertion affects the current flow across the radial resistance. In this simulation, three different scenarios were created: king bolt at pole section 14, pole section 12 and pole section 10. In the first scenario, a current "spike" was created at section 14. The leakage current was increased from 1.7 mA to 3.4 mA at pole section 15. As the king bolt was shifted down to section 12 and 10, the effect became less apparent due to the fact that the leakage dropped to approximately 1 mA at pole section 14 for all three

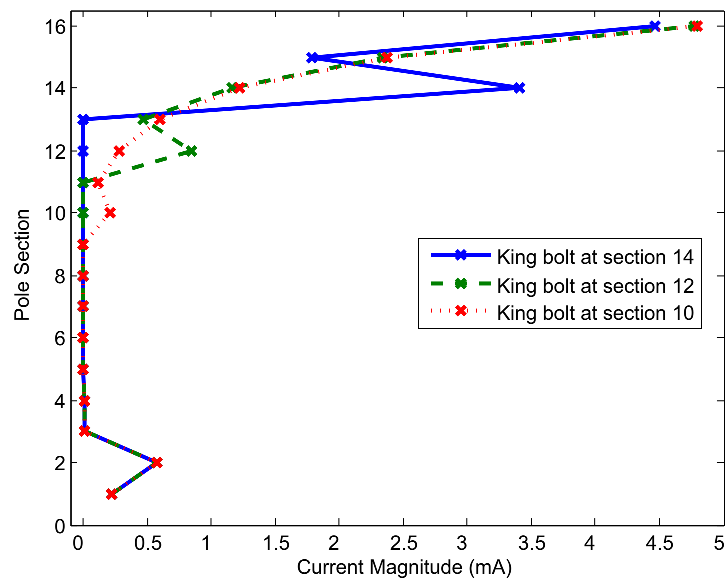

Figure 3.9: Current distribution of wet radial resistance with different locations of king bolt scenarios.

In term of energy or heat that develops along the wooden pole due to leakage current, the combination of sapwood, heartwood and radial current at the king bolt junction will exceed the glow current and fire inception current level as described by R. Filter in [44]. Based on Figure 3.6, 3.7 and 3.8, the leakage current is channeled through the king bolt insertion (at section 12) due to the lower resistance path provided by the king bolt. This effect is similar to the short circuit effect on the electrical network. Based on R. Filter's results [44], glow current as low as 2 mA or 4.3 mA (average) is needed to provide persistent incandescent glow on the CCA treated wooden pole. Fire inception current was observed of 7.3 mA was recorded in his experiments, where sparks, surface tracking, heavy single track and moderate smoke were observed. Similar fire inception current was observed in our experimental results on CCA treated hardwood in Chapter 5 of this thesis.

3.4 Summary

This chapter demonstrates the use of the ladder network model in studying the current distribution in wooden poles. The model in this research was developed based on the physical dimensions of a red pine CCA-treated 12-meter pole. Since the heartwood and sapwood resistances are represented by lump parameters, many different forms of circuit analysis, which cannot be obtained experimentally, were able to be done by using the computer simulation.

Many previous reports describe how the loose metal contact between wood and metal insertion contributes to the occurrence of pole fire [87]. However, the results in Figure 3.7 suggest that higher current concentration occurs at the metal-wood junction, regardless of whether an air gap exists between the wood and the metal. The current concentration, as shown in this figure, were solely due to the reduction in the overall resistance as a result of metal insertion.

The ladder network model also helps to establish an important fact whereby the bulk of leakage current flows under the surface of the wood. The heartwood section carries the bulk current from the top to the bottom of the wooden pole and the king bolt insertions set the upper limits for the amount of the current flow. Furthermore, the impact of the king bolt can be clearly seen when it is located close to the leakage current source; in this case, it occurred due to a polluted insulator. In addition, the introduction of another metal bolt and an additional structure, such as a pole mounted transformer, should be thoroughly analyzed. In conclusion, better pole design that takes into account the current distribution of the sapwood, radial and heartwood resistance could provide an answer to long-standing pole fire problems.

Chapter 4

Proposed Pole-Top Fire Mitigation Technique: Mid-pole Bonding System

4.1 Introduction

In general, a computer simulation is an imitation of a real physical system, phenomenon or process using a special software program package for research study purposes [139]. For example, computer simulation capabilities are being widely used to represent real things such as vehicles, robots or natural systems in order to understand them more easily and then solve or improve any existing problems [140–142]. Thus, a simulation model that is based on practical approximations of and assumptions about the real system can be utilized to gain more understanding of the system model and then manipulated for any purposes. The greatest advantage is that this computer simulation study allows us to see how the model performs by changing any variables or any input, and to obtain outcomes that approximate to the actual system. This simulation study also offers the possibility of carrying out many trial and error experiments and tests, which, in reality, are too costly, dangerous or impractical.

A computer simulation study of the power distribution of wooden pole is really important for a further understanding of pole-top fire events. Based on a computer simulation study of the modeled wooden pole in Chapter 3, radial resistance results yielded significant information in terms of explaining the causes of pole-top fire. The radial current distribution along the modeled wooden pole structure showed current concentration effects, especially at the bolt insertion sections [133, 143]. Further development and manipulation of the current wooden pole model became essential to realize the proposed pole-top fire mitigation techniques. As a result, the completed wooden pole model with cross-arm was constructed based on the original wooden-pole ladder-network model. Then a new mid-pole bonding system was developed to overcome the weakness and disadvantages of the current techniques [120].

The first part of this chapter presents the development of the complete wooden-pole model with wood and steel cross-arm based on the ladder network model [17]. The modified ladder network model can be used to show the metal insertion effect inside the wooden pole structure, based on radial current distribution simulation results. On the other hand, an electrical circuit of existing mitigation techniques has been constructed on the modified wooden pole model and compared with the new proposed mitigation method. A comparative study will be made based on different configurations of these techniques. The performance of the discussed electrical models will be based on how much the leakage current can be reduced, especially at the wooden pole cross-arm junction [133, 143].

4.2 Proposed Mid-Pole Bonding System

In this research, a new cost-effective shunting arrangement is proposed which utilizes 3 insulated cables to bypass the leakage current away from the critical metal-wood junction. Figure 4.1 shows the physical mid-pole bonding system arrangement between a metallic band and leakage current sources with the insulated cables. Figure 4.2 depicts the shunting cables termination configuration from the three insulator pins to the termination point i.e. the metallic band. The greatest advantage of this mid-pole bonding system is that it offers a very simple arrangement with low-cost implementation. In addition, this proposed method can be installed on any kind of pole configuration and retrofitted to wooden pole in service in electrical distribution systems. A further description of the mid-pole bonding system will be presented and discussed in the next section.

4.2.1 System Description

As depicted in Figure 4.3, the metallic band was created purposely as a leakage current termination point for the mid-pole bonding system. 1 mm aluminum was chosen to make this metallic band, due to its flexible character and conductive superiority. Good contact between the aluminum band and pole surfaces allowed more leakage current to be diverted through shunting cables to this termination point. Then this leakage current could flow easily into the wooden pole structure and then to the ground. Table 4.1 summarized the detail dimensions and parameters of the metallic band. The chosen dimensions were enough to secure the metallic band tightly onto the wooden pole. In addition, 3 holes were made on the metallic band and 3 bolts and nuts were used for termination purposes.

In general, aluminum has a higher thermal conductivity compared to other

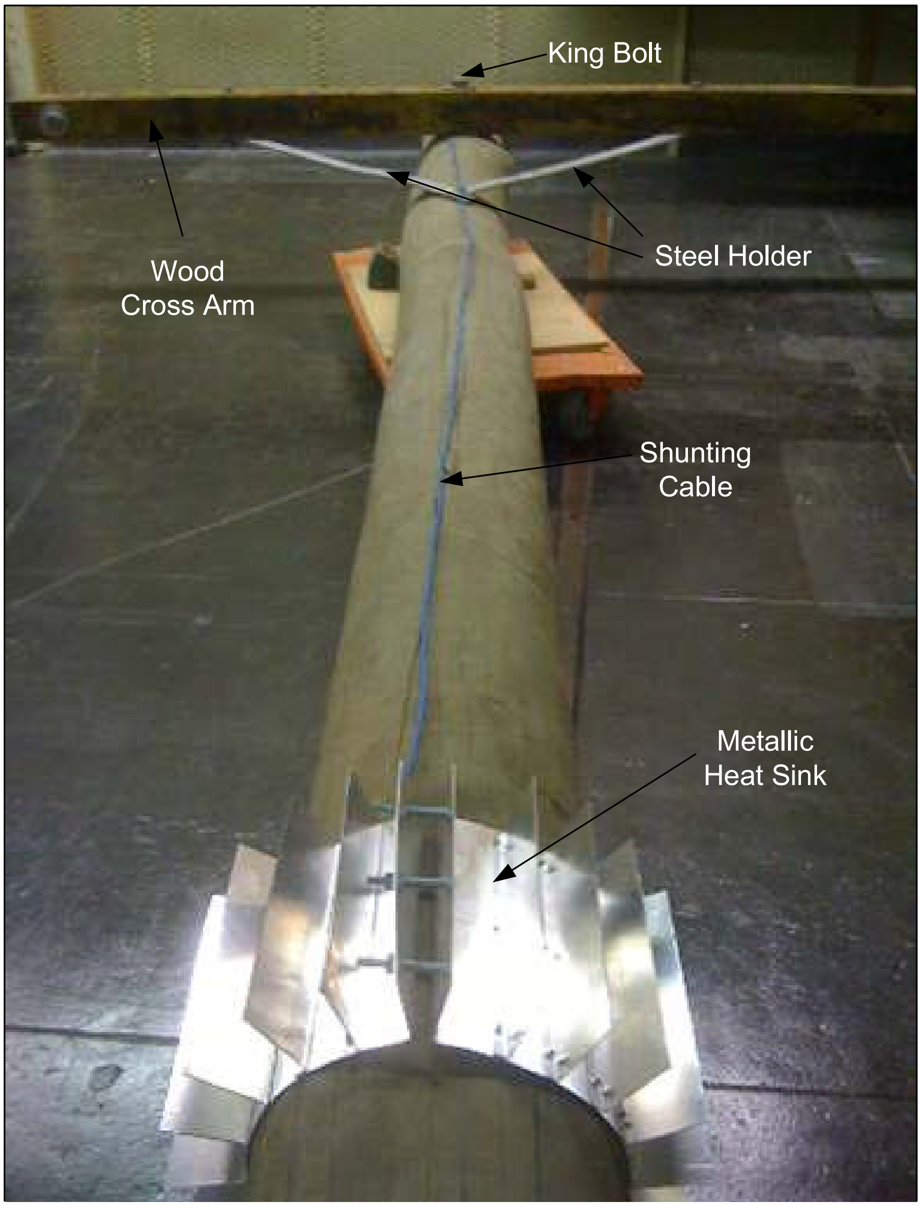

Figure 4.1: Mid-pole bonding system

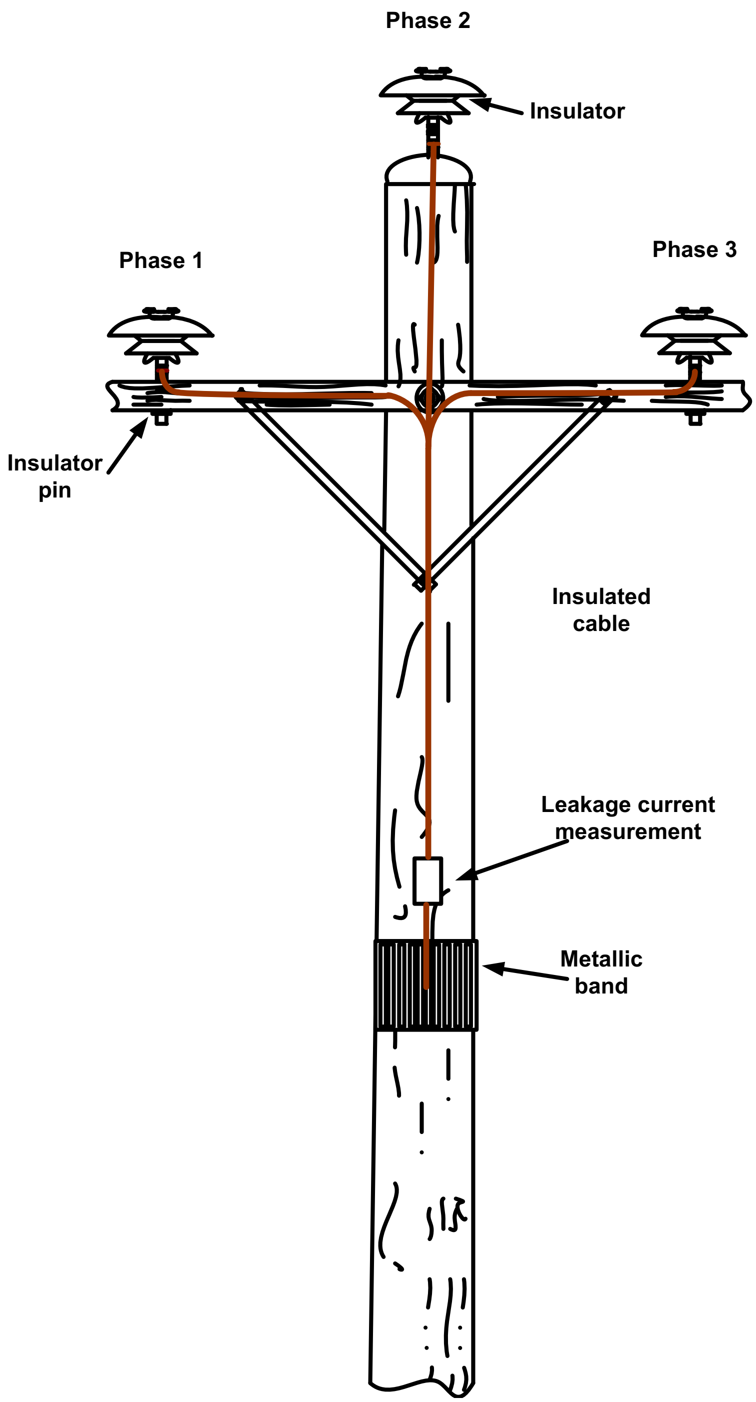

Figure 4.2: New mid-pole bonding arrangement

Figure 4.3: Metallic band

materials [144]. Thus, any thermal increase generated by the leakage current at this termination point can be dissipated easily into the air. To improve the heat dissipation efficiency, 21 aluminum fins were installed and bonded to this metallic band with rivets. Table 4.2 summarizes the heat sink performance in terms of the thermal resistivity resulting from manipulation of the fins; the thermal resistivity was based on equations 4.1 to 4.3 [145, 146]. As depicted in Table 4.2, the thermal resistance of the metallic band was small which meant more heat was transferable to the air as the number of fins were increased. Finally, the location at which this metallic band was secured onto the wooden pole structure was very important. More leakage current was able to be diverted, if the metallic band was fastened more toward to the bottom section of the wooden pole. A minimum location of 2 to 3 meters from the ground was required to minimize the electrical contact between the metallic band and the public.

Parameter	Descriptions
Metallic band	height, H = 0.2 m ; width, W = 0.07 m, thickness, t = 0.001 m
Fin	height, H_{fin} = 0.05 m ; width, W_{fin} = 0.2 m, thickness, t_{fin} = 0.001 m
A_{base}	H x W = 0.14 m^2
A_{fin}	2(H_{fin} x W_{fin}) = 0.02 m^2
k_{fin}	250 W/m ^{o}C (Thermal conductivity of aluminum [147])
h	assumed at 50 W/m^2 ^{o}C (Convective heat transfer coefficient of air [148])

Table 4.1: Metallic band dimensions and parameters

No. of Fin	Thermal Resistance (^{o}C/W)
0	0.143
5	0.093
10	0.068
15	0.054
21	0.043

Table 4.2: Heat dissipation of designed heat sink

$$\text{Thermal Resistance}, R_{HS} = \frac{1}{h(A_{base} + N_{fin} n A_{fin})} \tag{4.1}$$

$$\text{Fin efficiency}, n = \frac{\tanh(mH_{fin})}{mH_{fin}} \tag{4.2}$$

$$\text{Fin parameter}, m = \sqrt{\frac{2h}{k_{fin} t_{fin}}} \tag{4.3}$$

Physically, the source of leakage current was at the phase lines that are located at the top of the insulator. The polluted insulators allow leakage current flow through insulator pins to the wooden pole structures. Therefore, the leakage current must be immediately diverted away from the insulator pin to reduce the risk of current concentration at the metal wood insertion. As shown in Figure 4.4, the attachment of the shunting cables can be made at the insulator pin with cable clamps. Small screws, nuts and washers can attach the shunting cables firmly with cable clamps at the insulator pins and metallic band. Cable clips can be used with

(a) Cable termination at pole-top insulator (b) Cable termination at cross-arm insulator

(c) Termination of 3 insulated cables (d) Cable termination at the metallic band

Figure 4.4: Cable terminations for mid-pole bonding system

nails to hold the shunting cables tightly on the wooden pole structure.

The main purpose of shunting cables is to divert the leakage current away from the metal wood insertion, especially at the wooden pole cross-arm junction. As discussed in Chapter 2, normally the leakage current magnitude is within the mA range. Therefore the cable size for this mid-pole bonding system should have enough capacity to bring down the leakage current to the aluminum band. According to [149], 1 mm^2 to 10mm^2 sizes can be used and that is suitable for the shunting cables in the mid-pole bonding system. The most important thing is that these cables need a robust insulated cover for outdoor protection to withstand sun light and high temperature exposure. Another option is a leakage current measurement unit which can be included in this system for current monitoring purposes. Passive or active component units can be used to monitor the leakage current through online or offline measurement.

It has been a great concern over the basic impulse level (BIL) of wooden pole with mid-pole bonding system particularly when lightning strike. Generally, the impulse strength of the wood alone or with combination of porcelain insulator/cross-arm depends on the moisture contents of the wood. In detail, the influence of moisture contents in the wood effects the impulse strength, either in the form of natural moisture or moisture absorbed into the wood as a result from the rain [41]. Lusignan and Miller reported that the flashover voltage for wood and the combinations of wood-porcelain demonstrated variability of about $\pm$15 to 20 percent of the average (550 $\pm$100kVp/m for poles) under dry condition [150]. The author believes that the mid-pole bonding system will reduce the BIL of wooden pole which is dependent on the metallic band termination position. Therefore, the application of mid-pole bonding on wooden pole structure has to be compromised with the BIL. Unfortunately, due to the limitation of the facilities in the high voltage laboratory, BIL investigation of wooden pole with mid-pole bonding system will not be included in this study.

4.3 Enhanced Ladder Network Model for Simulating Mid-Pole Bonding System

Cross-arm is one of the essential parts of the wooden pole structure for an electrical distribution network. Cross-arm is a cross-piece and an arm or supporter bracket which crosses at the top section of the pole to hold the insulators that support the conductors and keep them separated. It has to be able to support the horizontal loads with very good mechanical strength under all circumstances, such as where the conductors are under tension, where the insulators carry great weight and where adverse weather occurs (wind, rain or snow). According to [151], the cross-arm concept generates many designs; for this study, it is limited to a 3-phase single support cross-arm for 11 kV wooden pole lines, as shown in Figure 4.5. The king bolt is used as a fastener to join the cross-arm and wooden pole together tightly with a washer and a nut. The steel bars act as the bracket holders to stabilize the cross-arm, especially to counter both the burden of the heavy insulators and phase wires, and the effect of weather loads.

A complete electrical model of a wooden pole structure can be established based on a full understanding of the ladder network model [17]. A cross-arm electrical model can be included with a few adaptations of the existing ladder network model. Firstly, the king bolt of the wooden pole should act as a reference point which is parallel to the radial resistance, $\mathbf{R}_r$ of wooden pole. Then the through king bolt will hold the cross-arm and wooden pole firmly. By assuming the through king bolt is parallel with the radial resistance of the cross-arm, the complete electrical model can be developed. Based on this idea, the effect of air resistance inside the wooden pole hole can be included in this enhanced ladder network model. In addition, the steel bar holders with bolts and insulator pins can also be added to

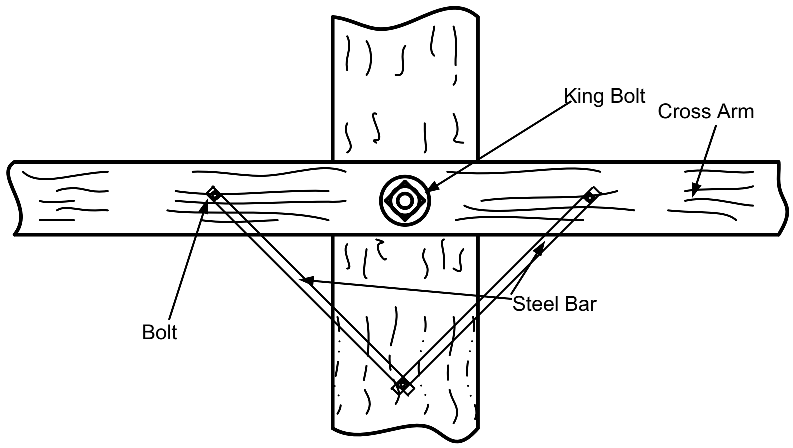

Figure 4.5: Wooden pole with cross-arm and supporting steel bars

the developed computer model. Therefore, this modified ladder network model can be exploited for further investigation of the wooden pole-top fire through a simulation study.

Founded on the ladder network model [17], an enhanced electrical model of wooden pole with mid-pole bonding system can be developed, as depicts in Figure 4.6. The $\mathbf{R}_{kb}$, king bolt is located at section 14 of the wooden pole model. It is parallel to $\mathbf{R}_{r}$ of the wooden pole and the radial resistance of the wooden cross-arm. The 2-meter wooden cross-arm is divided into 5 steps (0.4m for each step) and the cross-arm heartwood resistance is excluded in this cross-arm model. Both $\mathbf{R}_{st}$ steel holder resistances are connected to the second and fourth cross-arm sections with a small bolt, $\mathbf{R}_{b}$, to the 13th section of the wooden pole. In addition, $\mathbf{R}_{metallicband}$ is located at section 4 of the wooden pole ladder network model. $\mathbf{R}_{shunt}$ cables are used as shunting cables which run from the insulator pins to the $\mathbf{R}_{metallicband}$.

For the simulation study, 11 kV line voltage source produces leakage current in the mA range on the assumption that the polluted insulator has an overall

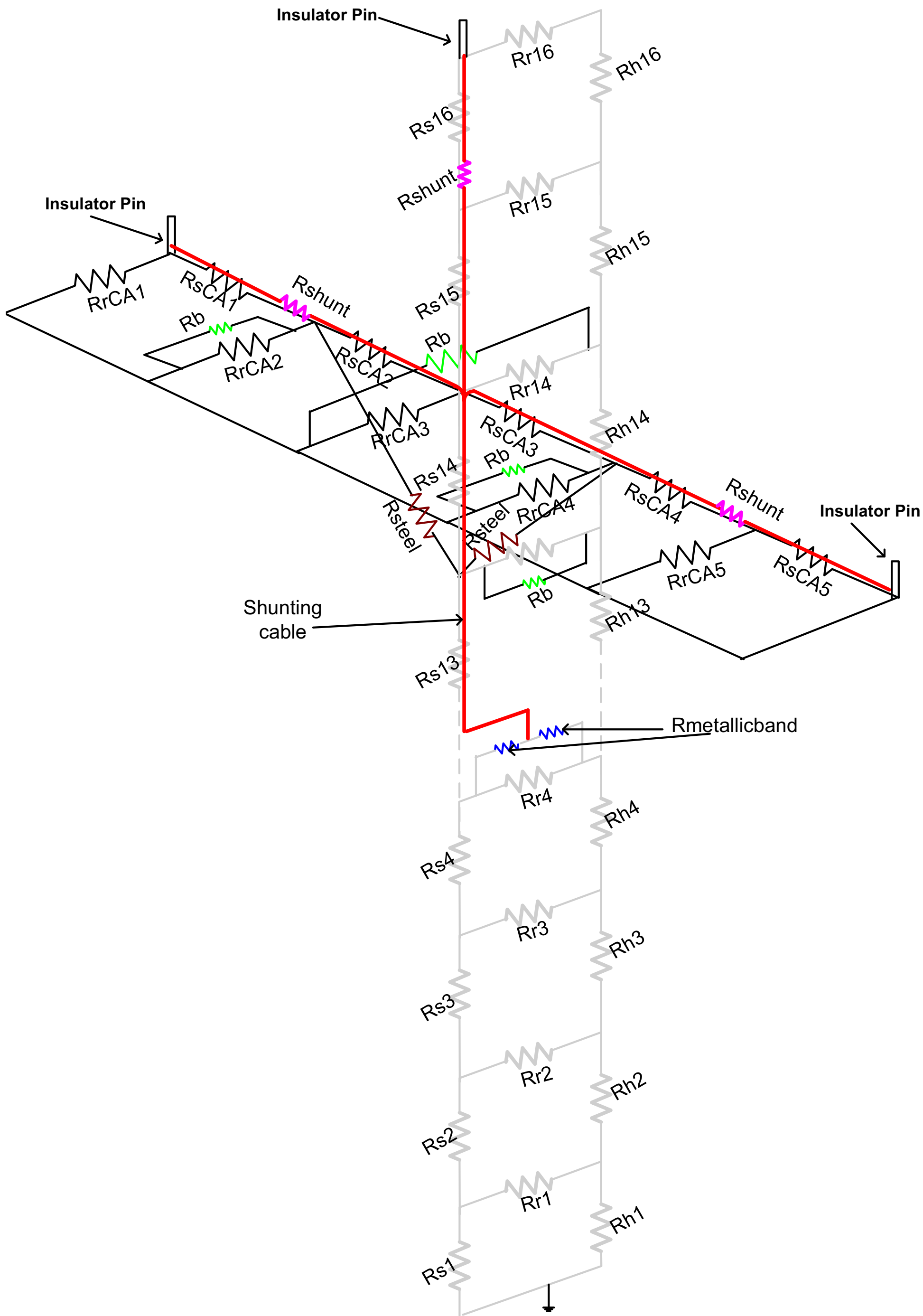

Figure 4.6: Electrical model for mid-pole bonding system (including steel bar and king bolt)

resistance value of 1 MΩ. As shown in Figure 4.6, the wooden pole is presented in 16 sections, where the 16^{th} section is located at the top of the wooden pole. A wooden cross-arm is attached to the wooden pole at section 14 and the king bolt resistance $\mathbf{R}_{kb}$ is parallel to the radial resistance of the wooden pole and the radial resistance of cross-arm $\mathbf{R}_{rCA}$. In addition, $\mathbf{R}_{metallicband}$ is located at section 10 of the wooden pole. This simulation study is focussed on the current distribution of the radial resistance, $\mathbf{R}_r$, along the wooden pole section under dry (11.7% of moisture content) and wet (22.7% of moisture content) conditions. Radial current distribution along 16 sections of the enhanced wooden pole model will provide significant information that relates to the effect of the steel bar and cross-arm under dry and wet conditions. Information about sapwood and heartwood current distribution is excluded in this study.

Figure 4.7 and 4.8 shows the radial current of wooden pole for conditions of

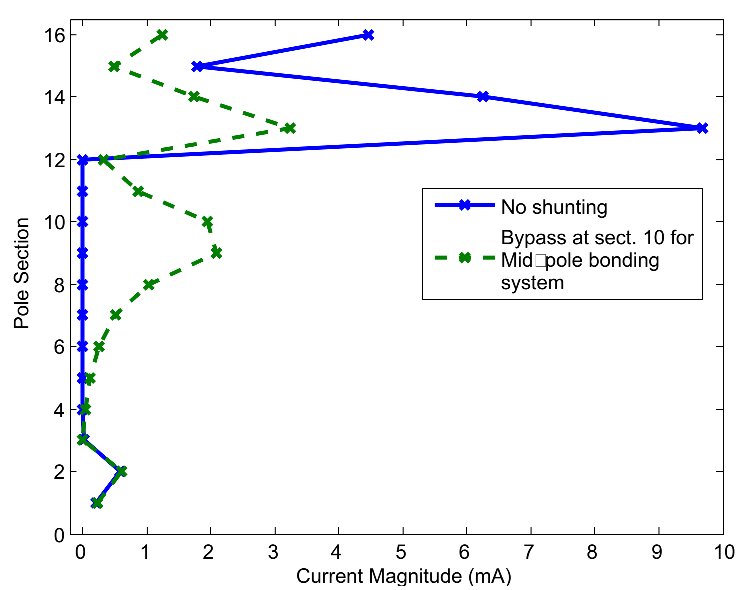

Figure 4.7: Comparison of radial current distribution in mid-pole bonding system and normal system

leakage current flow from Phase 2 (refer Figure 4.2). As shown in Figure 4.7, the radial current distribution was large for the wooden pole without a shunting system under wet conditions. About 6.3 mA and 9.7 mA radial current magnitude was recorded at sections 14 and 13 which had $\mathbf{R}_{kb}$ and $\mathbf{R}_b$ insertions. Then, the radial current distribution decreased as it flowed to the ground through the wooden pole structure. A small increase of radial current was plotted at section 2 and was caused by a lower radial resistance magnitude due to the high percentage of moisture content. Based on this study, the introduction of $\mathbf{R}_b$ on the enhanced model caused another spot of radial current concentration, especially at section 13. Based on this study, it can be concluded that $\mathbf{R}_b$ insertion has a higher risk of fire ignition compared to $\mathbf{R}_{kb}$ insertion at section 14.

On the other hand, the mid-pole bonding system successfully reduced the radial current concentration at sections 14 and 13 to 1.7 mA and 3.2 mA, as shown in Figure 4.7. These reductions were due to the role of the shunting cables which diverted the leakage current to the metallic band at section 10 directly from the insulator pin. However, another spot of radial current concentration at section 10 resulted from the metallic band termination. But, higher radial current concentration at this section did not cause any fire risk. This was because the metallic band was only secured on the surface of the wooden pole and did not penetrate the wood stakes at section 10.

In addition, Figure 4.8 depicts the comparison of radial current distribution for the mid-pole bonding system under dry and wet conditions. For this simulation study, the leakage current was diverted from the insulator pin at Phase 2 to section 10 of wooden pole through a shunting cable. Under dry conditions, the radial current distribution, which is in the μA range, was very small compared to that under wet conditions. Based on both graphs, it is evident that the $\mathbf{R}_{kb}$ and $\mathbf{R}_b$

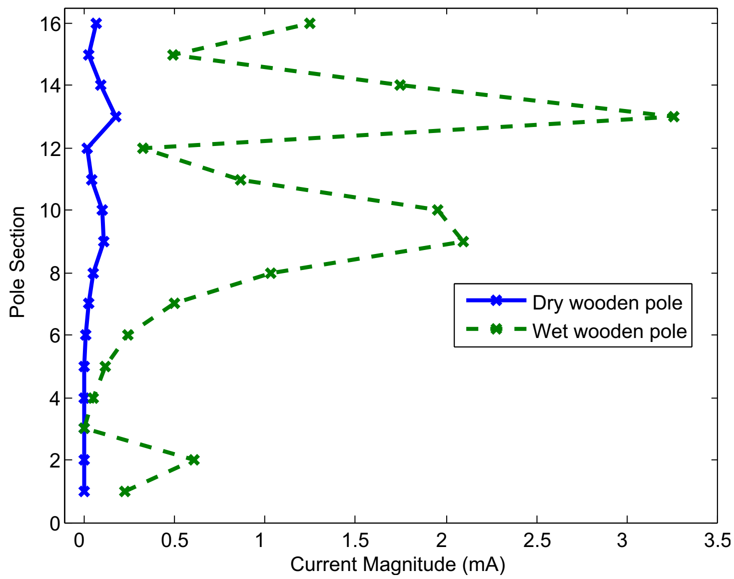

Figure 4.8: Radial current distribution of mid-pole bonding system

insertions caused the radial current concentration at the pole-cross-arm junction. However, the mid-pole bonding system managed to reduce the current concentration by more than 65%. This proves that the enhanced wooden pole model based on the ladder network model is really useful in terms of a pole-top fire mitigation study.

4.4 Performance Study of Mid-Pole Bonding System and Simulation Comparison

Research on the preventive measures related to pole-top fire began in the 1900s. For example, a stainless-steel cross-arm is often installed in distribution systems where the mechanical stresses on the line are too high for any other alternative [152]. In areas that suffer from heavy pollution, stainless steel has been a good alternative to wood. The copper jumper arrangements proposed by P.M Ross

	Mitigation system	Physical arrangement
1.	Ross shunting 1	Figure 4.9
2.	Ross shunting 2	Figure 4.10
3.	Steel cross-arm	Figure 4.13

Table 4.3: Developed mitigation system

were selected for the pole-top fire comparative study. The performance of these two mitigation techniques was chosen for investigation on terms of their relative radial leakage current distribution. Therefore a similar approach has been used to develop the electrical model of a stainless steel cross-arm and copper jumper arrangement on the enhanced ladder network. Table 4.3 summarizes the mitigation systems that were developed in this study. The performance of these two selected mitigation arrangements will be examined and compared with our new mid-pole bonding system.

Figure 4.9 and 4.10 shows the possible shunting arrangements originally proposed and designed by Ross [12], which aimed to decrease pole-top fire risk. In these arrangements, four copper bands or metal sheets were attached to the

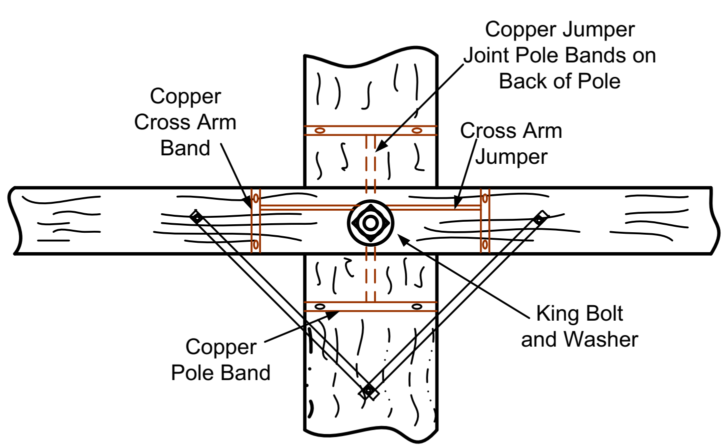

Figure 4.9: Shunting arrangement 1 for cross-arm by Ross [12]

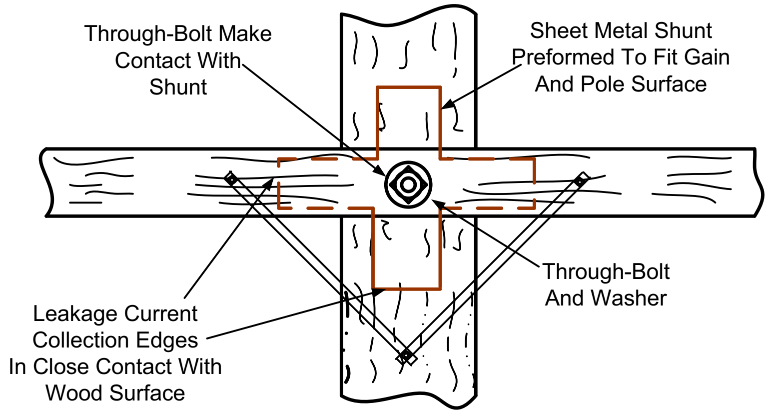

Figure 4.10: Shunting arrangement 2 for cross-arm by Ross [12]

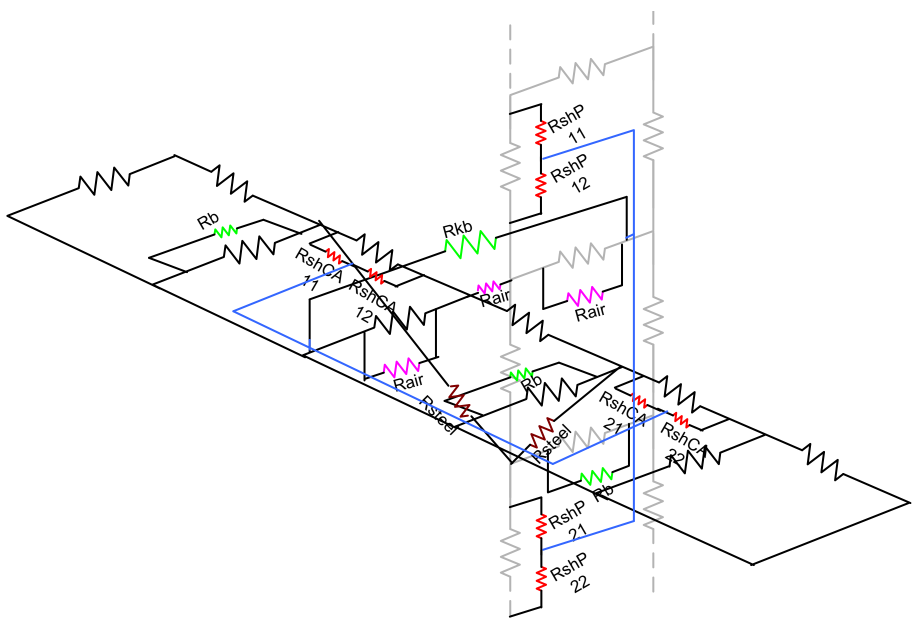

Figure 4.11: Electrical model for Ross shunting arrangement 1

wooden cross-arm and wooden pole. The developed electrical models of these shunting arrangements are shown in Figure 4.11 and 4.12. The shunting arrangement resistances for cross-arm and pole, $\mathbf{R}_{shCA}$ and $\mathbf{R}_{shP}$, were connected to the

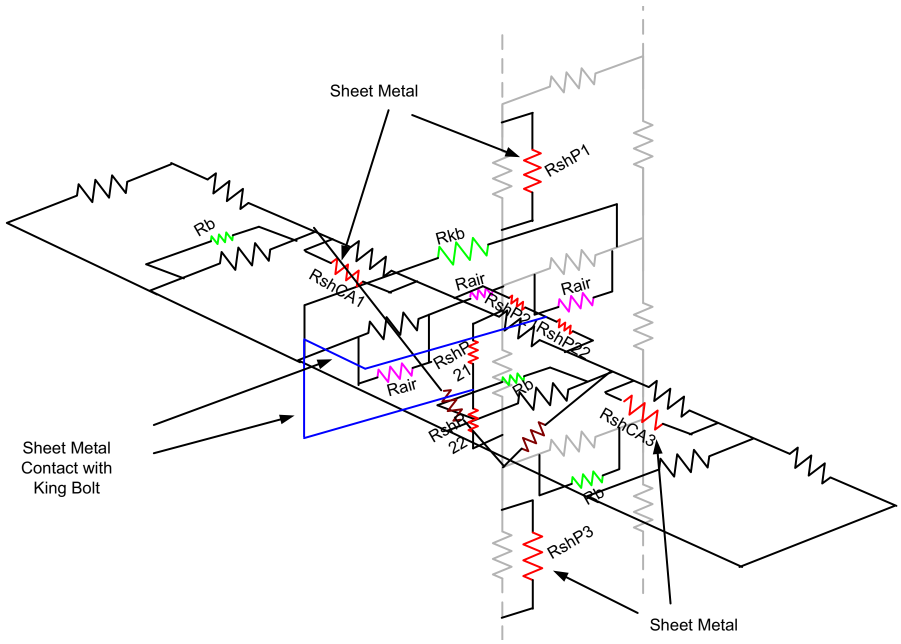

Figure 4.12: Electrical model for Ross shunting arrangement 2

king bolt with or without two sets of copper jumpers to avoid voltage concentration at the cross-arm pole junction. In these simulation models, the effects of an air gap, ($\mathbf{R}_{AIR}$) in between on both metal-wood and wooden pole, and metal-wood and cross-arm junction are taken into consideration.

Figure 4.13 shows an arrangement of the stainless steel cross-arm with pole structure. This 2-meter length steel cross-arm was made of a 3-mm thick galvanized steel and five holes were pre-drilled for the insulator and bolt attachments. Similar to the wooden cross-arm, the king bolt was used to hold and secure the steel cross-arm to the wooden pole at the center section. The steel holders were used to hold the cross-arm in position which carried the tension of the life lines and the weight of the insulators. Figure 4.14 depicts the electrical model of the steel cross-arm based on the ladder network model. It is divided into two parts and each part contains four elements ($\mathbf{R}_{steelCA1}$, $\mathbf{R}_{steelCA2}$, $\mathbf{R}_{steelCA3}$, $\mathbf{R}_{steelCA4}$)

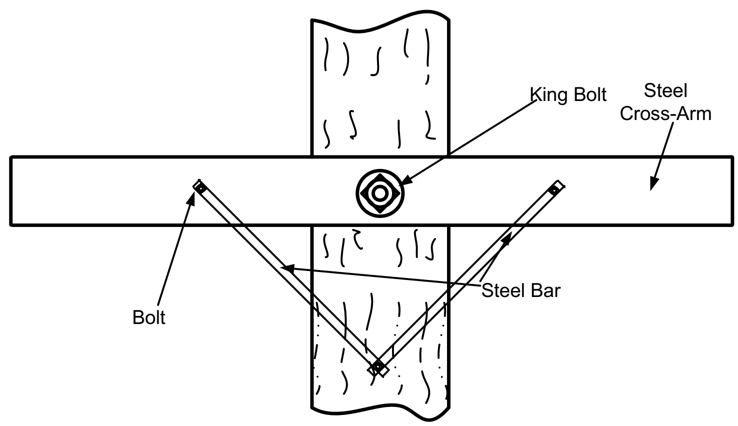

Figure 4.13: Wooden pole with cross-arm and supporting steel bars

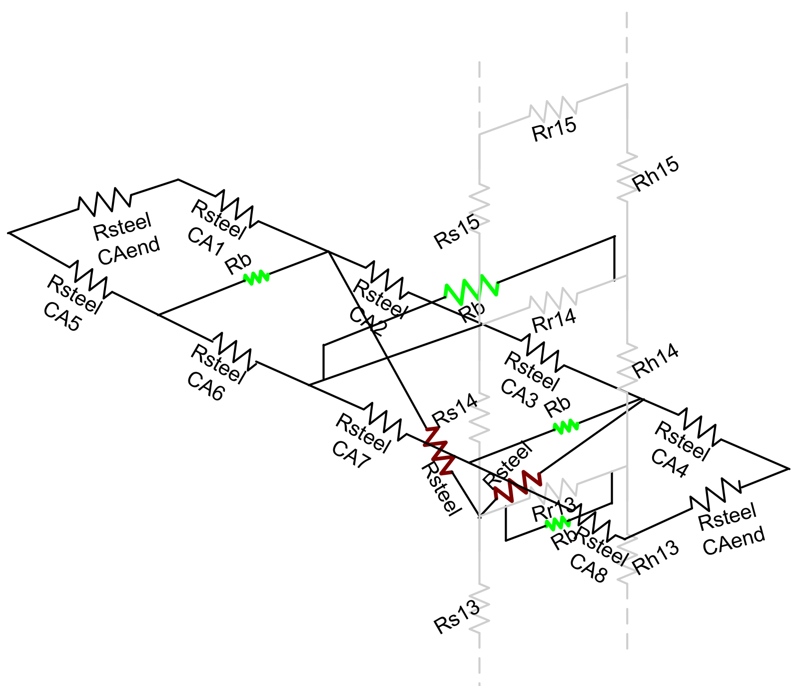

Figure 4.14: Electrical model for wooden pole and steel cross-arm(including steel bar and king bolt)

and ($\mathbf{R}_{steelCA5}$, $\mathbf{R}_{steelCA6}$, $\mathbf{R}_{steelCA7}$, $\mathbf{R}_{steelCA8}$) and finally the $\mathbf{R}_{steelend}$ connects both parts.

In summary, the successful manipulation of the original wooden pole ladder network model allowed us to move forward to the next level of the pole-top fire study. Significant information was able to be determined during an intensive simulation study of the radial current distribution along the enhanced ladder network model. The developed Ross shunting technique and steel cross-arm helped to explain the performance of both methods. The comparative simulation study of the mid-pole bonding system with, variously, the Ross shunting method and the steel cross-arm will be discussed in the next section.

4.4.1 Simulation Results

Similar to previous studies, the leakage current was assumed to flow from the polluted insulator located at the top section of the wooden pole i.e. at Phase 2 (refer to Figure 4.2) to the ground under wet conditions. Figure 4.15 depicts a comparative study of radial current distribution between wooden and steel cross-arm. The graph shows that the radial current distribution for wooden cross-arm is almost identical to the steel cross-arm simulation results; 6.3 mA and 9.7 mA radial current were recorded at sections 14 and 13. The effect of the king bolt insertion parallel to the radial resistance of the wooden pole and cross arm at section 12 caused the overall resistances at this section to be very small. Similar conditions for $\mathbf{R}_b$ insertion also reduced the overall resistance at section 13. However $\mathbf{R}_b$ resistance was small compared to $\mathbf{R}_{kb}$ resistance. Therefore a rapid change in the radial current was plotted between section 14 and 13 for both cross-arms. Consequently, the radial current reduced significantly as it flowed toward the bottom section of the wooden pole.

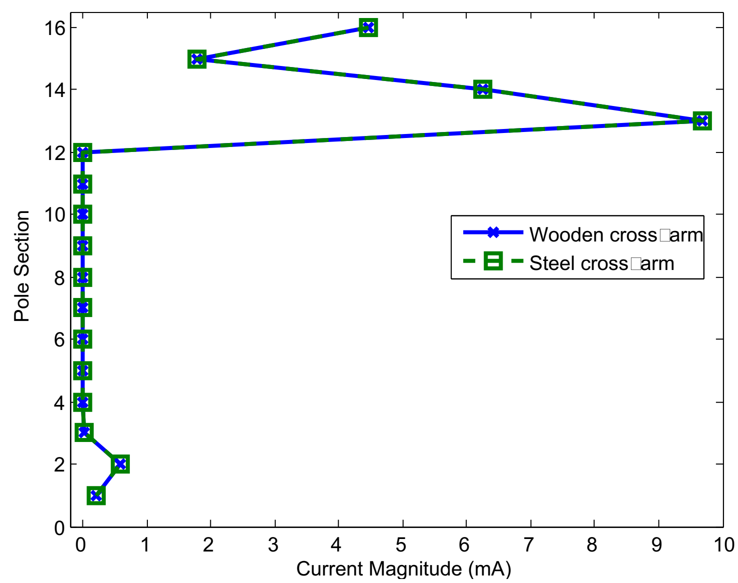

Figure 4.15: Comparison of radial current distribution between wooden and steel cross-arm under wet conditions

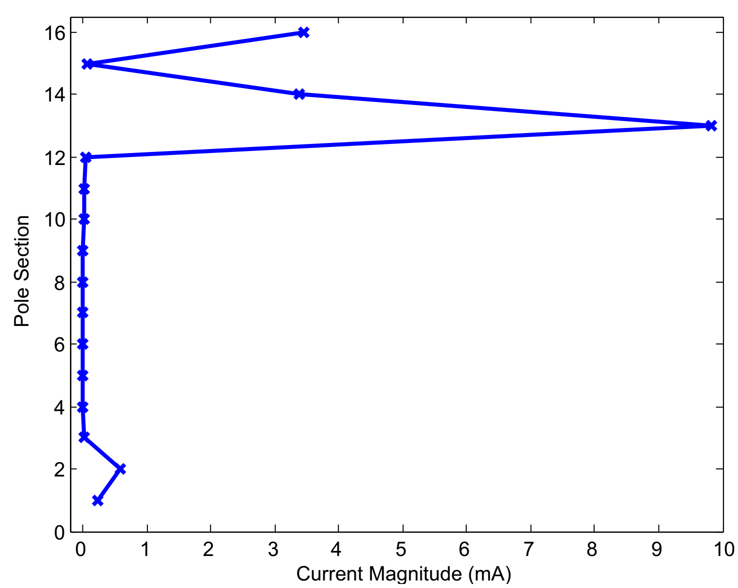

Figure 4.16: Radial current distribution of Ross's shunting arrangement 1

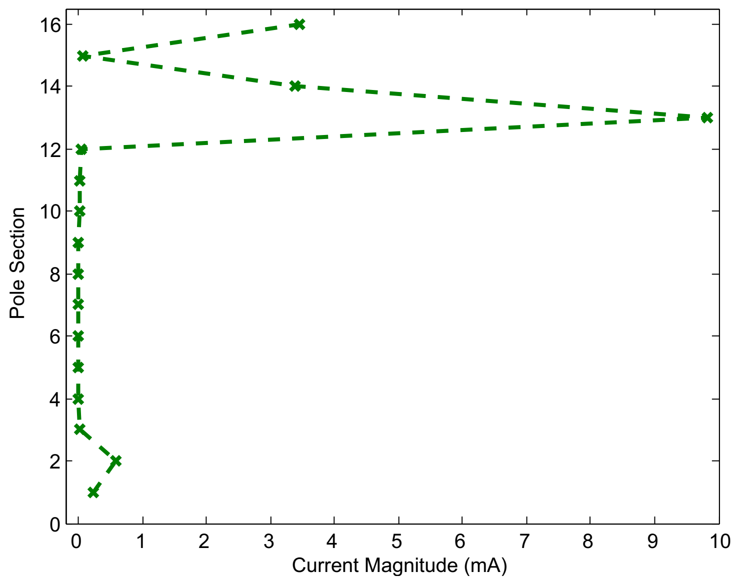

Figure 4.17: Radial current distribution of Ross's shunting arrangement 2

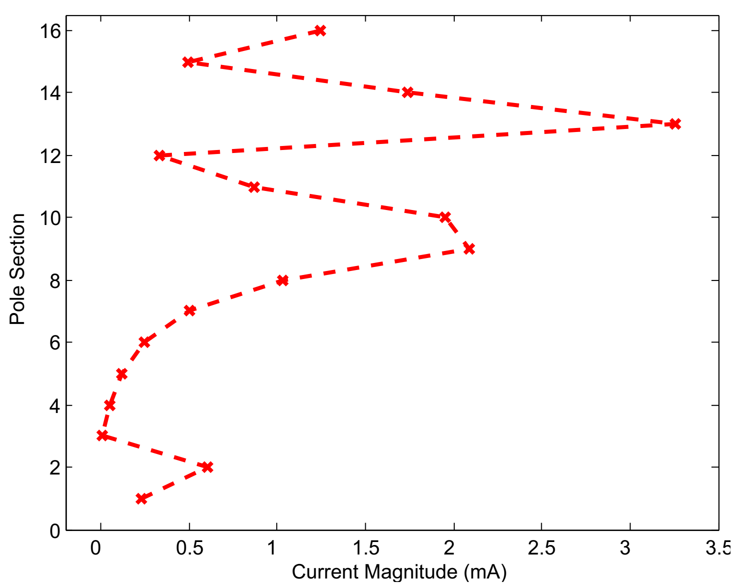

Figure 4.18: Radial current distribution of mid-pole bonding system with bypass at section 10

Radial current distributions under wet conditions were obtained from both Ross's shunting arrangements and the mid-pole bonding system simulation and are presented in Figure 4.16, Figure 4.17 and Figure 4.18. Radial current distribution of the Ross shunting arrangement 1 is similar to that of the Ross shunting arrangement 2. The results show that the shunting arrangements proposed by Ross were unsuccessful in reducing the radial current concentration at R_b in section 13, which had about 9.8 mA. However they managed to lower the radial current concentration at R_{kb} in section 14 to 3.3 mA compared to no shunting system. The copper jumper that tied up the four copper bands and that was electrically bonded to the king bolt slightly reduced the radial current concentration at section 14 but did not work for R_b section. In addition, the mid-pole bonding system managed to reduce current concentration at section 13 to 3.2 mA after bypassing the leakage current to section 10 of the wooden pole. The current concentration at R_{kb} also reduced to 1.7 mA, compared to that using Ross's method. There was about 66.37% and 72.16% reduction of radial current concentration at section 13 and 14 for this mid-pole bonding system.

Figures 4.19 and 4.20 show the distribution of radial current for the mid-pole bonding system with varying bypass terminations under dry conditions. As discussed, the mid-pole bonding system successfully reduced the radial current concentration at section 13 and 14 of the wooden pole. In Figure 4.19, it can be seen that the radial current concentration reduced to 1.5 mA at section 14 and 2.4 mA at section 13. As the termination of the metallic band moved downwards, more leakage current flowed through the shunting to the ground. Therefore at section 13 and 14 of Figure 4.20, the current reduced to 1.8 mA and to 1.1 mA respectively. The result demonstrates that the concept of bypassing the leakage current from the insulator pin to lower section of wooden pole is sound. By diverting the total

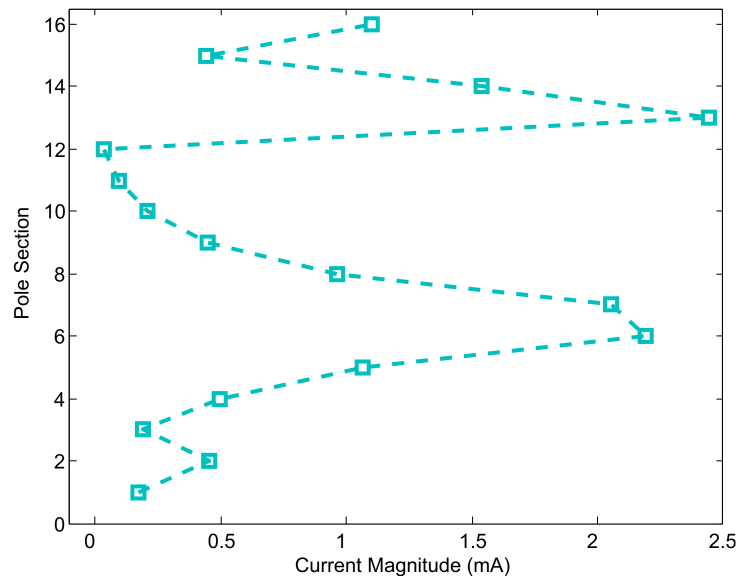

Figure 4.19: Radial current distribution of mid-pole bonding system with bypass at section 7

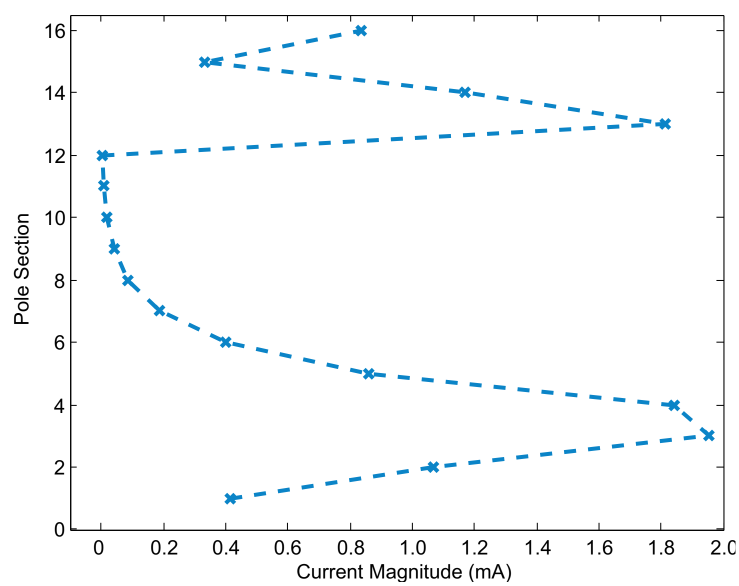

Figure 4.20: Radial current distribution of mid-pole bonding system with bypass at section 4

leakage current from the insulator straight to the mid-pole section, it accomplished the aim of reducing the radial current concentration at the pole cross-arm junction. The radial current increment at bypass termination, especially at section 10, 7 and 4 of the wooden pole, did not cause a problem because the metallic band was only secured on the surfaces and did not intrude into the wooden pole section.

4.5 Simulation of Three-Phase Leakage Current

The three-phase leakage current study attempted to determine the radial current distribution characteristics due to the failure of the insulators. In this instance, at least two insulators were assumed to fail at the same time and to permit a leakage current flow from either Phase 1 and Phase 2, Phase 1 and Phase 3, Phase 2 and Phase 3 (refer Figure 4.2) or from all these failed insulators to the ground. Assumptions were made for these situations that somehow these combined events could have happened due to the pollution caused by weather of uneven insulator surfaces. For example, a light shower with wind may have successfully cleaned up only one insulator in one direction but may still not have covered all in-service insulators. For this study, all line phases were set at a 11 kV voltage magnitude with 120^o angle difference between each phase, similar to actual conditions. In particular, this three-phase line was connected under a balanced delta configuration, in which line voltage is equal to phase voltage, while the line current is equal to phase current times the square root of 3. Finally, the insulators were set at 1 MΩ) to simulate the medium surface pollution level and the simulation was run under wet conditions.

Figure 4.21 depicts the results of the MATLAB simulation for all possible conditions. In case (a), the leakage current was flowing from Phase 1, Phase 2 and

Phase 3 to the ground and causing the radial current concentration at section 13 and section 14. About 6.3 mA and 0.5 mA current magnitudes were recorded flowing, respectively, at the king bolt and bolt steel holder sections under a normal configuration. With the Ross shunting technique, the current concentration at section 14 was reduced to 3.4 mA. Furthermore, a slight increase of radial current magnitude at section 13 with the Ross method was compared to the normal

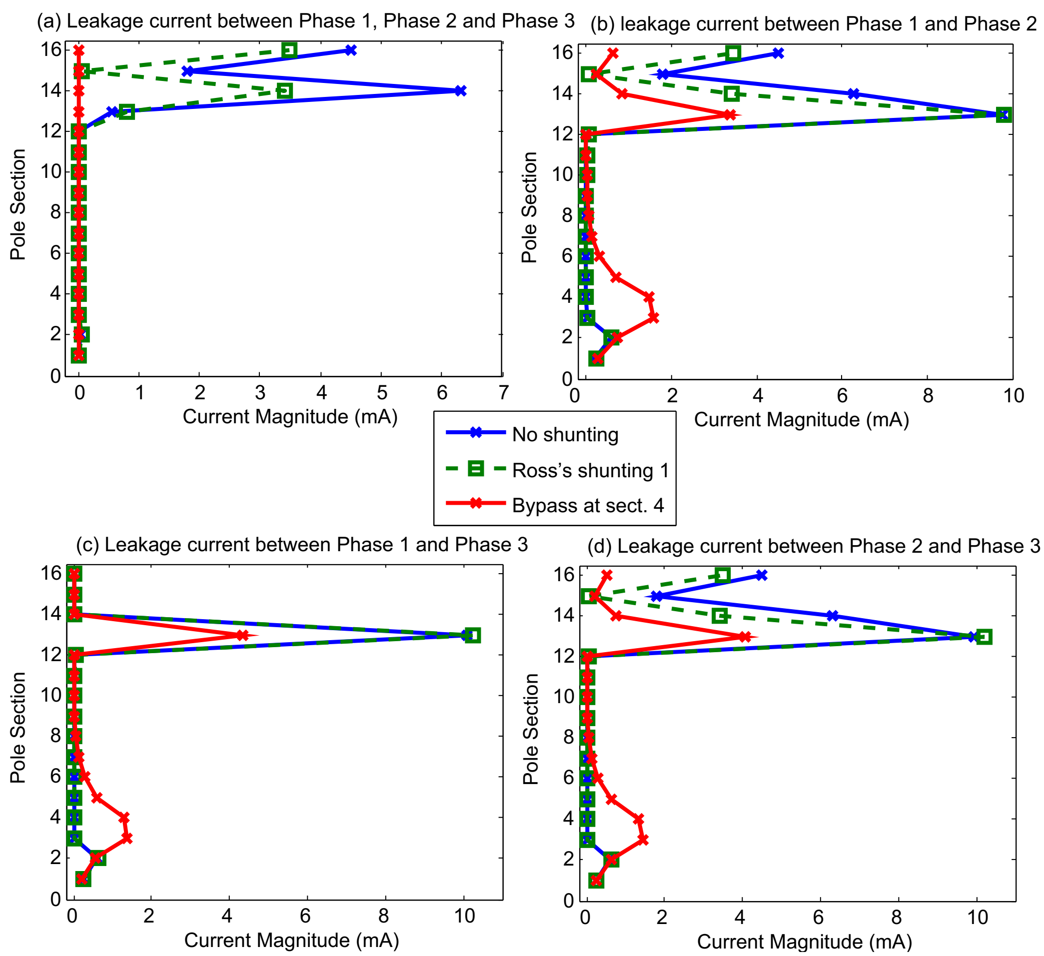

Figure 4.21: Comparison of radial current distribution for phase-to-phase leakage current with wooden cross-arm with grounding

configuration. Finally, with the mid-pole bonding system, all the potential current concentrations, particularly at sections 13 and 14, were successfully eliminated.

A similar pattern of simulation results was plotted for the circumstances of (b) and (d) as shown in Figure 4.21. In these cases, the leakage current was flowing between one of insulators at the cross-arm and the insulator at the top section of wooden pole to the ground. As depicted in Figure 4.21, the radial current that was mostly concentrated at the bolt section securing the steel bar holders was compared to the radial current at the king bolt section. In case (b), 9.7 mA and 6.0 mA current at section 13 and 14 was stepped down to 3.3 mA and 0.8 mA with a bypass of the leakage current to the metallic band at section 4. On the other hand, the Ross shunting method managed to cut down current concentration, especially at section 13, to about 3 mA. An identical radial current distribution was plotted for case (d), indicating that the mid-pole bonding system was successful for both conditions. In contrast, the radial current was only concentrated at section 13 for case (c), particularly under normal and Ross configurations. A very small radial current was recorded at section 14 and 10mA current was concentrated at section 13. These results were almost identical with the simulation results of the single-phase leakage current study from cross-arm to ground in Section 4.4.2. The current magnitude at section 13 was reduced from 10 mA to 4 mA with the mid-pole bonding system.

The simulation results of Figure 4.22 explain another situation of leakage current phenomena on the wooden pole structure. In detail, this study tried to simulate and find the reason for the leakage current that occurred between phases. It can happen if the wooden poles are not properly grounded or the grounding system is not in good order. In some cases, the wooden poles are not grounded physically, as is the case where the bottom section of the wooden pole is buried at

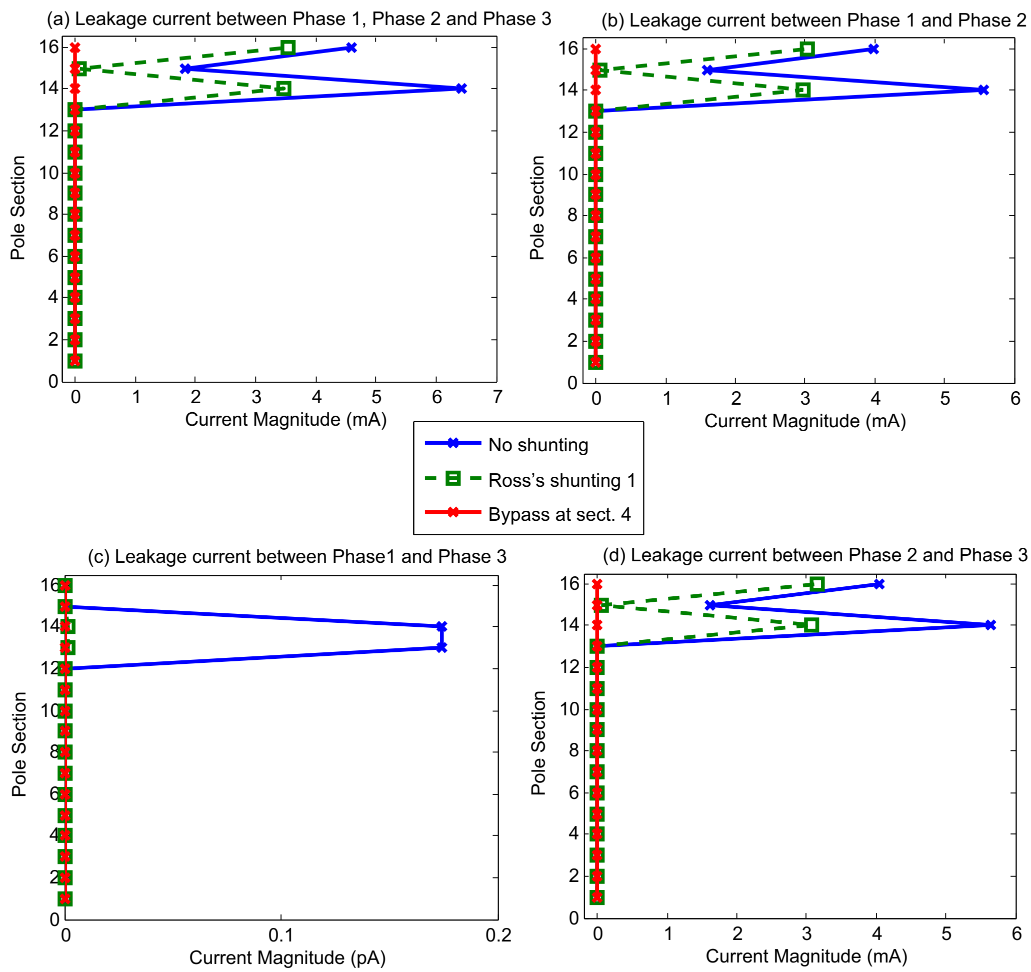

Figure 4.22: Comparison of radial current distribution for phase-to-phase leakage current with wooden cross-arm without grounding

depth into the ground. As depicted in Figure 4.22, the radial current is concentrated only at section 14 for cases (a),(b) and (d) in the range of 5 mA to 6 mA for normal conditions. However, a very small current distribution was plotted for the radial current magnitude caused by two failed insulators at the cross-arm i.e. for case (c). On the other hand, the Ross shunting method successfully reduced the current magnitude at section 14 to about 3 mA for all cases (a), (b) and (d). The current concentration at section 14 was eliminated to zero by applying the mid-pole bonding system to the wooden pole structure. Based on these simulation studies, no current flowed from section 13 to 1 due to the effect of phase-to-phase leakage current.

4.6 Summary

In this chapter, the electrical model for wooden pole with cross-arm was introduced. In particular, the electrical model of wooden and steel cross-arm was developed based on the ladder network model. Furthermore, the copper jumper arrangement at the wooden-cross-arm junction that was introduced by P.M Ross was also modeled for performance comparison purposes. On the other hand, a new mid-pole bonding system was proposed in this research to overcome the current disadvantages of the pole fire mitigation arrangement. The simulation results show that the king bolt junction displayed a large current concentration and the steel bar holder bolt located at section 13 also introduced another high magnitude leakage current spot. It was proven that any metal insertion on the wooden pole structure that was closed to leakage current source was very prone to the development of fire initiation.

The replacement of the wooden cross-arm with a steel cross-arm did not improve the wooden pole-fire resistance. Based on the simulation study, it had a similar radial current distribution to the normal wooden cross-arm configuration. On the other hand, the shunting arrangement proposed by P.M Ross was unable to reduce the radial current concentration at section 13 and 14 by a large margin, except in the cases of phase-to-phase leakage current. Additionally, the mid-pole bonding system mitigated the leakage current effectively from the metal-cross-arm junction. In summary, this study proves that a high leakage current

Figure 4.23: Pole-top fire at steel bar holder bolt due to leakage current phenomena

is concentrated on the metal insertion at the pole-cross-arm junction under wet conditions in contrast to dry conditions. Figure 4.23 depicts one of the pole-top fire phenomena in the electrical distribution system. It can be used as evidence that a fire could be triggered at the bolt or any pole-metal insertion point, especially at the wooden pole cross-arm junction. The proposed mid-pole bonding system gives promising results and could provide critical direction in future pole design. Table 4.4 summarizes the ladder network simulation results, in particular to highlight the performance of all considered mitigation methods. Finally, the experimental investigation of this research was carried out in the RMIT University high voltage facility and is discussed in Chapter 5.

Condition	Cases	With Grounding	No Grounding	(%) Changes	
				Sect. 13	Sect. 14
Single phase	Phase 2	Steel cross-arm		0%	0%
		Ross Shunting 1		-1.61%	45.93%
		Ross Shunting 2		-1.61%	45.93%
		Bypass at sect. 10		66.37%	72.16%
		Bypass at sect.7		74.77%	75.38%
		Bypass at sect. 4		81.27%	81.33%
	Phase 1	Ross Shunting 1		1.07%	0%
		Bypass at sect. 4		75.08%	0%
	Phase 3	Ross Shunting 1		-3.43%	0%
		Bypass at sect. 4		66.62%	0%
Phase-to-phase	Phase 1, 2 and 3	Ross Shunting 1		-41.51%	45.92%
		Bypass at sect. 4		99.43%	99.99%
	Phase 1 and 2	Ross Shunting 1		-0.18%	45.93%
		Bypass at sect. 4		65.41%	86.36%
	Phase 1 and 3	Ross Shunting 1		-1.37%	0%
		Bypass at sect. 4		56.91%	0%
	Phase 2 and 3	Ross Shunting 1		-2.62%	45.92%
		Bypass at sect. 4		59.15%	88.24%
	Phase 1,2 and 3		Ross Shunting 1	0%	45.98%
			Bypass at sect. 4	0%	100%
	Phase 1 and 2		Ross Shunting 1	0%	46.64%
			Bypass at sect. 4	0%	100%
	Phase 1 and 3		Ross Shunting 1	0%	0%
			Bypass at sect. 4	0%	0%
	Phase 2 and 3		Ross Shunting 1	0%	45.45%
			Bypass at sect. 4	0%	100%

Table 4.4: Comparison of simulation results for ladder network model

Chapter 5

Experimental Study on Novel Mid-Pole Bonding System

5.1 Introduction

A mid-pole bonding system for pole-top fire prevention based on a ladder network model study was proposed in Chapter 4. This technique manages to reduce current concentration at the wooden pole cross-arm junction based on a MATLAB simulation study. An experiment, the result of which will be compared with the simulation study, is needed to prove our hypothesis. On the other hand, there is a lack of knowledge about the heating process of the wooden pole supporting structure due to the high level of leakage current. A proper laboratory observation is needed in order to investigate this leakage current effect.

A small-scale laboratory setup was created in the RMIT University High Voltage Laboratory to study those two hypotheses. A 6.5-meter hardwood pole treated with CCA was used to realize the mid-pole bonding system testing and to examine the thermal distribution, especially at the cross-arm due to the likelihood of high leakage current at this juncture. This chapter presents an intensive laboratory test which studied the performance of the mid-pole bonding system and compared the results with the simulation work. It also demonstrates the leakage current effect, especially at the wooden pole cross-arm junction based on thermographic images. These experimental works will provide useful results with full information for a further understanding of the leakage current effect along the wooden pole structure.

5.2 Experimental Setup

Figure 5.1 depicts an experimental setup for the mid-pole bonding system experiment. For this study, the leakage current was produced by the resistive components of the polluted insulators; this was simulated using high voltage resistors that were connected to the high-voltage power supply. The high-voltage supply was connected in a series with a 4 MΩ resistor to simulate the polluted insulators that had suffered from medium surface pollution. As discussed in Chapter 4, a specially designed metallic band was installed at the middle section of the wooden pole to bypass the leakage current through a shunting cable with 21 fins. This metallic band was used for a current terminating point and for heat dissipation purposes. Another aluminium plate with nail was installed at the bottom section of the wooden pole to provide maximum electrical contact to the ground. Figure 5.2, Figure 5.3 and Figure 5.4 shows the high voltage transformer, voltage divider and resistor that were used during the experimental study.

For testing purposes, the leakage current was made to flow from 11 kV voltage source through the conductor that was connected, either to the metal pin of the metal cap at the top section of the wooden pole, or at the cross-arm to the ground.

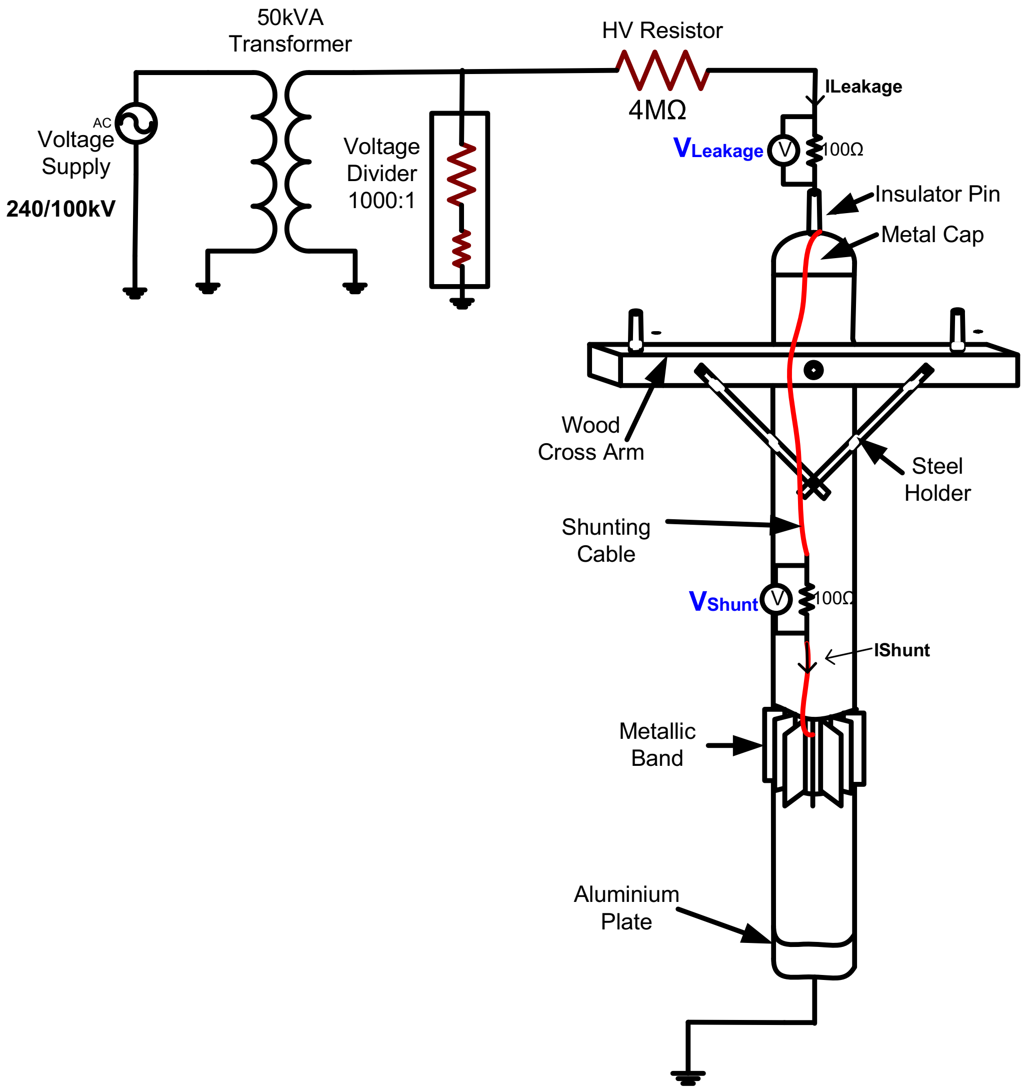

Figure 5.1: An experimental setup for mid-pole bonding system study

For the measurement setup, two 100 Ω low resistors were used and they were connected in a series measuring $\mathbf{V}_{Leakage}$ (at top section of wooden pole) and $\mathbf{V}_{Shunt}$ (at middle section of wooden pole). Both these resistors were connected to the floating oscilloscope through a coaxial cable for current measurement purposes i.e. the measured voltage divided by 100 Ω resistor. Floating measurement is needed

Figure 5.2: High voltage transformer

Figure 5.3: Voltage divider for high voltage measurement

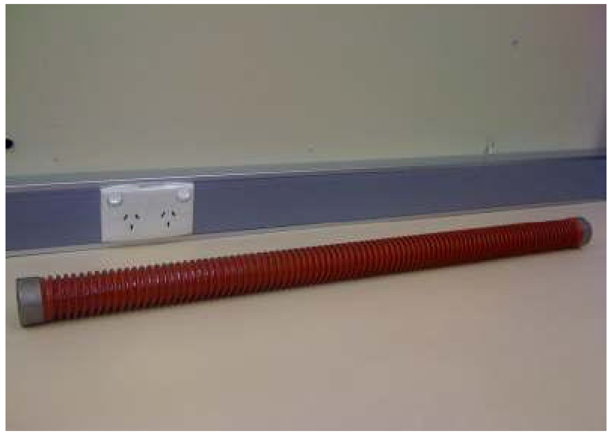

Figure 5.4: 1 MΩ high voltage resistor

purposely to capture the floating $\mathbf{V}_{Leakage}$ and $\mathbf{V}_{Shunt}$ accurately which it's was elevated far from the common earth. The common reference for two input channels of the floating oscilloscope is located at the junction of $\mathbf{V}_{Leakage}$ and $\mathbf{V}_{Shunt}$. The ratio between $\mathbf{I}_{Shunt}$ and $\mathbf{I}_{Leakage}$ gave an indication of the performance of the mid-pole bonding system. Finally these results were compared with the simulation study results.

This type of wooden cross-arm, as shown in Figure 5.5, is commonly found in power-system distribution networks of 11 kV and 22 kV around Australia. The wooden cross-arm is an untreated hardwood of 2 m x 0.1 m x 0.1 m dimension. On the other hand, stainless steel cross-arm has also been used as a support structure in electrical distribution networks. As depicted in Figure 5.6, the cross-arm is made of a 3-mm thick galvanized steel with 5 holes that are pre-drilled for insulators and bolt connection. Only the wooden cross-arm was used for the mid-pole bonding system experiments but both steel and wooden cross-arms were used for the thermographic study.

For the cross-arm thermographic study, two high voltage resistors of 2 MΩ

Figure 5.5: Wooden cross-arm

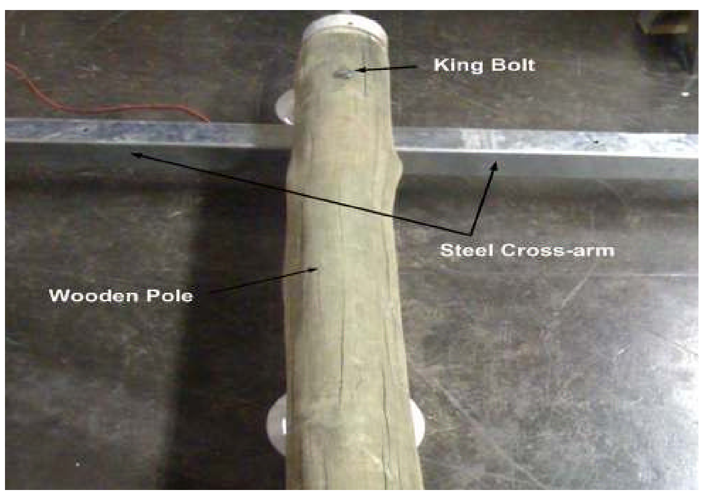

Figure 5.6: Steel cross-arm

and 100 kΩ were used to simulate medium and severe surface contaminations for the polluted insulators. For this setup, the current magnitude was measured at the primary side of the transformer and, by using the transformer transformation ratio, the leakage current level of 5 mA and 14 mA, which represents the current

Figure 5.7: Thermovision A320 thermal camera

magnitude at the secondary side was calculated on a 6.5-meter wooden pole. It was assumed that the polluted insulator allowed whole leakage current to flow to the king bolt through the cross-arm body, especially for the stainless steel cross-arm type. Therefore, the conductor was connected directly to the king bolt. A similar configuration was adopted for the wooden cross-arm thermographic study.

The Thermovision A320 thermal camera was used to measure the spot temperatures on the surface of the king bolt, cross-arm and pole. The A320 is designed to deliver an accurate thermographic imaging and repeatable temperature measurements in a wide range of applications. Each Thermal image is built from 76,800 individual picture elements that are sampled by the camera's on-board electronics and software to measure temperature. The thermal camera is installed at a 1-meter distance from the test object and the near-real time 16 bit 320 x 240 image data is recorded and stored at 10-minute intervals during the test.

5.3 Mid-Pole Bonding System Study on Wooden Pole

Based on our previous results in Chapter 4, the mid-pole bonding system successfully reduced the leakage current concentration at the wooden pole and cross-arm junction by at least 60%. This calculation was based on the reduction of the radial current magnitude, especially at the bolt section that fastened the steel bar holders and secured the cross-arm structure. By diverting the leakage current from the insulator pin to the metal band located at the middle section of the wooden pole structure, the chances of any unwanted process that could trigger fire was reduced. In particular, the relative magnitudes of $\mathbf{I}_{Shunt}$ and $\mathbf{I}_{Leakage}$ were exploited. Through this experimental study, it was impossible to measure the radial current distribution on the actual wooden pole structure. Therefore, the ratio between $\mathbf{I}_{Shunt}$ and $\mathbf{I}_{Leakage}$ was used to demonstrate the performance of the mid-pole bonding system.

For this study, the leakage current was assumed to flow either from the insulator pin at the top section of the wooden pole or from the cross-arm to the ground. A shunt conductor was connected from the leakage current source to the metallic band at the middle section of the wooden pole i.e. at 3 m, 4 m and 5m from the top section. It was planned that the single-phase voltage supply be varied between 1kV to 11kV to simulate the consistency of the current ratio, $\mathbf{I}_{Ratio}$ between $\mathbf{I}_{Shunt}$ and $\mathbf{I}_{Leakage}$. However, the floating oscilloscope was turned off at the 10 kV voltage level. It is due to excessive current flow into oscilloscope through coaxial cables which exceed its limitation. Therefore the voltage supply was limited to 9 kV.

Figure 5.8 and Figure 5.9 show the $\mathbf{I}_{Leakage}$ and $\mathbf{I}_{Shunt}$ distribution for the tested wooden pole with mid-pole bonding system. As the voltage supply increased, the $\mathbf{I}_{Leakage}$ moved upward until 9 kV limited by 4 MΩ resistor. $\mathbf{I}_{Shunt}$ also increased, depending on where the shunting cable was terminated. For example, by shunting the leakage current from the top of the wooden pole to the metallic band at 5 meters from the top section at 9 kV voltage level, 2.04 mA $\mathbf{I}_{Leakage}$ and 1.22 mA $\mathbf{I}_{Shunt}$ was recorded, as shown in Figure 5.8(c). For a similar condition with leakage

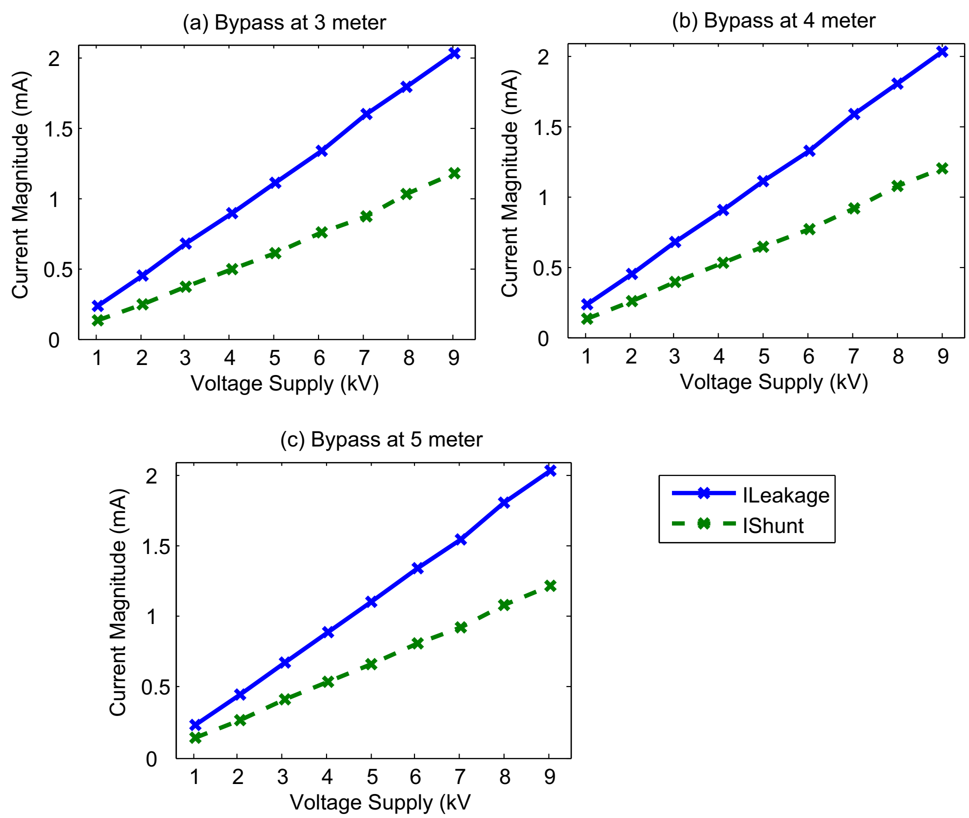

Figure 5.8: Mid-pole bonding system on wooden pole for leakage current from top section of wooden pole to ground

current flow from the cross-arm insulator pin, 1.85 mA $\mathbf{I}_{Leakage}$ and 1.04 mA $\mathbf{I}_{Shunt}$ was observed, as depicted in Figure 5.9(c). Based on these readings, at least 50% of leakage current magnitude was successfully diverted to the middle section of the wooden pole.

Table 5.1 summarized the results of the $\mathbf{I}_{Ratio}$ percentage recorded during the lab testing. For example, almost 60.32% and 57.00% $\mathbf{I}_{Leakage}$ were diverted through the shunting cable to the metal band at 5-meter position in the lab experiments for both cases. On the other hand, less percentage of $\mathbf{I}_{Ratio}$ was computed from the floating oscilloscope during lab testing in the case of leakage current which started

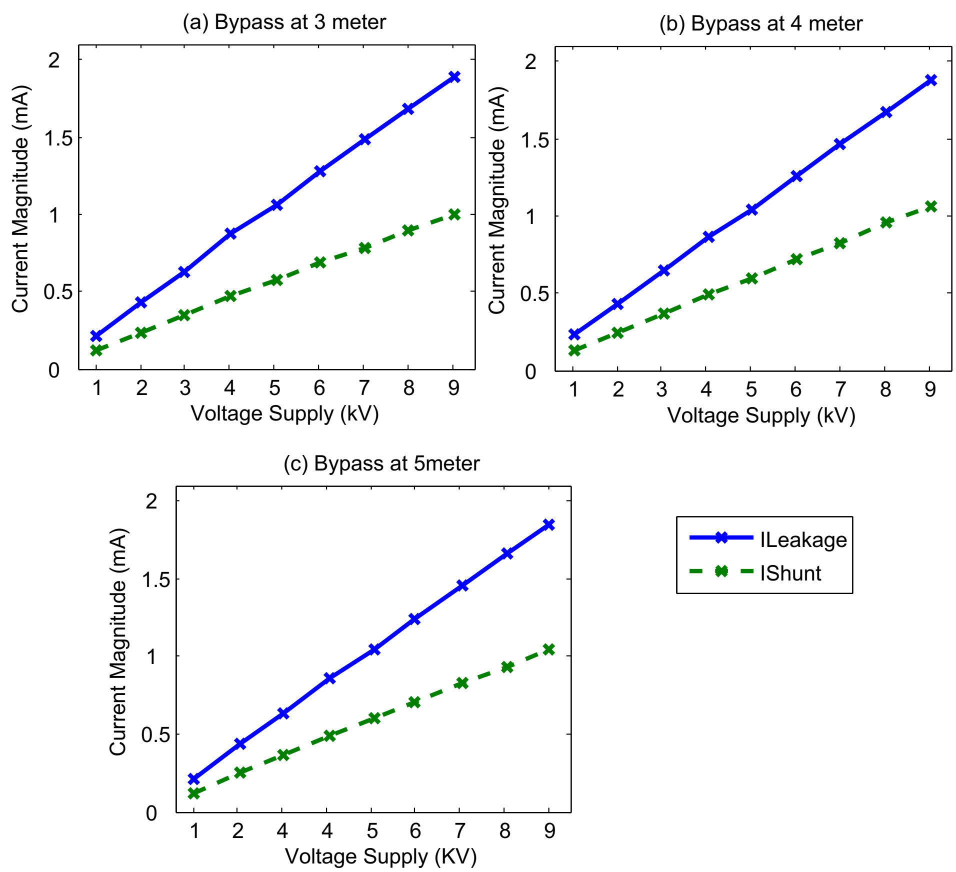

Figure 5.9: Mid-pole bonding system on wooden pole for leakage current from cross-arm to ground

to flow at the cross-arm. For example, about 53.93% and 56.96% $\mathbf{I}_{Leakage}$ were shunted at 3 and 4 meters compared to that in the case of the leakage current from the top of wooden pole. In addition, a simulation study for the $\mathbf{I}_{Ratio}$, was set up for the mid-pole bonding system. As shown in Table 5.2, the simulation results had a higher $\mathbf{I}_{Ratio}$ compared to the experimental test for both test conditions. Overall, the percentage of the $\mathbf{I}_{Ratio}$ magnitude decreased as the metallic band termination moved far from the ground. For instance, 74.95% $\mathbf{I}_{Leakage}$ was diverted at 5 meters and it reduced to 71.92% for leakage current at 3 meters from the top of the wooden

	$\mathbf{I}_{Ratio}$ for mid-pole bonding system		
Experimental Setup	Bypass at 3m	Bypass at 4m	Bypass at 5m
Leakage Current from top of Wooden Pole	56.05%	58.42%	60.32%
Leakage Current from cross-arm	53.93%	56.96%	57.00%

Table 5.1: Average I_{Ratio} for both experimental setups at each bypass termination

	I_{Ratio} for mid-pole bonding system		
Simulation Setup	Bypass at 3m	Bypass at 4m	Bypass at 5m
Leakage Current from top of Wooden Pole	71.92%	73.49%	74.95%
Leakage Current from cross-arm	80.25%	81.39%	82.45%

Table 5.2: Average I_{Ratio} for both simulation setups at each bypass termination

pole. Based on these studies, the mid-pole shunting system successfully reduced the amount of current flowing through the wooden pole structure by shunting the severe leakage current away from the burning spot i.e. the wooden pole cross-arm junction.

5.4 Thermographic Study of Cross-Arm

Wooden cross-arm has been used around the world as a preferred support structure for insulators in electrical distribution networks. Wooden cross-arm offers excellent electrical and mechanical performance and is known to have a service lifespan of more than 20 years [153]. In recent years, across the world, many of the existing wooden cross-arms have been replaced by stainless steel cross-arms or fibre cross-arms. This is due to the fact that wooden cross-arm is prone to pocket-burning or fire in areas that are subjected to high-level pollution, dust and salt spray. In the coastal areas where heavy salt spray from seas is high, the contaminated layer on the insulator surfaces degrades the surface resistivity. As discussed in Chapter 2, Chapter 3 and Chapter 4, the leakage current flow due to surface contamination can reach hundreds of milliamperes and cause spot burning and pole-top fire.

The main objective of this study was to investigate the thermal and electrical properties of cross-arm on wooden pole. This study showed the thermal distribution in stainless steel cross-arm and compared it with wooden cross-arm. This thermographic study was performed using a Thermovision A320 thermal camera measuring the spot temperatures at the king bolt and pole-cross-arm sections and adjacent surfaces for 60 minutes duration. The time-lapse images of the heating process are presented. As part of this study, a thermographic study based on the mid-pole bonding system is also presented. Finally, most of the results presented in this section were presented in a published paper [154].

5.4.1 Thermographic Study of Wooden Cross-Arm with Leakage Current of 5 mA and 14 mA

There are many past studies which focus on the leakage current level on high voltage insulators. However there is a lack of knowledge in the heating process of the supporting structure due to the high level of leakage current. Many past researchers have suggested that the heating process was mainly contributed to by the micro-arc that took place at the metal-wood interface in the insert. The following results are based on the time-lapse images taken by a thermal camera of respectively cross-arm at, 5 mA (with 2MΩ resistor) and 14 mA (with 100kΩ resistor) leakage current level.

Figure 5.10 and Figure 5.11 illustrates the heating process at the wooden cross-arm for the 6.5-meter wooden pole. The spot temperatures that are shown in these figures represent the temperature at the metallic surface of the king bolt (spot 1), the temperature at the wood surface (spot 2), the temperatures at the cross-arm and pole interface (spot 3) and the temperature at the surface of the cross-arm (spot 4). The temperature measurement at spot 1 is the most critical in this study. The initial temperature at spot 1 was 23.7^{o}C before the 5mA current was applied.

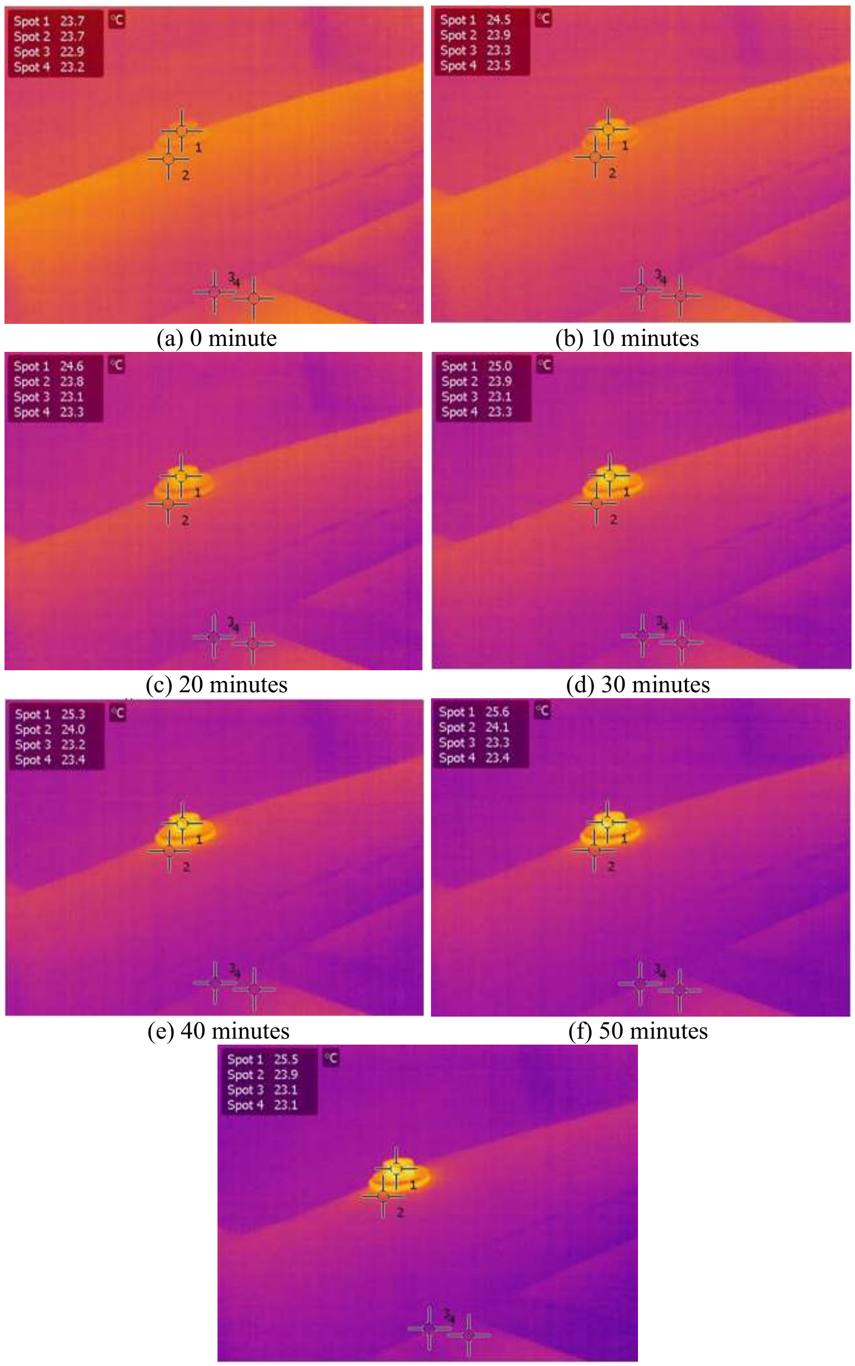

(a) 0 minute
(b) 10 minutes
(c) 20 minutes
(d) 30 minutes
(e) 40 minutes
(f) 50 minutes
(g) 60 minutes

Figure 5.10: Thermographic images for wooden cross-arm at 5 mA

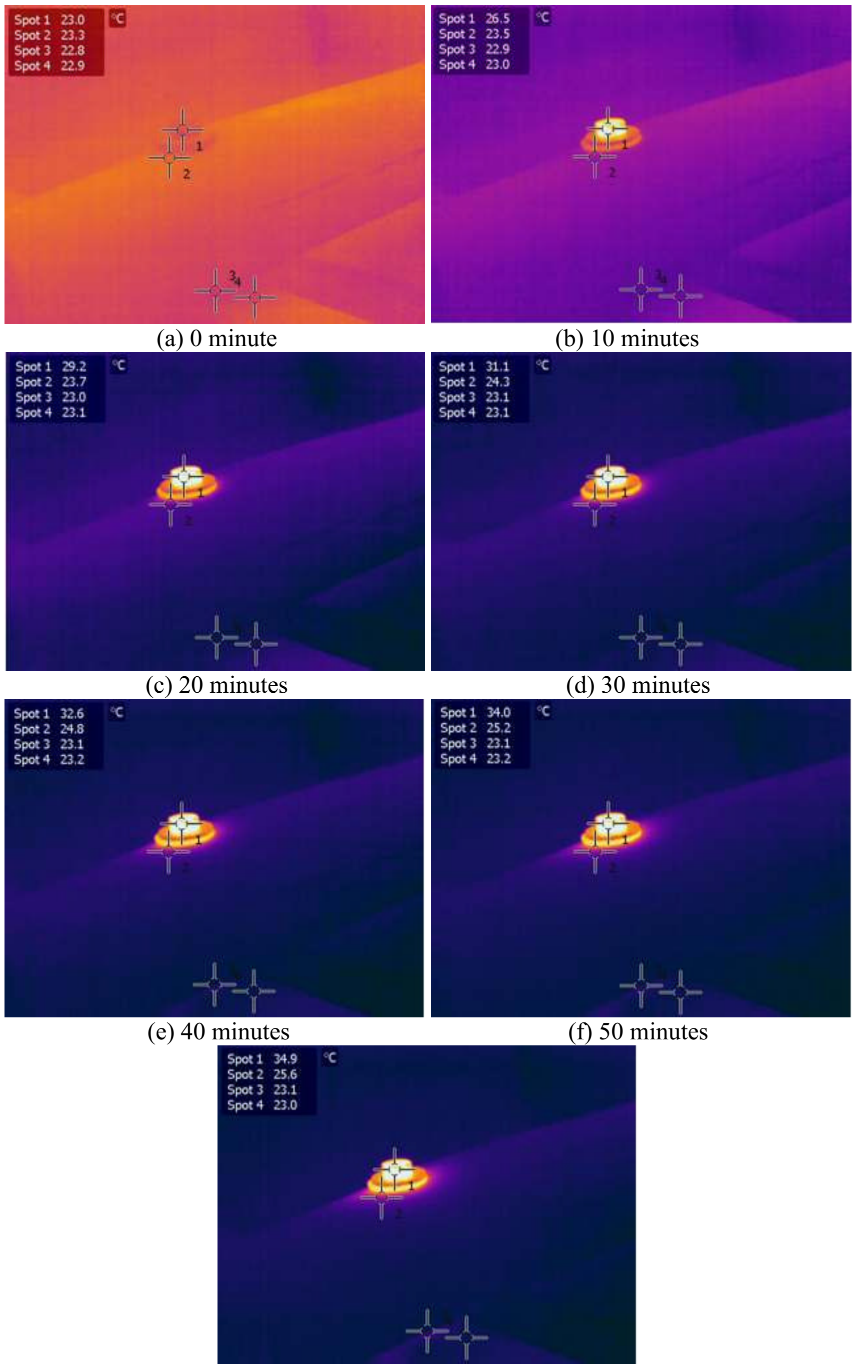

(a) 0 minute (b) 10 minutes

(c) 20 minutes (d) 30 minutes

(e) 40 minutes (f) 50 minutes

(g) 60 minutes

Figure 5.11: Thermographic images for wooden cross-arm at 14 mA

When the 11 kV high voltage supply was switched on, the temperature at spot 1 increased to 24.5^{o}C in a period of 10 minutes and finally reached 25.5^{o}C at the end of the test period. On the other hand, the temperature at spots 2,3 and 4 did not experience the same level of temperature rise and the final readings were 23.9^{o}C, 23.1^{o}C and 23.1^{o}C respectively. A maximum change of 1.8^{o}C was observed at spot 1 after 60 minutes testing.

In the case of 14 mA, the temperature at spot 1 increased from the initial value of 23.0^{o}C to 26.5^{o}C after a 10-minute period. The temperature continued to rise gradually to 29.2^{o}C after 20 minutes and finally a maximum temperature of 34.9^{o}C was recorded at the end of the test period. The temperature at spots 2, 3 and 4 also showed some changes as depicted in Figure 5.11. A maximum of 11.9^{o}C was observed at spot 1 after 60 minutes testing.

5.4.2 Thermographic Study of Steel Cross-Arm with Leakage Current of 5 mA and 14 mA

Figure 5.12 and Figure 5.13 depict the time-lapse thermographic images of the heating process of the stainless steel cross-arm at 5 mA and 14 mA. A similar 2 MΩ and 100 kΩ current limiter was used with 11 kV voltage supply to simulate the leakage current level. The temperature at spot 1 increased from 22.4^{o}C at 0 minutes to 23.2^{o}C in a 10-minute period at 5 mA. This spot temperature grew steadily to 25.3^{o}C in the 60-minute testing period. A maximum change of 2.9^{o}C was observed at spot 1 after a 60-minute test. In contrast, for 14 mA leakage current level, the temperature reading at spot 1 increased gradually from an initial temperature of 22.5^{o}C to 25.2^{o}C after 10 minutes. The temperature of the king bolt changed progressively to 27.0^{o}C after 20 minutes and reached 31.0^{o}C at the end of the 60-minute test. A maximum change of 8.5^{o}C was observed at spot 1

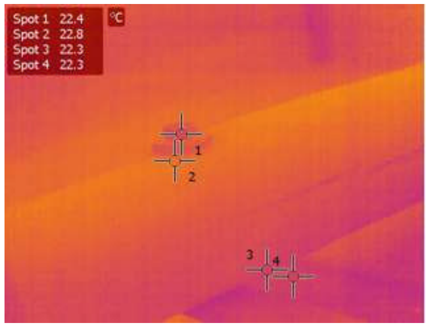

(a) 0 minute

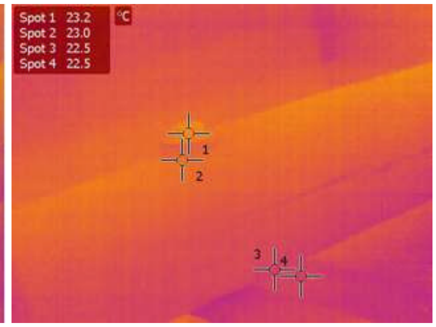

(b) 10 minutes

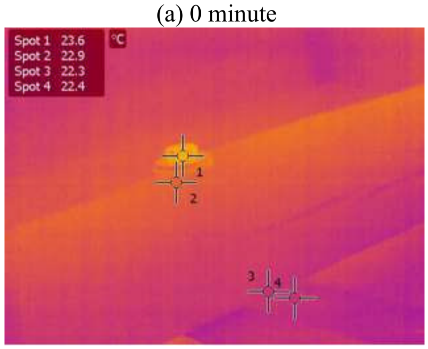

(c) 20 minutes

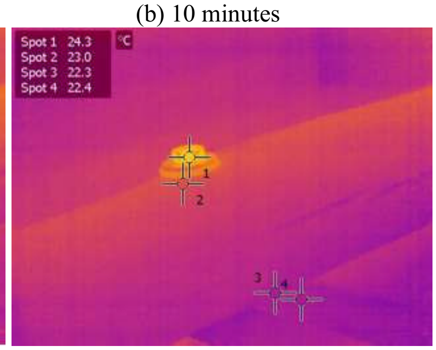

(d) 30 minutes

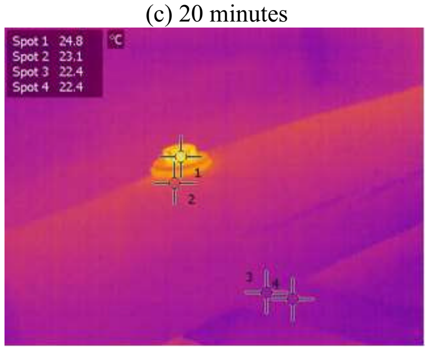

(e) 40 minutes

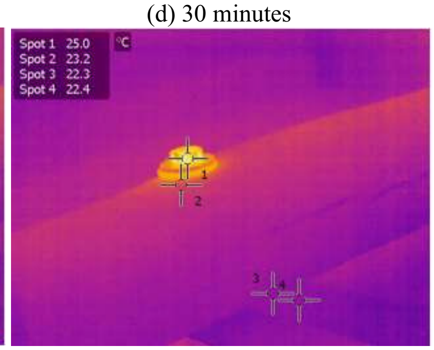

(f) 50 minutes

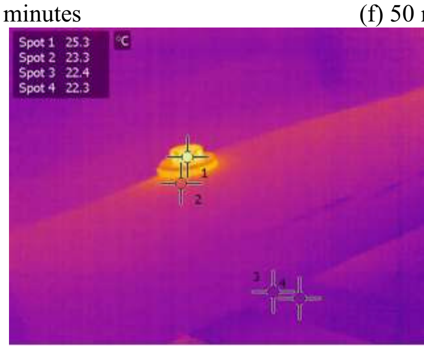

(g) 60 minutes

Figure 5.12: Thermographic images for steel cross-arm at 5 mA

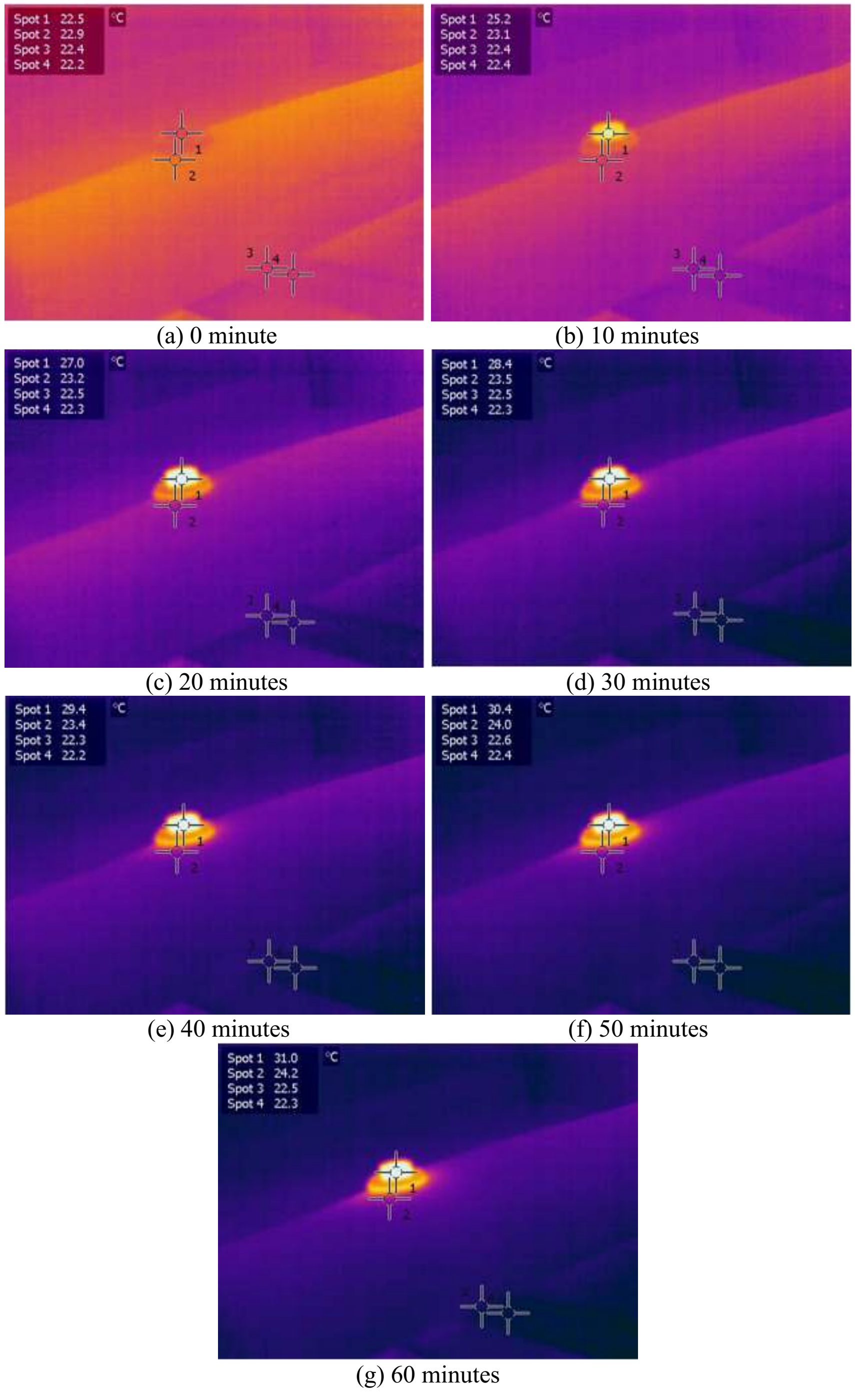

Figure 5.13: Thermographic images for steel cross-arm at 14 mA

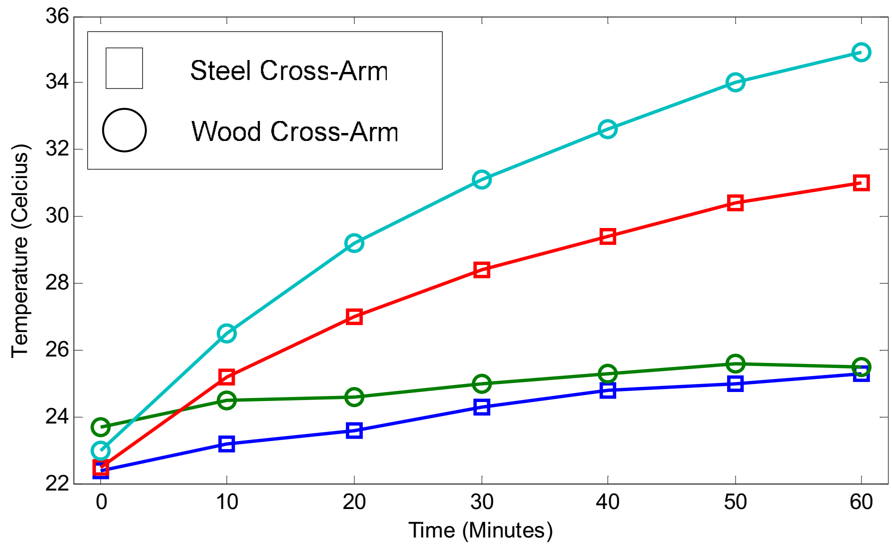

Figure 5.14: King bolt temperature for steel and wooden cross-arm

after 60 minutes' testing.

When the pole was subjected to a low leakage current level of 5 mA, both types of cross-arm showed a similar heating process. On the other hand, these two cross-arms went through a different heating process when subjected to higher leakage current. The heating rate of the king bolt at the steel cross-arm was far less compared to that of the wooden cross-arm, as shown in Figure 5.14. From our results, it is clearly shown that the king bolt experiences the highest temperature rise compared to other spot measurements during the test period. This is due to the fact that the king bolt has a higher thermal conductivity compared to wood. In terms of reducing the risk of pole-top fire or pocket burning, the thermographic test results showed that the steel cross-arm didn't give much benefit compared to the benefits of wooden cross-arm. During the one-hour test period, an unpleasant smell was noticed at 15 mA leakage current level. At this stage, the scent of wood burning could be detected within the laboratory. In particular, a small burnt spot was detected at the wood with king bolt washer and nails for aluminium plate which located at the bottom section of wooden pole during visual inspection.

5.4.3 Thermographic Study of Mid-Pole Bonding System

The mid-pole bonding system was used to reduce the heating effect of the king bolt. This current diverter system was installed on the wooden pole with a steel cross-arm which diverted the leakage current through the shunting cable to a metallic band located at 5 meters from the top of the wooden pole. Figure 5.15 shows the heating process for the steel cross-arm over a two-hour period. The temperature reading was taken from spot 1 and it is clearly demonstrated that the mid-pole bonding system reduced the temperature by 0.6^{o}C. As shown in Figure 5.15, the king bolt temperature increased from 23.0^{o}C to 24.4^{o}C for the setup without a mid-pole bonding system during the two-hour test period. This is equivalent to a

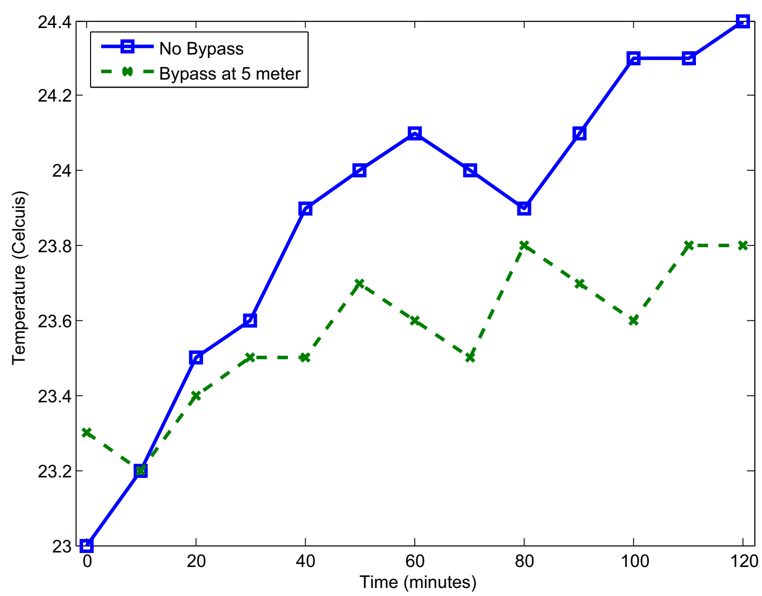

Figure 5.15: Comparison of king bolt temperature with steel cross-arm

change of 1.4^{o}C. In contrast, the king bolt temperature rose slowly from 23.3^{o}C to 23.8^{o}C and a change of 0.5^{o}C was observed. Based on this study a large amount of leakage current magnitude was bypassed through the shunting cable and reduced the radial current concentration effect on the king bolt. Therefore the mid-pole bonding system successfully reduced the leakage current effect on the king bolt.

As part of this study, we also demonstrated the effectiveness of the mid-pole bonding system on the wooden pole structure. This mid-pole bonding system managed to reduce the heating effect at the king bolt, as illustrated in Figure 5.16. By extending the results in Figure 5.15 with a linear regression method, the best fitting line of the king bolt temperature was plotted for the next ten-hour testing period. This linear regression method was used to predict and estimate the

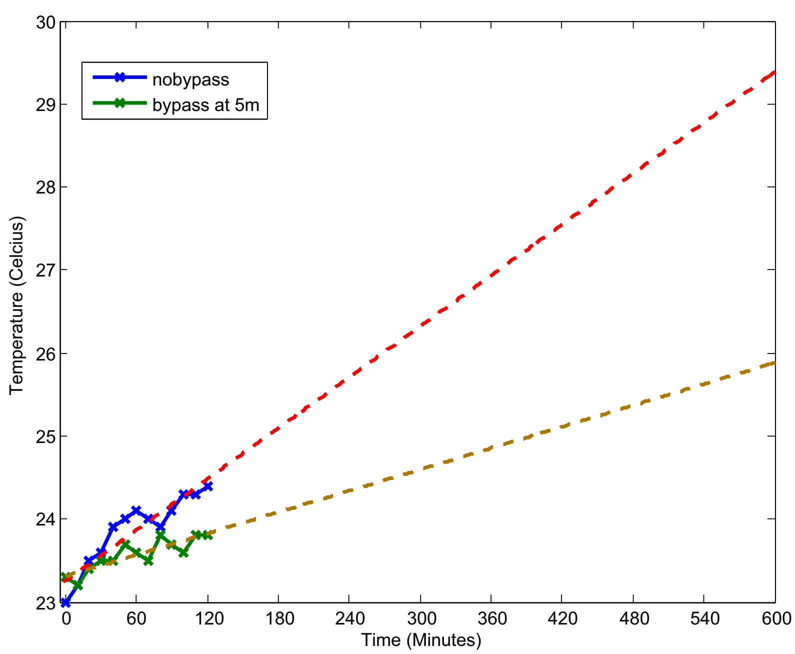

Figure 5.16: Linear regression of king bolt temperature with mid-pole bonding system for steel cross-arm

temperature of the king bolt, based on the least square approach of the recorded data. As shown in Figure 5.16, about 29.4 degree Celsius of the king bolt temperature can be reduced to 25.8^{o}C with the mid-pole bonding system over a ten-hour period. This is equivalent to a difference of 3.6^{o}C. In conclusion, a slow king bolt temperature development is significant in the long term and will decrease the degree of thermal generated at the king bolt.

5.5 Summary

This chapter investigated the performance of the mid-pole bonding system and the thermal characteristics of steel and wooden cross-arms at different levels of leakage current. This research was conducted at the RMIT University High Voltage Laboratory. The leakage current flow due to surface contamination on the insulator increased the king bolt temperature to a hazardous level on both cross-arms. High leakage current caused the king bolt to heat up at a more rapid rate than low leakage current. The recorded thermographic images provided a more highly accurate spot temperature reading of the heating process on the king bolt. In addition, the mid-pole bonding system successfully reduced the risk of raised temperature at the king bolt, especially in the long term. The results offer new insights into the initial stage of pole-top burning at the king bolt junction. Continuous monitoring of the king bolt temperature should be included as part of regular wooden pole inspection and any asset management program. Finally, the comparative study between testing and simulation also shows the huge potential of the new mid-pole bonding system. In conclusion, this mid-pole bonding system has significant potential to eliminate the risk of pole-top fire by diverting a large amount of leakage current and thereby reducing the heating effect of the king bolt.

Chapter 6

Conclusions and Future Works

Pole-top fire in electrical distribution networks has become a great concern to all utility companies in their effort to provide reliable, secure and safe power supply to customers. The two main causes of pole-top fire—a mechanical failure on a wooden pole structure causing power supply interruption, and sparks triggered by falling live lines in dry vegetation areas—have already become a common issue discussed in the media. Power provider agencies are working hard to maintain, improve and upgrade their assets, so that these issues and any associated problems can be minimized and avoided. At the same time, extensive and continuous research work at a higher education level can support and provide advanced solutions for the current related issues.

This thesis commenced with the objective of understanding a wooden pole ladder network model for the pole-top fire issue. To achieve this, the author manipulated and modified the existing ladder network model onto a completed structure of a distributed wooden pole. The model developed by the author demonstrates a new accomplishment in leakage current effect in wood.

This research program presented an analytical procedure using computer simulations and experimental work, which is presented as follows:

1. A comprehensive examination of the ladder network model consisting of sapwood, radial and heartwood resistances influenced by CCA treatment and moisture levels in wood, together with the leakage current effect related to pole-top fire.
2. Modification of the existing ladder network model to include the wooden cross-arm, steel cross-arm and Ross shunting methods in the current model.
3. The introduction and proposition of an original mid-pole bonding system to overcome leakage current concentration at the wooden pole cross-arm junction.
4. A cross-examination in a high-voltage laboratory of the computer model and the real wooden pole, both with mid-pole bonding, in terms of their leakage current bypass percentage.
5. A thermal characterization of the wooden cross-arm, steel cross-arm and mid-pole bonding system with wooden pole using a thermographic camera.

In the next section, conclusive statements that show the major findings in this research program and recommendations for future works will be presented.

6.1 Conclusions

The research program goals have been successfully accomplished by developing and manipulating the ladder network model of wooden pole for pole-top fire research. As a result, many significant outcomes have been discovered in the field of pole-top fire study on an 11 kV distribution network 3-phase system. From these achievements, all the outcomes and original contributions are summarized and listed below:

- A computer model of wooden pole has been successfully developed in a MATLAB environment, based on the ladder network principles. Type of treatment i.e. CCA-treated, moisture levels of the wood, realistic pole dimensions, step size, levels of insulator surface contamination are included respectively. A king bolt was inserted into the 16 sections of wooden pole and the resulting built model became the foundation of the research work. To the author's knowledge, this is the first pole-top fire research study that is based on the established ladder network model.

- To the best of the author's knowledge, a radial current distribution result of the developed model is a novel discovery in terms of explaining the leakage current effect on wooden pole structures. Compared to the sapwood and heartwood current distribution along 16 sections of wooden pole, the metal insertion effect with radial current distribution is clearly shown. The influence of moisture content in the wood significantly changes the resistances of the developed ladder network whereby wet conditions cause a higher leakage current concentration at the metal insertion in contrast to the concentration under dry weather conditions.

- A new completed wooden pole model with wooden cross-arm was developed and introduced onto the ladder network model. This original development was based on the author's critical thinking which resulted in the king bolt being manipulated as a reference point before introducing it from the point of radial resistance of the cross-arm. The heartwood resistances were not included, due to the wooden cross-arm's physical appearance. The effect of a loosed bolt was able to be included, which was represented by air resistance that is parallel with a king bolt resistance at section 14 of the wooden pole. Another secured bolt was introduced in this model to hold the cross-arm firmly on a wooden pole with steel bar holders. It caused another leakage current concentration point, especially at section 13 of the wooden pole.

- The copper jumper and copper cross-arm band electrical connections of the P.M Ross shunting techniques were also successfully introduced into the enhanced wooden pole model. Two Ross shunting methods were developed and used for mitigation performance study purposes. Based on computer simulation work, the Ross shunting techniques failed to reduce leakage current concentration at sections 14 and 13. Copper-band configurations clearly increased radial current magnitude at sections 13 and 14 in the case of single-phase leakage current. A small reduction at section 14 was recorded for the Ross shunting method in the case of phase-to-phase leakage current; this is not very significant for overall performance.

- A new steel cross-arm model was successfully introduced in this research work. Similar to the wooden cross-arm, two steel bar holders were included to keep it steady on the wooden pole structure. Interestingly, the radial current distribution of this configuration is the same as that of the wooden cross-arm. It can be concluded then that the steel cross-arm did not decrease the risk of pole-top fire.

- The novel mid-pole bonding system was successful in overcoming the leakage current concentration at the wooden pole cross-arm junction for all study cases. All the limitations of Ross's shunting techniques and steel cross-arm were eliminated using this new mitigation method. By mitigating the leakage current from pin insulators with insulated conductors, and securing a metal band at the bottom section of the wooden pole, the magnitude of current concentration at sections 13 and 14 were reduced significantly. Based on the simulation study of the ladder network model, the risk of pole-top fire can be eliminated by implementing this technique on a wooden pole structure. The comparative summary of the simulation work is shown in Table 4.4.

- Critical experimental work was successfully performed in the RMIT high voltage laboratory to verify the performance of the mid-pole bonding system on a 6.5 meter wooden pole structure. Another ladder network computer model was also successfully developed to imitate the tested pole dimension, type of treatment and also the moisture level of the wood. A specially designed metallic band from aluminium sheet was used for the mid-pole bonding system testing. More than 50% leakage current was bypassed through shunting cable in the laboratory study, compared to 70% in the simulation work. If the test is done with a 12-meter wooden pole length, better results will be recorded for the mid-pole bonding system.

- The temperature growth under the influence of leakage current at the wooden pole cross-arm junction was successfully recorded and monitored with a thermographic camera. It shows that the development of temperature on the king bolt is almost similar in steel and wooden cross-arm. It proves that there is no significant contribution from steel cross-arm, the mechanical strength of which is greater than that of wood. Finally, the success of the mid-pole bonding system is shown in terms of temperature development on the king bolt, which records a very small temperature change compared to that in a normal setup.

In conclusion, based on a simulation study, this research work clearly demonstrates the successful implementation and potential of ladder network model in explaining pole-top fire problem. The flexibility of the ladder network model for allowing further improvement and extension is highly appreciated by the author and will lead to wider and more comprehensive research work to overcome the disadvantages of current solutions. A new mid-pole bonding system that offers simple implementation and a low cost solution should be utilized by distribution companies for their electrical distribution networks. Hopefully, this work will contribute much to this field of research and provide benefits to humankind.

6.2 Recommendation for Future Work

In order to have research continuity in this field, a few recommendations have been identified which have large research potential throughout this research work. The proposed exploration work for the future includes:

1. Further Development of Ladder Network Model

    - The new wooden pole ladder network model is based on the combined resistances of sapwood, radial and heartwood which are distributed throughout the numerous pole sections from the top to the bottom. The author believes that by dividing each section into small segments, the leakage current concentration on the metal insertion could be localized to small segments of the pole section. This will result in very detailed simulation work on the wooden pole model.
    - To include other variables such as capacitive and inductive parameters into the ladder network model which demands advanced critical thinking

and a deeper understanding on the part of interested researchers. The author believes it will provide significant and interesting results in terms of explaining pole-top fire events. It could be used for further investigation on an impulse study of the ladder network model.

2. Further investigation to determine another significant parameter that can be used to explain the metal insertion effect on wooden pole structures using finite element method. It is possible to display the effect of king bolt with a voltage distribution or other parameters from the ladder network model.

3. Further investigation to determine the BIL of the mid-pole bonding system on the wooden pole structure.

4. The actual on-site installation of a mid-pole bonding system in a distribution network, especially for very high-risk fire prone areas. This implementation could provide further understanding of the mid-pole bonding system in terms of its effectiveness and performance. Technical modifications for further improvements can be made according to on-site conditions. Currently, the Horizon Power company in Western Australia has expressed interest in applying this new method in their electrical distribution network. Discussions are still at an early stage and hopefully this mid-pole bonding system can be installed on their wooden poles soon.

5. A continuous monitoring of king bolt temperature as a part of asset management action in a distribution network.

Appendix A

Wooden Pole

Section	**Height (m)**	**l (m)**	**r (m)**	**R (m)**	**P (m)**	$\mathbf{A}_s$ **(m^2)**	$\mathbf{A}_h$ **(m^2)**
1	0.00 to 0.75	0.75	0.142	0.181	0.0395	0.0352	0.0633
2	0.75 to 1.50	0.75	0.138	0.177	0.0388	0.0336	0.0600
3	1.50 to 2.25	0.75	0.134	0.172	0.0382	0.0322	0.0567
4	2.25 to 3.00	0.75	0.130	0.168	0.0375	0.0307	0.0535
5	3.00 to 3.75	0.75	0.126	0.163	0.0367	0.0292	0.0505
6	3.75 to 4.50	0.75	0.123	0.159	0.0360	0.0278	0.0476
7	4.50 to 5.25	0.75	0.119	0.154	0.0353	0.0264	0.0447
8	5.25 to 6.00	0.75	0.115	0.150	0.0347	0.0251	0.0419
9	6.00 to 6.75	0.75	0.111	0.145	0.0340	0.0238	0.0391
10	6.75 to 7.50	0.75	0.107	0.141	0.0334	0.0226	0.0365
11	7.50 to 8.25	0.75	0.104	0.136	0.0326	0.0213	0.0341
12	8.25 to 9.00	0.75	0.100	0.132	0.0319	0.0201	0.0316
13	9.00 to 9.75	0.75	0.096	0.127	0.0312	0.0189	0.0293
14	9.75 to 10.50	0.75	0.092	0.123	0.0306	0.0178	0.0270
15	10.50 to 11.25	0.75	0.089	0.118	0.0298	0.0166	0.0249
16	11.25 to 12.00	0.75	0.085	0.114	0.0293	0.0156	0.0228

Table A.1: Physical dimensions of pole

Section	**Height (m)**	**R_s (MC%)**	**R_h (MC%)**	**R_s (Ω)**	**R_h (Ω)**	**R_r (Ω)**
1	0.00 to 0.75	16.70	30.00	1874977.045	493.55	3431207.99
2	0.75 to 1.50	16.70	25.35	1961289.153	7575.22	3589159.15
3	1.50 to 2.25	11.70	20.70	36426610.62	116442.85	66660697.43
4	2.25 to 3.00	11.70	20.70	38186244.63	123317.59	69880827.66
5	3.00 to 3.75	11.70	20.70	40156301.72	130613.52	73486032.14
6	3.75 to 4.50	11.70	20.70	42200815.29	138801.85	77227491.99
7	4.50 to 5.25	11.70	20.70	44408514.51	147785.05	81267581.54
8	5.25 to 6.00	11.70	20.70	46662707.70	157669.40	85392755.09
9	6.00 to 6.75	11.70	20.70	49243544.43	168579.60	90115686.31
10	6.75 to 7.50	11.70	20.70	51893562.19	180662.70	94965218.82
11	7.50 to 8.25	11.70	20.70	55054912.41	193720.66	100750489.70
12	8.25 to 9.00	11.70	20.70	58392490.56	208662.28	106858257.70
13	9.00 to 9.75	11.70	20.70	62051127.12	225401.67	113553562.60
14	9.75 to 10.50	11.70	20.70	65858523.87	244239.23	120521098.70
15	10.50 to 11.25	11.70	16.70	70434822.89	2649451.55	128895725.90
16	11.25 to 12.00	11.70	16.70	74915930.82	2897558.42	137096153.40

Table A.2: Resistances of dry pole

Section	**Height (m)**	**R_s (MC%)**	**R_h (MC%)**	**R_s (Ω)**	**R_h (Ω)**	**R_r (Ω)**
1	0.00 to 0.75	27.70	30.00	3334.23	493.55	6101.64
2	0.75 to 1.50	27.70	30.00	3487.72	521.06	6382.52
3	1.50 to 2.25	22.70	30.00	64776.69	550.95	118541.34
4	2.25 to 3.00	22.70	30.00	67905.81	583.47	124267.63
5	3.00 to 3.75	22.70	30.00	71409.12	617.99	130678.69
6	3.75 to 4.50	22.70	30.00	75044.84	656.74	137332.05
7	4.50 to 5.25	22.70	30.00	78970.74	699.24	144516.46
8	5.25 to 6.00	22.70	30.00	82979.33	746.01	151852.17
9	6.00 to 6.75	22.70	30.00	87568.78	797.63	160250.86
10	6.75 to 7.50	22.70	30.00	92281.25	854.80	168874.69
11	7.50 to 8.25	22.70	30.00	97903.01	916.59	179162.52
12	8.25 to 9.00	22.70	30.00	103838.16	987.28	190023.83
13	9.00 to 9.75	22.70	30.00	110344.24	1066.49	201929.96
14	9.75 to 10.50	22.70	30.00	117114.85	1155.62	214320.18
15	10.50 to 11.25	22.70	27.70	125252.79	4711.46	229212.61
16	11.25 to 12.00	22.70	27.70	133221.45	5152.66	243795.26

Table A.3: Resistances of wet pole

Bibliography

[1] Bryan Wewers. Garden valley 34.5-kv distribution line. http://www.idahopower.com/images/aboutus/planningforfuture/projectnews/structureHorseshoeBend.gif.

[2] The stobie concrete pole. *Engineering*, 122:416–417, 1926.

[3] Swis pole top fire history. http://www.mediastatements.wa.gov.au/Lists/Statements/Attachments/120808/Swis\%20Pole\%20Top\%20Fire\%20History.pdf, 2004.

[4] Power line fault and bush fire near cape naturaliste lighthouse dunborough western australia. Technical Report EIS 2009-559, EnergySafety Western Australia, March 3 2009.

[5] Finding alternatives to persistent organic pollutants (pops) for termite management. Technical report, UNITED NATIONS ENVIRONMENT PROGRAMME (UNEP), 2000.

[6] The lightning phenomenon. http://www.seratech.com.sg/ionostar.htm.

[7] Transmission structures. http://www.atcllc.com/IT10.shtml.

[8] Hobbs. Pole top fire knocks out power along southmoor. http://www.pikespeakfreepress.com/?p=736, November 30 2008.

[9] Bushfire management plant 2007-2008. Technical report, Western Power, 2008.

[10] J.C. Jureit and A.C. Middleton. Pole bonding. Technical Report 3344225, United States Patent Office, 26 Sept. 1967.

[11] A.E. Loxton. Investigation into prevention of fires on 22kv wood pole lines. Eskom Report TRR/P98/510, 1998.

[12] Paul M. Ross. Wood structure burning by leakage current. *Electrical Engineering*, 66:472–474, 1947.

[13] 2009 victorian bushfires royal commission. `http://www.royalcommission.vic.gov.au/Commission-Reports`.

[14] Lesley Francis and Jack Norton. A review : Australian timber pole resources for energy network. Technical report, Department of Primary Industries & Fisheries, The State of Queensland, Australia, 2006.

[15] As 2209: Timber - poles for overhead lines. Technical report, Australian Standard, 1994.

[16] As1604: Specification for preservative treatment. Technical report, Australian Standard, 2005.

[17] R. Filter and J.D. Mintz. An improved 60 hz wood pole model. *IEEE Transaction on Power Delivery*, 5:442–448, 1990.

[18] Focue: Asset management. *Power Engineer*, 19(2):10 –11, april-may 2005.

[19] M.E. Beehler. Managing risk on available transmission capacity using performance contracting. In *IEEE 8th International Conference on Transmission*

Distribution Construction, Operation Live-Line Maintenance Proceedings, 1998., pages 167 –171, 26-30 1998.

[20] Iec 60826: Design criteria of overhead transmission lines. Technical report, International Electrotechnical Commission, October 1 2003.

[21] Bs en 50423-3:2005: Overhead electrical lines exceeding ac 1 kv up to and including ac 45 kv. Technical report, British Standard, December 2005.

[22] Roger A. Sedjo. Wood materials used as a means to reduce greenhouse gases (ghgs): An examination of wooden utility poles. *Mitigation and Adaptation Strategies for Global Change*, 7(2):191 – 200, 2002.

[23] Department of Sustainability and Environment Australia. Bushfire history - major bushfires in victoria. `http://www.dse.vic.gov.au/DSE/nrenfoe.nsf/childdocs/-D79E4FB0C437E1B6CA256DA60008B9EF?open`, November 10 2009.

[24] Geraldine Mitchell. Faulty fitting blamed for black saturday fire disaster. `http://www.heraldsun.com.au/news/special-reports/faulty-fitting-blamed-for-black-saturday-fire-disaster/story-fn4chuwg-1225799760632`, November 19 2009.

[25] Jane Cowan. Powerline inspection failures out in the open. `http://www.abc.net.au/news/stories/2009/11/24/2751722.htm`, November 24 2009.

[26] Jane Cowan. Lifting the shroud: Powerlines and the kilmore fire. `http://www.abc.net.au/news/stories/2009/11/23/2751068.htm`, November 23 2009.

[27] Bushfire near river and folewood roads toodyay western australia. Technical report, EnergySafety Western Australia, Febuary 15 2010.

[28] B.Wareing. *Wood Pole Overhead Lines*. The Institution of Electrical Engineers, 1st edition, 2005.

[29] Paul C. Gargiulo. *Utility Poles, Preservatives and Soil Contamination*. PhD thesis, Faculty in Earth and Environmental Science, The City University of New York, 2000.

[30] Michael Daniel Folse. *Probability Based Design of Wood Pole Transmission Structures*. PhD thesis, Civil Engineering Department, Colorado State University, 1981.

[31] Roger A. Sedjo. Wood material used as a means to reduce greenhouse gases (ghgs): An examination of wooden utility poles. *Mitigation and Adaptation Strategies for Global Change*, 7(2):191–200, June 2002.

[32] B. Hart. Hv overhead line-the scandinavian experience. *Power Engineering Journal*, 8(3):119–123, Jun 1994.

[33] Flavio L.R. Vidor, Marcal Pires, Berenice A. Dedavid, Pedro D.B. Montani, and Adriano Gabiatti. Inspection of wooden poles in electrical power distribution networks in southern brazil. *IEEE Transaction on Power Delivery*, 25(1):479–484, Jan 2010.

[34] As 5604: Timber - natural durability ratings. Technical report, Australian Standard, 2005.

[35] Wood preservation. Technical report, NSW Heritage Office, March 1998.

[36] R.E. Harness and E.L. Walters. Woodpeckers and utility pole damage. *IEEE Industry Applications Magazine*, 11(2):68–73, March 2005.

[37] N.K. Wallis. *The Australian Timber Handbook*. Angus and Robertson Ltd, 3rd edition, 1970.

[38] J.J.Morrell. *Wood pole maintenance manual*. Forest Research Laboratory, Oregon State University, 1996.

[39] R.H. Colley. Poles and pole treatment. *Electrical Engineering*, 61(9):685–691, Sept. 1942.

[40] George M. Hunt. Wood pole practice vi : Treatments and processes for preservation of poles. *Journal of Electric Light and Power*, 7(1):58–70, Jan. 1929.

[41] Mat Darveniza. *Electrical Properties of Wood and Line Design*. University of Queensland Press, St. Lucia, 1st edition, 1980.

[42] E.Brandt, N. Becker, H. Pohlmann, H.J. Fuchs, H. Muller, W. Booz, and G. Thierauf. Structural stability and reliability of various designs of medium-voltage overhead-line constructions. In *10th International Conference on Electricity Distribution*, pages 173–178. IEE Conference Publication, May 1989.

[43] J.D. Maclean. The preservative treatment of various species for poles and crossarms. *Electrical engineering*, 65:549–554, Augt-Sept. 1946.

[44] R. Filter. The influence of wood pole preservatives on wood fire and electrical safety. *IEEE Transactions on Power Apparatus and Systems*, 103:3089–3095, 1984.

[45] G.E. Phillips and D.E. Mclear. Treatment effects and strength grading for cca treated red pine poles. *IEEE Transactions on Power Delivery*, 4(2):1262–1268, April 1989.

[46] Sandor Poncsak, Duygu Kocaefe, Ramdane Younsi, Yasar Kocaefe, and

Louis Gastonguay. Thermal treatment of electrical poles. *Wood Science and Technology*, 43(5-6):471–486, August 2009.

[47] Ieee guide for preservative treatment of wood distribution and transmission line structures. IEEE Standard 1217-2001, IEEE Power Engineering Society, 2001.

[48] James R. Goodman and Andrew H. Stewart. Wood pole management - utility case studies. *IEEE Transactions on Power Delivery*, 5(1):422–426, 1990.

[49] Nelson G. Bingel III and Phil J. Halsch. Utility pole computerized maintenance management systems. In *Proceedings of the IEEE International Conference on Transmission and Distribution Construction and Live Line Maintenance, ESMO*, pages 340–345, 1998.

[50] Robert F. Nelson. Reliability-centered power line management - inspection process, measurement techniques and data management considerations. In *Proceedings of the 1998 IEE Colloquium on Distribution Overhead Lines - Economics, Practice and Technology of Reliability Assessment*, pages 3/1–3/24, May 1998.

[51] Steve Horsman. Condition and design assessment of wood pole overhead lines. In *IEE Colloquium (Digest)*, pages 15–22, March 2000.

[52] D. Hughes. Component issues. In *IEE Colloquium (Digest)*, pages 9–14, 2000. March.

[53] C. Glover. Asset management: reliability centred maintenance and overhead lines. In *IEE Seminar on Improved Reliability of Woodpole Overhead Lines*, pages 5/1–5/5, March 2000.

[54] Flavio L.R. Vidor, Marcal Pires, Berenice A. Dedavid, Pedro D.B. Montani, and Adriano Gabiatti. Inspection of wooden poles in electrical power distribution networks in southern brazil. *IEEE Transactions on Power Delivery*, 25(1):479–484, 2010.

[55] F.M. Gravito and N.D.S. Filho. Inspection and maintenance of wooden poles structures. In *Transmission and Distribution Construction, Operations, and Live Line Maintenance (ESMO) Conference*, pages 151–155, April 2003.

[56] M. Newbill. Bonnaville power administration's wood pole management program. In *Transmission and Distribution Construction and Live Line Maintenance 1993*, pages 185–198, Sept. 1993.

[57] C.C. Whitworth, A.W.G. Duller, D.I. Jones, and G.K. Earp. Aerial video inspection of overhead power lines. *Power Engineering Journal*, 15(1):25–32, Feb. 2001.

[58] Jason R. Stack, Ronald G. HArley, Paul Springer, and James A. Mahaffey. Estimation of wooden crodd-arm integrity using artificial neural network and laser vibrometry. *IEEE Transaction on Power Delivery*, 18(4):1539–1544, October 2003.

[59] J. Frate, D. Gagnon, R. Vilandre, and R. Dansereau. Evaluation of overhead line and joint performance with high-definition thermography. In *Transmission and Distribution Construction, Operation and Live Line Maintenance Proceeding*, pages 145–151, 2000.

[60] E. Ezer. Measurement of wood pole strength-polux a new nondestructive inspection method. In *Rural Electric Power Conference*, pages 6/1–6/7, 2001.

[61] K. Hamami Khalid, Ng Kok Cheong, and S.A. Fuad. Microwave reflection sensor for determination of decay in wooden pole cross-arms. In *Properties and Application of Dielectric Material*, pages 595–598, 2000.

[62] K.M. Tsang and W.L. Chan. Overhead line wooden pole condition sensing by acoustic method. *Sensor and Actuator A : Physical*, 143(2):251–255, 2008.

[63] A. Douglas Shaw. Sonic vibration technique for rot detection in wood poles. *IEEE Transaction on Instrumentation and Measurement*, 23(3):240–244, 1974.

[64] Yoshiro Tomikawa, Yukiharu Iwase, Kishio Arita, and Hiroaki Yamada. Nondestructive inspection of a wooden pole using ultrasonic computed tomography. *IEEE Transaction on Ultrasonic, Ferroelectrics and Frequency Control*, 33(4):354–358, July 1986.

[65] J.L. Sandoz and O. Vanackere. Wood poles ageing and non destructive testing tool. In *14th International Conference and Exhibition on Electricity Distribution*, pages 26/1–26/6, June 1997.

[66] A. Wyckhuyse and X. Maldague. A study of wood inspection by infrared thermography, part i: Wood pole inspection by infrared thermography. *Research in Nondestructive Evaluation*, 13(1):1–12, Sept. 2001.

[67] A. Wyckhuyse and X. Maldague. A study of wood inspection by infrared thermography, part ii: Thermography for wood defects detection. *Research in Nondestructive Evaluation*, 13(1):13–21, Sept. 2001.

[68] J.L. Sandoz and Y. Benoit. New technologies for wooden poles network asset

management. In *18th International Conference and Exhibition on Electricity Distribution*, pages 4–1, 2005.

[69] S. Refsnaes, L. Rolfseng, E. Solvang, and J. Heggset. Timing of wood pole replacement based on lifetime estimation. In *2006 International Conference on Probabilistic Methods Applied to Power Systems*, pages 594 – 601, 2006.

[70] H. Li, J. Zhang, and G. Bhuyan. Reliability assessment of electrical overhead distribution wood poles. In *2006 International Conference on Probabilistic Methods Applied to Power Systems*, pages 1–4, 2006.

[71] R.H. Stillman. Probabilistic derivation of overstress for overhead distribution in-line structures. *IEEE Transactions on Reliability*, 43(3):366–374, 1994.

[72] A.D. Bartlett, J.L.L. Roberts, and D. Hearnshaw. Overhead power lines designed to contain failure. In *IEE Conference Publication*, pages 3.1.1 – 3.1.9, 1993.

[73] G. Orawski. Overhead lines. the state of the art. *Power Engineering Journal*, 7(5):221–231, 1993.

[74] Yujia Zhou, Anil Pahwa, and Shie-Shien Yang. Modeling weather-related failures of overhead distribution lines. *IEEE Transactions on Power Systems*, 21(4):1683–1690, 2006.

[75] R.H.Stillman. Modeling failure data of overhead distribution systems. *IEEE Transactions on Power Delivery*, 15(4):1238–1242, 2000.

[76] Gouri S. Bhuyan. Condition based serviceability and reliability assessment of wood pole structures. In *Proceedings of the IEEE International Conference on Transmission and Distribution Construction and Live Line Maintenance, ESMO*, pages 333–339, 1998.

[77] M. Clement and A. Marty. Computer aided maintenance for distribution lines an expert system approach of failure risk evaluation. In *IEE Conference Publication*, pages 250–154, 1991.

[78] R.H. Stillman, M.S. Mackisack, B. Sharp, and C. Lee. Case studies in survival analysis of overhead line components. In *Second International Conference on 'The Reliability of Transmission and Distribution Equipment'*, pages 210–215, 1995.

[79] Dee E. Parrish. Distribution lightning protection - past, present, future. *IEEE Transactions on Industry Applications*, IA-18(2):183–187, March 1982.

[80] S.A. Sokolovsky and V.G. Santotsky. Environmental impact on the insulation of 10kv distribution power lines. In *Conference on Electrical Insulation and Dielectric Phenomena, 1998. Annual Report.*, volume 1, pages 56–59, Oct. 1998.

[81] R. Bhattarai, N. Harid, H. Griffiths, and A. Haddad. Application of surge arresters for lightning protection of 33kv wood pole distribution lines. In *2009 20th International Conference and Exhibition on Electricity Distribution*, pages 1–4, June 2009.

[82] T.E. McDermott, T.A. Short, and J.G. Anderson. Lightning protection of distribution lines. *IEEE Transactions on Power Delivery*, 9(1):138–152, Jan. 1994.

[83] H.M. Lacey. The lightning protection of high-voltage overhead transmission and distribution systems. *Proceedings of the IEE - Part II: Power Engineering*, 96(50):287–299, April 1949.

[84] Guoping Shen, Jian Yuan, and Yan Luo. Over-voltage protector for overhead

insulated distribution lines. In *Electrical Insulation Conference and Electrical Manufacturing Expo, 2007*, pages 26–29, Oct. 2007.

[85] Yu Wang, Xishan Wen, Lei Lan, Wanqi Ye, Jutian Li, and Jingqian Wang. Effects of impulse voltage waveforms on lightning shielding simulation test of transmission lines. In *Power and Energy Engineering Conference, 2009. APPEEC 2009. Asia-Pacific*, pages 1–4, March 2009.

[86] M. De Nigris, A. Sironi, I. Bonfanti, F. Giornelli, C. Valagussa, and Li Kai Shing. Most recent developments in surge arresters technology and testing. In *1998 International Conference on Power System Technology, 1998. Proceedings. POWERCON '98*, pages 194–201, Aug., 1998.

[87] Mat Darveniza, G.J. Limbourn, and S.A. Prentice. Line design and electrical properties of wood. *IEEE Transaction on Power Apparatus ans Systems*, 86:1344–1356, 1967.

[88] Gary L. Johnson and B. F. Walraven. Tentative cure for transmission pole fires. *Transmission and Distribution*, 25:80–90, 1973.

[89] G. E. Lusk and Sioe. T. Mak. Ehv wood pole fire: Their causes and potential cures. *IEEE Transaction of Power Apparatus System*, 95:621–629, 1976.

[90] Paul M. Ross. Burning of wood structures by leakage currents. *AIEE Transaction*, 66:279–187, 1947.

[91] W.H. Wickham, H.A. Adler, and M.S. Oldacre. Pole fire due to insulator contamination. *Electrical Engineering*, 67:212, 1948.

[92] W. Lethersich. Behaviour of red fir poles for 11kv lines under electrical stress due to insulator failure. *Institution of Electrical Engineer*, 93:387–393, 1946.

[93] Donald Sebesta. Grounded bracket stop pole-top fire. *Electrical World*, 190:110–112, 1978.

[94] Jenh-Yih Chen and R.J. Chang. Field eperience with overhead distribution equipment under severe contamination. *IEEE Transactions on Power Delivery*, 11:1640–1645, 1996.

[95] K.L. Wong, S. Pathak, and X. Yu. Aging effect on leakage current flow in wooden poles. *IEEE Transaction on Dielectrics and Electrical Insulation*, 16:133–138, 2009.

[96] K.L. Wong, S. Pathak, and X. Yu. Leakage current flow through wooden pole structures of varying age on overhead distribution system. In *Australasian Universities Power Engineering Conference (AUPEC2007)*, pages 1–6, Perth, Western Australia, 2007.

[97] M. Al-Dabbagh and S. Pathak. Leakage current estimation of h.v insulators on power distribution lines. In *2005 IEEE Region 10 TENCON 2005*, pages 1–4, 2005.

[98] A.E. Loxton, A.C. Britten, and I.A. Fergusson. Recent experience in eskom with pole-top fires on 22 kv wood pole lines. In *IEEE AFRICON 4th AFRICON, 1996*, volume 2, pages 705–710, Sept. 1996.

[99] C.R. Abrams. Leakage current suppression cuts pole-fire losses. *Electric Light and Power*, 44(8):52–53, Aug. 1966.

[100] P. Pelacchi. Automatic hot line insulator washing device positioned by helicopter. In *1998 IEEE 8th International Conference on Transmission and Distribution Construction, Operation and Live-Line Maintenance Proceedings, 1998. ESMO '98.*, page 133, April 1998.

[101] R. de Parny. Helicopter airborne services live line work. In *Sixth International Conference on Transmission and Distribution Construction and Live Line Maintenance, 1993. Proceedings from ESMO-93.*, pages 74 –87, Sept 1993.

[102] M.E. Fields. Silicone coating project (insulators). In *Conference Record of 1995 Annual Pulp and Paper Industry Technical Conference, 1995.*, pages 178–182, June 1995.

[103] M. Portillo, L. Fernandez, and A. Andres. An innovative method for insulators washing in energised lines. In *1998 IEEE 8th International Conference on Transmission and Distribution Construction, Operation and Live-Line Maintenance Proceedings, 1998. ESMO '98.*, page 132, April 1998.

[104] E.A. Cherney, R. Hackam, and S.H. Kim. Porcelain insulator maintenance with rtv silicone rubber coating. *IEEE Transaction on Power Delivery*, 6(3):1177–1781, 1991.

[105] E.A. Cherney. Rtv silicone rubber coating for substation insulator maintenance. In *Proceeding Pulp and Paper Industry Technical Conference*, pages 170–174, 1993.

[106] Suwarno. Silicone compound coating on ceramics insulators under various environmental conditions. In *Proceedings of the 7th International Conference on Properties and Applications of Dielectric Materials, 2003.*, volume 3, pages 1015–1018, June 2003.

[107] K. Siderakis and D. Agoris. Performance of rtv silicone rubber coatings installed in coastal systems. *Electric Power Systems Research*, 78(2):248 – 254, 2008.

[108] I.A. Metwally, A. Al-Maqrashi, S. Al-Sumry, and S. Al-Harthy. Performance improvement of 33kv line-post insulators in harsh environment. *Electric Power Systems Research*, 76(9-10):778–785, 2005.

[109] R.J. Chang, M. Shah, L. Tsai, and M. Takaseki. Design of insulators for severe contamination. In *Proc. 5th International Conference Properties and Application of Dielectric Material*, volume 2, pages 778–781, May 1997.

[110] S. Grzybowski and T. Disyadej. Electrical performance of fiberglass crossarm in distribution and transmission lines. In *Transmission and Distribution Conference and Exposition, 2008. IEEE/PES*, pages 1–5, April 2008.

[111] S. Shihab, V. Melik, L. Zhou, G. Melik, and N. Alame. On-line pollution leakage current monitoring system. In *Proceedings of the 4th International Conference on Properties and Applications of Dielectric Materials, 1994.*, volume 2, pages 538–541, July 1994.

[112] C.J. Bennoch, M.D. Judd, and J.S. Pearson. System for on-line monitoring of pollution levels on solid insulators. In *Conference Record of the 2002 IEEE International Symposium on Electrical Insulation, 2002.*, pages 237–240, April 2002.

[113] I.A.Metwally, S. Al-Sumry, and S. Al-Harthy. Online condition monitoring of line-insulator leakage currents. *International Journal of Emerging Electric Power Systems*, 5(1):1–15, 2006.

[114] A.E. Vlastos and T. Orbeck. Outdoor leakage current monitoring of silicone composite insulators in coastal service conditions. *IEEE Transaction on Power Delivery*, 11(2):1066–1070, April 1996.

[115] A.O. Austin. Protection of wooden pole by an interrupted or shunt path. Technical Report 1863080, United States Patent Office, 14 June 1932.

[116] K.A. Hawley. Mean for utilizing wood pole to aid insulators. Technical Report 1866804, United States Patent Office, 12 July 1932.

[117] T.N. Cofer and A.J. Borchers. Transmission line support. Technical Report 2844643, United States Patent Office, 22 July 1958.

[118] W.H. Duvenduck and B. Mont. Line pole grounding system. Technical Report 3621107, United States Patent, 16 Nov. 1971.

[119] David McKenzie and Brian Clancy. Wire act to fix power poles. `http:www.weeklytimesnow.com.au`, Febuary 18 2009.

[120] K. L. Wong and M.F. Rahmat. Feasibility study of leakage current shunting method based on the ladder network model. *IEEE Transactions on Power Delivery*, 25(2):1133–1137, April 2010.

[121] Xinghuo Yu. Rmit power systems research. http://mams.rmit.edu.au/eherxl8xtkkv1.pdf.

[122] P.B. Stewart. The electrical resistance of wood poles. In *Proc. of AWPA*, pages 353–385, January 1936.

[123] J.H. Winter and H.E. Ziegenfuss. Electrical resistance to ground of equipment mounted on wood poles. *Power Apparatus and Systems, Part III. Transactions of the American Institute of Electrical Engineers*, 77(3):765 – 768, April 1958.

[124] J.G. Segelken and M.S. Mason. An electrical test for moisture content of southern pine round timber. In *Proc. of AWPA*, pages 33–365, Feb. 1941.

[125] A.R. Katz and D.G. Miller. Effect of some preservatives on the electrical resistance of red pine. In *Proc. of AWPA*, pages 204–217, 1963.

[126] R. Younsi, D. Kocaefe, S. Poncsak, Y. Kocaefe, and L. Gastonguay. Cfd modeling and experimental validation of heat and mass transfer in wood poles subjected to high temperatures: a conjugate approach. *Heat and Mass Transfer*, 44(12):'497–1509, 2008.

[127] N. Franco and P.J. Pellicane. Three-dimensional model for wood-pole-strength predictions. *Journal of structural engineering New York, N.Y.*, 119(7):2199–2214, 1993.

[128] P.J. Pellicane and N. Fanco. Modeling wood pole failure: Part 1. finite element stress analysis. *Wood Science and Technology*, 28(3):219–228, March 1994.

[129] P.J. Pellicane and N. Fanco. Modeling wood pole failure: Part 2. material and geometric considerations. *Wood Science and Technology*, 28(4):261–274, May 1994.

[130] Joraslav Mackerle. Finite element analyses in wood research: a bibliography. *Wood Science and Technology*, 39(7):579–600, Oct. 2005.

[131] Atsuo Chiba, Katsuo Isaka, Tsuneo Matsuo, Yoshihide Yokoi, Masyoshi Nagata, and Minoru Kitagawa. Application of finite element method to analysis of induced current densities inside human model exposed to 60-hz electric field. *IEEE transactions on power apparatus and systems*, 103(7):1985–1902, 1984.

[132] A.I.E.E Committee. Impulse flashovers of combinations of line insulators, air gaps and wood structural members. *Transactions of the American Institute*

of Electrical Engineers, Part III (Power Apparatus and Systems), 75:16–21, 1956.

[133] K. L. Wong and M.F. Rahmat. Study of leakage current distribution in wooden pole using ladder network model. *IEEE Transactions on Power Delivery*, 25(2):995–1000, April 2010.

[134] Western power pole management : Regulatory compliance audit. Technical report, Department of Consumer and Employment Protection, Government of Western Australia, 2005.

[135] CEA Project No. 118-D-393. The electrical characteristics of wood poles. Technical report, Canadian Electrical Association, 1987.

[136] Australian government bureau of meteorology. `www.bom.gov.au/climate/`.

[137] Australian government bureau of meteorology. `www.bom.gov.au/climate/averages/tables/cw_086071_All.shtml`.

[138] Australian government bureau of meteorology. `www.bom.gov.au/climate/dwo/201102/html/IDCJDW3050.201102.shtml`.

[139] Sidney Yip, Gran Grimvall, Ju Li, John C. Mauro, Cai-Zhuang Wang, and Kai-Ming Ho. *Scientific Modeling and Simulations*, volume 68. Springer Netherlands, 2009.

[140] I. Troch, P. Kopacek, and K. Desoyer. Models for robots a simulation approach. *Automatic Programming*, 12(Part 1):307–310, 1985.

[141] Toshio Sata, Fumihiko Kimura, Hiroyuki Hiraoka, and Masayuki Enomoto. An approach to model-based robot software for industrial applications. *Computers in Industry,*, 7:211–225, 1986.

[142] E. Onieva, V. Milanes, C. Gonzlez, T. De Pedro, J. Perez, and J. Alonso. Throttle and brake pedals automation for populated areas. *Robotica*, 28(4):509 – 516, 2010.

[143] K.L. Wong and M.F. Rahmat. Investigation of leakage current in wooden pole using ladder network model. In *AUPEC '08. Australasian Universities Power Engineering Conference, 2008.*, pages 1–5, Dec. 2008.

[144] M. Kemal Atesmen. *Everyday heat transfer problems : sensitivities to governing variables.* New York : ASME Press, 2009.

[145] P. Teertstra, M.M. Yovanovich, J.R. Culham, and T. Lemczyk. Analytical forced convection modeling of plate fin heat sinks. In *Fifteenth Annual IEEE, Semiconductor Thermal Measurement and Management Symposium 1999*, pages 34 –41, 1999.

[146] Robert E. Simons. Estimating parallel plate-fin heat sink thermal resistance. `http://www.electronics-cooling.com/2003/02/estimating-parallel-plate-fin-heat-sink-thermal-resistance/`, Feb 2003.

[147] Thermal conductivity of some common materials. `http://www.engineeringtoolbox.com/thermal-conductivity-d_429.html`.

[148] Convective heat transfer. `http://www.engineeringtoolbox.com/convective-heat-transfer-d_430.html`.

[149] As3000: Wiring rules. Technical report, Australian Standard, 2007.

[150] J.T. Lusignan and C.J. Miller. What wood may add to primary insulation for with standing lightning. *A.I.E.E. Electrical Engineering Transaction I.E. Australia*, 59:534–540, 1940.

[151] Scott A. Liebel and Raymond E. Mueller. Douglas fir crossarms solid sawn vs. laminated comparison. In *Proceedings of the 1994 IEEE Power Engineering Society Transmission and Distribution Conference*, pages 581–586. IEEE, April 1994.

[152] Anthony J. Pansini. *Electrical Distribution Engineering.* Fairmont Press, 3rd edition, 2006.

[153] R.A.C. Altafim, J.F.R. Silva, H.C. Basso, C. Calil Junior, J.C. Sartori, and C.R. Murakami. Study of timber cross-arms coated with castor oil based polyurethana resin: electrical and mechanical tests. In *Conference Record of the 2004 IEEE International Symposium on Electrical Insulation 2004*, pages 556–559, Sept. 2004.

[154] M.F. Rahmat and K.L. Wong. Thermographic study of stainless steel cross-arm on overhead distribution system. In *AUPEC '09. Australasian Universities Power Engineering Conference, 2009*, pages 1–6, Sept 2009.